FINAL REPORT

SPATIO-TEMPORAL WATER AVAILABILITY UNDER CHANGING CLIMATE AND LAND-USE SCENARIOS IN WAINGANGA RIVER BASIN

आपो हि ष्ठा मयोभुवः

WATER RESOURCES SYSTEMS DIVISION

NATIONAL INSTITUTE OF HYDROLOGY
ROORKEE- 247 667, UTTRAKHAND, INDIA

JUNE 2025

STUDY TEAM

Director	:	Dr M. K. Goel
Head	:	Dr A. R. Senthil Kumar, Scientist 'G'
Investigators	:	Dr Manish K. Nema, Scientist 'E' (PI)
		Dr P. K. Mishra, Scientist 'D'
		Dr R. K. Jaiswal, Scientist 'F'

ABSTRACT

Water availability of a river basin is primarily governed by climatic factors and basin characteristics. Changes in these two may alter the various attributes of water resources and hydrology of the region. With the pronounced enrichment of carbon emission in the atmosphere, worldwide warming is leading to changes in many climatic variables. Impacts of changing climate have been witnessed on every sphere of our planet. The hydrosphere, which is vital for sustaining life on earth, is closely linked to the various climatic phenomenon. The evaluation of the impacts of climate change on the hydrologic responses of river basins is vital for optimised planning and management of water resources for the sustenance of the developmental projects.

To meet the various demands such as food, water, settlement, etc. of the ever-growing population, the land-use and land cover (LULC) have changed drastically, i.e. urban sprawling. The LULC change can alter land surface interactive processes, thus affects the hydrological cycle. This research has examined the impacts of various scenarios of varying climate and land-use on the water availability of the Wainganga River basin, India.

As a first step, the trends and variability of regional climatic characteristics of the Wainganga basin were carried out for the past and future under two SSP scenarios, i.e. SSP2 4.5 and SSP5 8.5. Thus, the impact of changing future climate on rain is analyzed by way of assessing future rainfalls in terms of projected rainfalls for different time steps. The simulations of the changes of varying land-use for three periods in the coming future were performed for the study basin. Four bias-corrected and statistically downscaled GCM model variables with SSP2 4.5 and SSP5 8.5 are considered to ascertain the impacts of climate change. Precipitation and temperature for baseline (1981-2015) and three future periods: NFS: Near-Future Scenario (2025–2050), MFS: Mid-Future Scenario (2051–2075) and FFS: Far-Future Scenario (2076–2100) have been used for hydrological simulations using a semi-distributed hydrological model on a monthly time scale. An MLP-ANN-Markov process-based land-use change model was applied to predict the land-use conditions for the year 2030, 2040 and 2050 in future. For hydrological simulation Soil and Water Assessment Tool (SWAT) model with GIS-based GUI was calibrated for the period of twenty-five years of period (1980-2005) including three years of warm-up period and validated for five years of period (2000-2005). The study also includes the detailed uncertainty analysis to identify and quantify the various components for the assessment of hydrological response under changing climate and land-use of the basin.

The results of the study reveals that there are distinct impacts of changing climate and land-use on the hydrologic response of the WRB was observed, particularly in the monthly variations of

streamflow. Results of the study confirmed the decreased streamflow initially in the early periods of the 21st century and increased streamflow towards the mid and end of the 21st century under both SSP2 4.5 and SSP5 8.5. The Basin hydrology seems to be intensified during the mid and far future period, particularly under SSP-585 scenario. Average monthly streamflow decreased for July, August and September months from 0.4% to 30.5% for SSP245 and 6.0% to 14.9% for SSP585 during the near future period of the 21st century. The mid and far future periods are confirming the significant increase in these months, 4.1% to 34% for SSP245 and 8.1% to 65.2% for SSP585. In the Monsoon season, flows are getting larger in the mid and far future periods of the 21st century. The study results in the assessments of water availability in the future periods with various percentage of dependability and can aid policymakers for effective planning and implementation of different water resources strategies.

TABLE OF CONTENT

LIST OF TABLES

LIST OF FIGURES

CHAPTER 01: INTRODUCTION

1.1 GENERAL

Water resources influence every sphere of the life-sustaining environment of our planet. Its varying forms and availability in temporal and spatial scale is a matter of concern to humankind as fresh-water is not a ubiquitous natural resource. Thus, the assessment, planning, management and sustenance of water resources become essential for reasonable utilization. Water resources management plans require a systematic approach that considers not only the hydrological processes, viz. precipitation, evaporation, transpiration, groundwater recharge, runoff, etc. but also the associations and interactions among these processes. Anthropogenic interventions to the natural environment, including changing land-use, command area development and flow regulation, significantly affect seasonal and yearly hydrologic variations. Fossil fuel induced climatic changes and the natural cycle of climate also have implications on the river hydrology. A predictive understanding of the various processes of the hydrological cycle in an integrated way is required for adaptation to these changes and to mitigate the ill effects of changing climate.

The total amount of water in the different forms persists to be constant in the hydrological cycle. The ever-growing population and changing lifestyle are the leading causes of decreasing per capita availability of freshwater over the world. Further, the non-uniform spreading of utilisable freshwater in time and space makes the situation more complicated. The solution to the water crisis lies in better planning of available water for the optimum utilisation.

Water, an essential feature of the earth, vital for living, is at a vulnerable situation nowadays. The accessibility of freshwater is an evolving concern for sustaining the pace of development across the globe (Gallopín 2001). Referring to the United States Geological Survey (USGS), the total water on earth is 1386 million km^3, out of which over 96.5% is saline water in oceans. Rest is the freshwater, which is available in the form of precipitation, streams, rivers, groundwater and snow etc. From the total freshwater, only 10.53 million km^3 is present as fresh groundwater and 0.0021 million km^3 in lakes and rivers of the planet (Lal 2015). In the current scenario of the growing population, increased consumption of water and energy, industrialisation, urbanisation, global warming, desertification, etc., there is degradation in the quality and quantum of water resources. Future projections indicated that, about 33% of the world population would face severe water shortage by the year 2050.

Falkenmark (1995) classified the water present on the earth into two classes, green water and blue water. Green water is a large fraction of precipitation, which is held by the soil pores and accessible to the plant roots for the photo-synthesis and comes backs to the atmosphere via stomatal evaporation and transpiration. Blue water is the part of precipitation that converted into a surface runoff or sub-surface-runoff or both. It also accounts for the groundwater recharges. Human beings directly use blue water for their domestic, industrial, and food production purposes. Water is a renewable resource. Over the recent 100 years (from 1900 to 2010), the world population has increased above four times (exceedingly more than seven billion now). Various economic and developmental activities have significantly changed the land-use and cropping patterns across the globe to meet out the food and water demands of the growing population. Global crop area has doubled while the global irrigated area has increased six-fold. Over these 100 years, the total global withdrawal of water from natural sources to meet various needs has increased nearly eight times from 579 km^3 per year to 4179 km^3 per year whereas only 1277 km^3 per year is recharging the groundwater, thus creating a disparity in supply and demand. The agriculture sector is the primary consumer of water and shares about 70% of the global total water uses and the remaining share used by the industrial and municipal sectors. In the agricultural water, uses are estimated to be increased only by 13% by 2050 (Siebert et al. 2010, Wada et al. 2016). It should be clearly understood that only a limited amount of blue water resources is available for all three major sectors, including agriculture, domestic and industrial. So, keeping this fact in mind, there is a necessity for strategic plans for water resources and their efficient implementation.

Watershed is a natural integrator of all physical processes governing the hydrological cycle within its rain catchment and, so is a well-accepted entity for managing the soil and water systematically. The natural resources of a watershed such as land, water, and bio-resources, including the energy regime, are extremely interconnected and need an integrated approach for better management. Watershed management programmes involve the conservation of the soil, prevention of soil erosion, runoff retardation, improvement of forests and grasslands, and protection of water quality. The water balance studies are essential for the success of such programmes. These studies quantify the various water balance components over different periods for the defined objective of watershed management and development activities.

1.1.1 Water Balance in Watersheds

The water balance can be articulated as “overall mass conservation of water within a catchment for a defined period. It states that in a specified time, the difference between the water entering a basin and that flowing out (as surface or subsurface water) must be equal to the change in the storage in the soil water content. It is necessary to appreciate the present status and forthcoming trends of the water resources of a region over a defined period”. A basin water balance helps to strengthen decision making while planning and executing various water management strategies.

The flows are generated as one of the primary components of the water cycle of a watershed as a result of the mutual interaction of climatic variables, elevation profile, land-use pattern and type of soil of watershed. One of the main objectives of watershed management is to minimise soil erosion and sediment yield by reducing the peak rate of runoff. Hence, hydrological modelling is essential nowadays to estimate streamflow, rate of soil erosion and yield of sediment, for sustainable development (Arnold et al. 1998, Jain et al. 2010). Nowadays, the practice of contemporary tools has become a crucial part of the monitoring of watershed programmes. These tools and techniques include geospatial tools such as Geographic Information System (GIS) and remote sensing (RS), which assists in establishing precise water balance for better watershed management. Monitoring at a synoptic view of the basin, near real-time data observation, multi-temporal information are a few of the advantages (not limited) of remote sensing techniques which can provide a variety of data and analysed in the GIS for effective planning, implementation and monitoring of any water resources projects.

Atmospheric temperature is accepted as a primary index of the conditions of global and regional climate due to its aptitude to characterize the exchange processes of the radiation energy on the earth's surface with reasonable accuracy (Vinnikov et al. 1990). Solar energy is the main driver for many of the earth's processes, including the hydrological cycle. A warmer climate tends to the intensified the hydrological cycle, which results in advancing the rates of evaporation and an upsurge of precipitation. Some studies on temperature variability on the global scale (Jones et al. 1986, Folland and Parker 1990, Griggs and Noguer 2002) have proven the fact that the earth atmosphere has perceived substantial warming in last century. The studies on the mountainous region of the world like the Swiss and Polish Alps, the Rockies, upland of England and the Himalayas (Beniston et al. 1997, Shrestha et al. 1999, Wibig and Glowicki 2002, Rebetez and Dobbertin 2004, Trigo et al. 2005, Bhutiyani et al. 2007, Shekhar et al. 2010, Horton et al. 2015, Stryhal and Huth 2019) have demonstrated notable rising in air temperatures with alarming effects on their environment in terms of reducing number of snowfall days, early melting of snow cover etc.

1.1.2 Remote Sensing and GIS Applications in Hydrology

The application of remote sensing and GIS enables hydrologists to deal with spatially distributed hydrological processes on a very large scale. Remote sensing has greater capabilities to deal with the hydrological processes, primarily because of its inherent capacity to monitor the areas and entire river basins rather than simply few points (Congalton and Green 2009, Shilpakar et al. 2011, Shukla et al. 2016). GIS has advanced as a highly sophisticated and versatile geodetic data and information system to collect, store, analyse, display and share the huge datasets usually prerequisite for hydrological studies. GIS delivers representations of geo-spatial information on the earth resources, whereas hydrological simulations mainly deal with the quantity of water flowing in a stream and its flowing components over the land surface and beneath the sub-surface environment (Sreedevi et al. 2009, Kumar Shukla et al. 2016, Senay et al. 2016). Substantial technological developments are going on in GIS and remote-sensing domain, which would lead to the corresponding increase in the operational use of such hydrological models. The Soil and Water Assessment Tool (SWAT) model is one of them, for which the GIS software-based graphical user interfaces (GUI) are also available with proven capabilities such as ArcSWAT and QSWAT (Wilson and Weng 2011, Arnold et al. 2012, Jain and Sharma 2014, Khalkho 2017).

1.1.3 Hydrological Modeling

Hydrologic modeling plays a critical role in evaluation of catchment response for planning (Singh and Singh 1992, Singh and Frevert 2005), development and operation of various water resources schemes (Jain and Singh 2003, Letcher et al. 2007), flood forecasting (Jasper et al. 2002, Kauffeldt et al. 2016), pollution control (Tim and Jolly 1994, Di Luzio et al. 2004) and many other applications. Rainfall-runoff is a complicated relationship for any catchment as it influenced by several implicit and explicit factors such as distribution pattern of rainfall, interception, evapotranspiration, infiltration, percolation, abstraction, watershed topology, land-use and soil profile. The flow variability at a river gauging site may vary significantly throughout a year, depending on seasonal rainfall, abstraction or diversion of flow, watershed characteristics and many other factors and variables. These parameters may significantly impact the modeling effort and time and in turn, provide ample opportunities for new research prospects.

Runoff is a vital component of hydrological modeling. Estimation of runoff from the catchment is essential for flood peak assessment and mitigation, water conservation measures, assessment of recharge potential, water resources development and overall sustainable development of the catchment. Rainfall-runoff modeling is commonly used for prediction of catchment runoff, the flow of water and its constituents on some part of the land surface or subsurface environment of a drainage basin or watershed. More precisely, a rainfall-runoff model produces the surface runoff hydrograph as a response to rainfall as an input.

Generally, the model represents a system; models allow compilation of existing knowledge can serve as a language to communicate hypotheses and can be applied to gain understanding. Different models are formulated by keeping different aims, such as conceptual models to understand better, mathematical models to quantify, operational models to operationalise and graphical models to visualise the subject.

Models of hydrologic simulations can be broadly categorized into physical process-based and conceptual. As the name suggests, in the physically-based models, the physical processes and relationships among them may be characterised in a deterministic means governed by the laws of mass, momentum and energy conservation, whereas in the conceptual models the governing processes are characterized by the mathematically based relations. Considering the spatial aspect, the hydrological models to describe the catchment process can be classified as lumped (conceptual) or distributed. A distributed model takes cares of the spatial variability of land-use, soil-class, elevation, etc., while a lumped model does not take, the spatial characteristics and inputs of the watershed into the account.

Hydrologic models, mainly spatially distributed models, are extensively used to understand and quantify the impact of land-use changes on the river flow regimes. A number of hydrologic models are existing, varying in the type of nature, level of complexity and purpose of use (Jain and Singh 2003). Numerous models have been established by a lot of researchers to study the relationship between the rainfall and runoff, such as the rational method, Soil Conservation Services (SCS) Curve Number method, Green-Ampt method etc.

1.1.4 Impacts of Climate and Land-use Change

Water resource planners and authorities essentially consider the plausible impacts of changing climate, that might create supplementary pressure on the fresh-water availability for various usages for all the sectors at least on a large scale (MoWR, 2008). Apart from the impacts of the changing climate, the changes in the land-use and land-cover (LULC), such as rapid urbanisation, can lead to modifying the water cycle by effecting various means, i.e. changing rates of evapotranspiration, altered soil infiltration capacity, and changing the regimes properties of surface and subsurface. For sustainable water resource plans for future generations, it is critical to improving the current understanding of the potential and plausible impacts and consequences of the changing climate and land-use on streamflow, evapotranspiration and groundwater dynamics in basins.

Many impact investigations have evaluated the effects of changing climate on flows in the river basins (Arnell 1999, Middelkoop et al. 2001, Gosain et al. 2006, Jean-Pierre et al. 2010, Narsimlu et al. 2013, Basheer et al. 2016, Mall 2016, Zhang et al. 2016b, Nilawar and Waikar 2019). These studies found that streamflow impacted by climate change while considering a more extended period of datasets. For example, it has been reported that some considerable alterations are expected in the hydrologic behaviour of snow and glaciered areas in view of the rise global temperature such as, deviations in the monthly peak runoff and quick snowmelts (Arnell 1999).

Besides the climatic factors of an area, LULC plays a decisive role in governing the drainage of the area. Therefore, many researchers have tried to investigate the combined effects of climate and LULC changes on streamflow (Tomer and Schilling 2009, Tong et al. 2012, Kim et al. 2013a, Júnior et al. 2015, Wu et al. 2015, Zhang et al. 2016b, Garg et al. 2017, Stigter et al. 2017). The results of these studies showed that the impacts of climate change on the hydrological behaviour of the basin were more significant than those caused due to changes in the LULC. The sixth assessment report (AR6) of the IPCC published in the year 2023 uses new-fangled scenarios of greenhouse gases (GHGs) concentrations based on several Socioeconomic and developmental pathways. These scenarios, called Shared Socioeconomic Pathways (SSPs), are a set of GHGs concentration and emissions pathways designed to support adaptation, mitigation, planning and research on the impacts of climate change and the prospective policy interventions to these changes.

1.2 STUDY OBJECTIVES

Most of the hydrological processes are random, complex and regulated by climate and the physical properties of the catchment and human activities together. The interaction of these factors complicates the separation among the effects of land-use and climatic changes on river hydrology. However, much investigation has been carried out on the impact assessment of either climate change or land-use changes. Still, limited research can be seen that considers both climate change and land-use scenarios, simultaneously. The integrated land-use and climate change analysis can reveal and suggest the land-use planning and development strategies that can be adopted to mitigate potential future water scarcity and to cope with the ill effect on climate change. The challenges are still left to distinguish the impact of land-use change from that of concurrent climate variability.

The Wainganga River Basin (WRB) is one of the important perennial rivers in Central India (a major tributary of Godavari River system), which is mainly sustained by the base flows and caters to the states Madhya Pradesh, Maharashtra and Chhattisgarh. Wide-scale interventions and other water-related activities have occurred in the Wainganga River Basin (WRB), which sustains the northern industrial region of Nagpur and large expanses of highly irrigated rice-growing districts. The water demands of the basins have steadily increased over time, and among the diverse nature of the purposes driving such a continually growing demand for drinking water, an increased reliance on irrigated agriculture, as well as numerous developmental projects such as thermal power plants, are expected to intensify competition for the limited water resources. As a result, the study's goal is to examine the basin's water resources availability and, more importantly, to estimate the influence of current and future changes in climate and landuse on the Wainganga River basin's water balance. Based on the literature and identified gaps, the following specific objectives are outlined for the present study:

1. To study the historical climate change, morphological properties and land use/land cover change pattern over the Wainganga River basin
2. To calibrate and validate a hydrological model at different spatial scales for the river basin using current land use and observed climatic conditions
3. To develop future expected land-use change and climate change scenarios (CMIP6) for the base period and compare them with the observed period
4. To model spatial and temporal future water availability using climate and land-use change scenarios
5. To quantify the uncertainty in modeling analysis arising from model parameters and input conditions
6. To prepare adaptation/management strategies under changing climate and land-use scenarios

CHAPTER 02: STUDY AREA

2.1 GENERAL

This chapter describes the various physical features, climatic and hydrological characteristics, that are helpful for data processing, land-use modeling and hydrologic model simulation. It provides information about the location of study basin in India, its contributing tributaries, districts falling within the basin, climatic conditions, geography, elevation profile and general land-use of the basin.

2.2 LOCATION AND EXTENT

The Wainganga rises in the Seoni District of Madhya Pradesh at an elevation of 640 m above M.S.L. Wainganga basin extends over approximately 50,000 square kilometres up to the Ashti gauging site, which spreads across the States of Madhya Pradesh and Maharashtra. The total length of this river is ~638 km up to the Ashti gauging site just before the confluence with the Wardha River. In the beginning, it flows eastward for a distance of about 175 km and then Southward for a length of about 100 km in Seoni and Balaghat District of Madhya Pradesh. It also serves as a border between Madhya Pradesh and Maharashtra state for 32km. Before joining the Godavari, it flows about 479 km in the Bhandara, Chandrapur, and Gadchiroli District of Maharashtra. The Wainganga basin lies in the medium rainfall zone, situated between 900 mm and 1600 mm. Most of the rainfall is received during the southwest monsoon from June to October. In the winter, the minimum temperature varies from 70 C to 130 C. Maximum temperature ranges from 390 C to 470 C. Month of May is the hottest month, and December is the coldest month. The total area of the WRB is covered by the parts of 12 districts of the Maharashtra, Madhya Pradesh and Chhattisgarh (Table 2.1).

Table 2. 1 Details of the areal contribution of districts falling under the WRB

SN	Name of District (State)	Area (km^2)	Percentage
1	Bhandara (Maharashtra)	4023.9	7.8
2	Chandrapur (Maharashtra)	5850.3	11.3
3	Gadchiroli (Maharashtra)	5587.5	10.8
4	Gondia (Maharashtra)	5273.6	10.2
5	Nagpur (Maharashtra)	0.1	0.0
6	Balaghat (Madhya Pradesh)	6941.5	13.5
7	Betul (Madhya Pradesh)	972.3	1.9
8	Chhindwara (Madhya Pradesh)	8096.1	15.7
9	Mandla (Madhya Pradesh)	735.0	1.4
10	Seoni (Madhya Pradesh)	6504.6	12.6

11	Kanker (Chhattisgarh)	6547.1	12.7
12	Rajnandgaon (Chhattisgarh)	1015.2	2.0
	Total	51547.3	100.0

2.3 CLIMATE

The Wainganga River basin, located in central India, spans parts of Madhya Pradesh and Maharashtra and forms a significant sub-basin of the Godavari River system. The climate of the Wainganga basin is primarily tropical, characterized by three distinct seasons—summer, monsoon, and winter—each with its unique influence on the hydrological behavior, vegetation, and land use patterns in the region.

Summer (March to June): The summer season is typically hot and dry, with maximum temperatures often exceeding 40°C, especially in the lowland areas. The heat is more intense in the southern parts of the basin, such as Chandrapur and Gadchiroli districts in Maharashtra. Evapotranspiration rates are high during this period, leading to reduced soil moisture and water availability in surface reservoirs and rivers.

Monsoon (June to September): The basin receives the majority of its annual rainfall during the southwest monsoon season, which begins in mid-June and continues through September. Rainfall is largely orographic and varies significantly across the basin. The average annual precipitation ranges between 1,000 mm and 1,600 mm, with higher values in the upper catchments and forested areas, especially in the Seoni and Balaghat districts of Madhya Pradesh. This season is vital for groundwater recharge, streamflow, agricultural activity, and forest growth. However, it also increases the risk of flooding, especially in low-lying areas.

Winter (October to February): Winters are mild and dry, with minimum temperatures occasionally dropping below 10°C in the northern parts of the basin. The period from November to February is characterized by clear skies, low humidity, and negligible rainfall. It is also the main Rabi cropping season, dependent largely on soil moisture stored from the monsoon.

Rainfall Variability and Climate Extremes: Rainfall in the Wainganga basin is subject to high inter-annual variability. In some years, especially during El Niño events, the basin experiences drought-like conditions due to deficient monsoon rainfall. Conversely, La Niña years can bring excessive rainfall, leading to localized flooding. This variability poses challenges to water resource management, agriculture, and hydropower generation in the region.

Climatic Influences on Hydrology and Land Use:

The monsoon-dominated climate significantly influences the river's flow regime, making it highly seasonal. Peak flows occur during July and August, with low flows persisting during the pre-monsoon months. The climate also affects sediment transport, reservoir inflow, and the functioning of wetlands and forest ecosystems in the basin. Agriculture is largely rainfed, and the timing and quantity of rainfall directly determine crop success.

Climate Change Considerations: Recent studies indicate that climate change may be impacting rainfall patterns and temperature trends in the Wainganga basin. Observations suggest a gradual increase in extreme rainfall events and a slight rise in annual mean temperatures. These changes underscore the need for climate-resilient water resource planning and adaptive management practices in the basin.

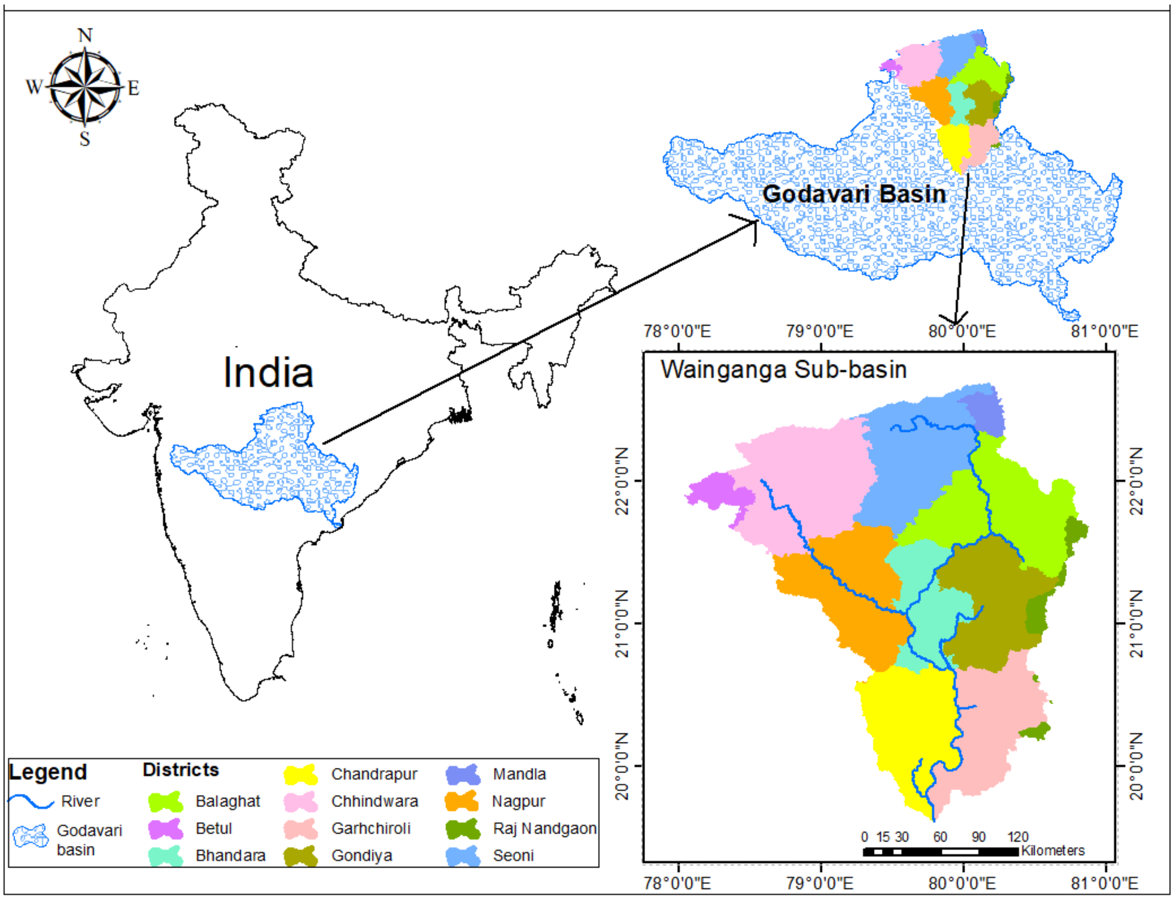

Fig. 2. 1 Location of the WRB and its sub-basins within India

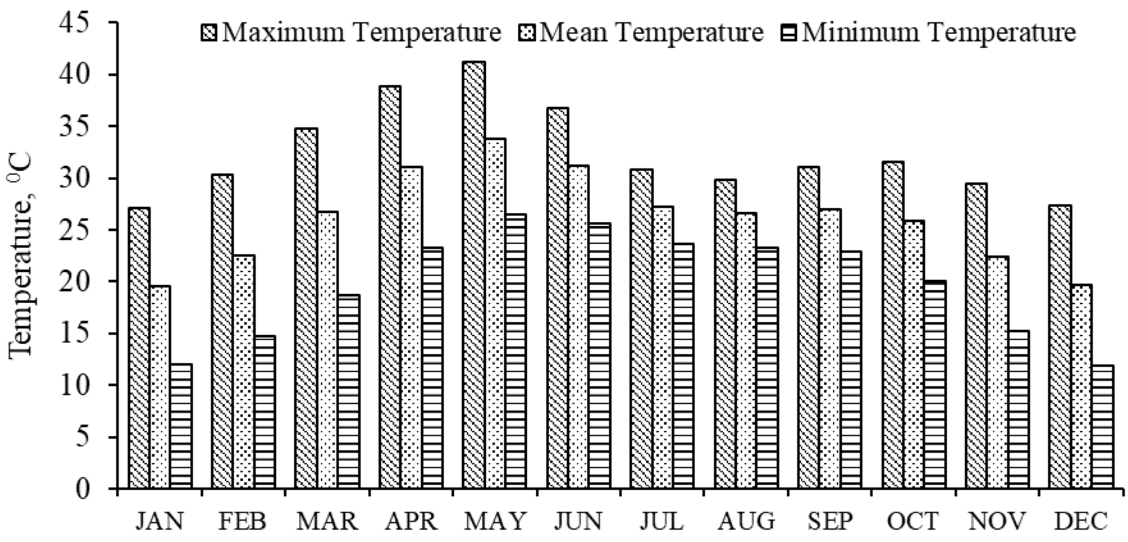

Fig. 2. 2 Average monthly temperature (1951-2014) of the study basin

Average rainfall ranges from 1050–1,600 mm/year, concentrated during the June–September southwest monsoon. The basin falls within a medium-to-high rainfall zone (990–160 cm/yr). The average annual variation in the sub-basins based on IMD gridded rainfall for 64 years (1951-2014) is shown in Fig. 2.3.

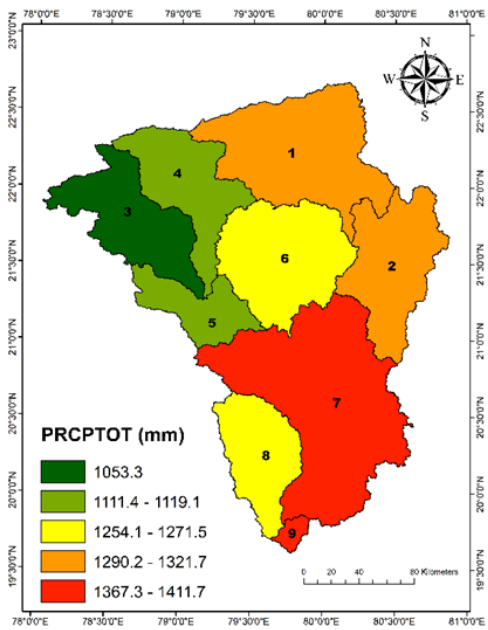

Fig. 2. 3 Average annual rainfall variation at subbasins (1951-2014) of the study basin

The basin experiences four well defined seasons viz. 1) southwest monsoon season, i.e. from June to end of September, followed by 2) post-monsoon season from October to November, 3) winter season from December to February and 4) pre-monsoon or summer season, i.e. from March to May. About 88% of the annual rainfall is contributed by the monsoon season, followed by 5%, 3% and 4% in post-monsoon, winter and pre-monsoon season, respectively.

2.4 HYDROLOGY

The Wainganga River is a major tributary of the Pranhita River, which ultimately joins the Godavari River one of India's largest river systems. Originating in the Mahadeo Hills near Gopalganj in Seoni District, Madhya Pradesh, the Wainganga River flows southward through the states of Madhya Pradesh and Maharashtra, covering a basin area of approximately 43,000 square kilometers before merging with the Wardha River to form the Pranhita. The hydrology of the Wainganga River basin is largely governed by the region's monsoon-driven climate, physiography, land use, and underlying geology.

The Wainganga River follows a dendritic drainage pattern, with several tributaries joining it along its course. Major tributaries include the Bagh, Chulband, Kathani, Kanhan, and Bawanthadi rivers. The basin's topography is undulating to hilly in the northern and central regions and relatively flatter in the southern stretches. These variations contribute to differences in runoff generation, erosion rates, and sediment transport across the basin. The river is perennial but exhibits strong seasonal variation in flow. High flows occur during the southwest monsoon season (June–September), contributing up to 80% of the annual discharge. The non-monsoon months experience reduced flow, with some tributaries becoming ephemeral, especially in dry years. The average monthly discharge at Ashti and rainfall profile of the WRB are shown in Fig. 2.4. The figure explains the high seasonality and dominance of the monsoon system in the study basin.

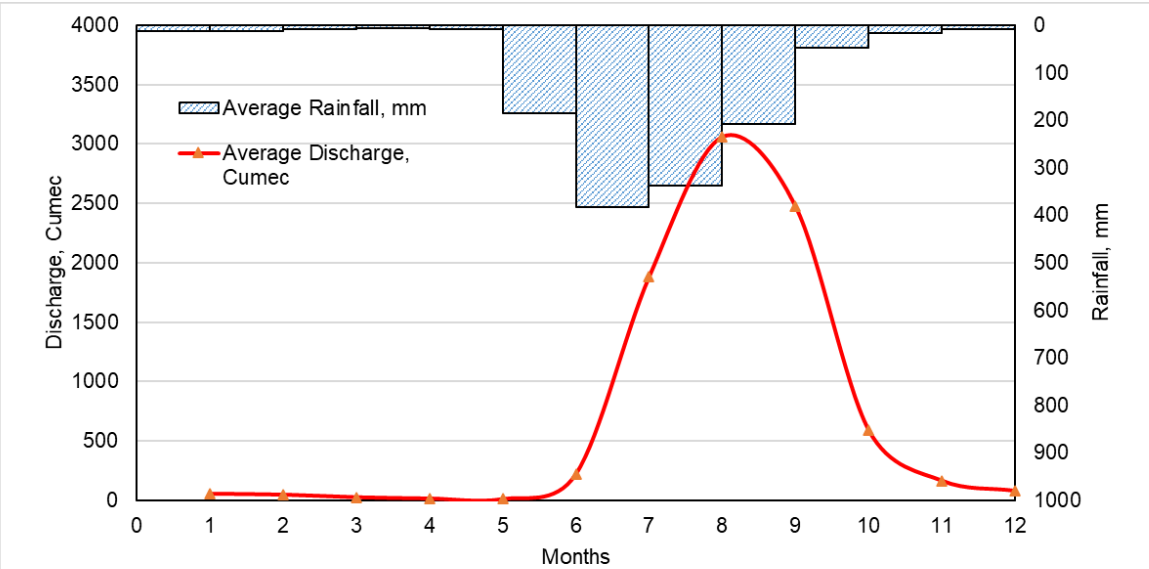

Fig. 2. 4 Average monthly discharge (at Ashti gauging site) and rainfall for the WRB

The surface water regime of the Wainganga basin is heavily influenced by monsoonal rainfall, which determines streamflow volume, peak discharge, and sediment yield. Runoff coefficients vary based on land use and soil type, with forested upper catchments yielding lower runoff and higher infiltration, while agricultural and degraded lands in the middle and lower basin produce higher surface runoff.

Several large and medium-scale irrigation and hydroelectric projects have been developed along the Wainganga and its tributaries, such as the Gosekhurd Dam in Maharashtra. These interventions regulate the river flow, support agriculture, and meet water demands for domestic and industrial use, but also alter the river's natural hydrological regime.

Groundwater plays a critical role in the basin's hydrology, particularly in sustaining baseflow during the dry season. The basin lies largely over Deccan Trap basaltic formations, which influence groundwater storage and movement. Shallow aquifers are recharged primarily during the monsoon, while deeper aquifers contribute to groundwater sustainability during lean periods. However, groundwater over-extraction in agricultural zones poses long-term risks to the hydrological balance.

The basin faces multiple hydrological challenges, including: Seasonal flooding in low-lying and downstream areas during intense monsoon rainfall; Water scarcity during prolonged dry spells or delayed monsoons; Decreasing baseflow and groundwater levels due to land use changes and increased extraction; Sedimentation in reservoirs and rivers due to upstream soil erosion.

A sound understanding of the basin's hydrology is essential for integrated water resources management. It supports sustainable planning of irrigation, flood control, reservoir operations, and climate adaptation strategies. Monitoring of streamflow, groundwater, and sediment load, combined with hydrological modeling, is critical for anticipating water availability and ensuring the resilience of the Wainganga River system.

The Central Water Commission (CWC) maintains several gauge and discharge (G&D) sites on the WRB and its tributaries for hydrological monitoring. These sites are crucial for flood forecasting and water resource management. Ashti is the last gauging site of the WRB and downstream of this site, the river confluences with the Godavari River. Thus, the discharge data series available at the outlet of the basin, i.e. Ashti manual gauging site has been used in this study.

The average annual flow at Ashti is ~1290 m^3/s (1980-2018) with a one-day highest peak of 27,874 m^3/s observed during July 13, 1994. In the summer season, which is the lean flow period for the region, few stretches of the river become intermittent, mainly in the upper part of the basin. The base flow is the governing factor for the WRB during the non-monsoon season.

2.6 GEOLOGY, ELEVATION AND SOIL

The Wainganga basin has varied rock formation and includes Precambrain rocks (granite gneisses) and Deccan traps which cover the major portion of the basin. Alluvial soils, laterite, granite, sandstone, shale, dolomite, mica, schist etc. are also seen in fragments. Major tributaries of Wainganga include Thel, Thanwar, Bagh, Chulband, Gadhvi, Khobragarhi and Kathani. All of these latter systems join the river along the left bank while Hirri, Bawanthari, Kanhan and Mul join Wainganga along the right bank.

Elevations range from 130 m to 1,200 m, with a distinct highland region in the north. The Digital Elevation Models (DEMs) highlight pronounced north-to-south gradients. All analysis of elevation was done using a digital elevation model (DEM) acquired from the United State Geological Survey (USGS) (https://earthexplorer.usgs.gov.in) website. The Shuttle Radar Topography Mission (SRTM) DEM of 1 Arc second spatial resolution was used for processing the DEM related operations.

Variations in most soil properties and characteristics in the region are closely related to their portion on the landscape. Soils of the basin are mainly developed by the action and interactions of relief, parent material and climate. The soil conditions along the valleys are rich with black regur loams while clay loams are also found along the river bed. These soils, known locally as kali soils, are very productive and suitable for rabi crops due to high moisture retention capacity. These loamy and clayey soils of the plain area are very fertile and suitable for agriculture. The soils of the study basin are mainly classified under the B and C hydrological soil groups. Soil have moderately low to moderately high runoff potential under saturated conditions. The inherent feature of soils such as porosity, permeability etc. have a significant effect in the hydrological studies because due to porosity, a lot of surface water filtrates into the Earth's crust which feeds the underground water.

Table 2. 2 The physio-chemical properties of soils in the WRB

Soil texture	Soil description	Hydrologic Soil Group	Soil layer (mm)	Bulk density (gm/cc)	water-holding capacity (mm H_20/mm soil)	Saturated hydraulic conductivity (mm/hr)	Organic Carbon (%)	Clay (%)	Silt (%)	Sand (%)	Rock (%)	USLE K-factor
Clay (CLAY)	Clay, Mixed, Hyperthermic, Lithic, Ustochrepts	C	300	1.665	0.252	2.032	0.7	54.9	31.8	13.3	0	0.163
			900	1.710	0.276	1.778	0.6	58.7	31.5	9.8	0	0.178
			1750	1.765	0.300	2.286	0.5	63.5	28.4	8.2	0	0.202
Gravelly Sandy Loam (GSCL)	Loamy-Skeletal. Kaohmtic, Hyperthermic, Typic Ustorthents	B	130	1.660	0.200	75.552	0.7	47.2	26.5	26.3	34	0.201
			400	1.700	0.180	42.809	0.5	51.3	24.0	24.7	36	0.198
Clay Loam (CYLM)	Fine-Loamy, Mixed, Hyperthermic, Typic Haplustalfs	C	250	1.575	0.171	1.778	0.6	47.2	29.8	23.1	0	0.109
			900	1.665	0.204	1.270	0.4	50.4	27.0	22.7	0	0.115
			1550	1.700	0.236	1.016	0.3	53.4	26.0	20.6	0	0.136
Silty Clay (SYCY)	Fine, Montmorillonitic, Hyperthermic, Typic Haplusterts	C	180	1.620	0.194	3.597	0.8	49.3	30.5	20.2	0	0.111
			620	1.650	0.215	3.551	0.5	52.5	30.0	17.6	0	0.103
			1000	1.700	0.226	3.505	0.4	55.3	30.0	14.7	0	0.094
Sandy Clay Loam (GSLM)	Fine-Loamy, Kaolinitic, Hyperthermic, Typic Haplustalfs	B	150	1.610	0.164	19.903	0.5	26.4	10.0	63.6	0	0.188
			750	1.625	0.185	10.977	0.3	31.4	14.3	53.3	0	0.195
			1200	1.660	0.214	3.901	0.3	34.5	14.0	51.5	0	0.221

2.7 LAND-USE

In WRB agriculture (65%) is a dominant land-use followed by dense and open forest (34%). The land-use and land-cover maps are crucial information needed for hydrological modeling. For the study basin, LULC maps for the year 2000, 2005, 2010 and 2015 were downloaded from the European Space Agency (ESA). The information regarding the LULC has been discussed in detail under Chapter 4. The LULC Maps of the period 2000 and 2020 for the study area are shown in Fig. 2.5, and their statistical information is described in Table 2.3. For more information on these global LULC datasets, the web http://maps.elie.ucl.ac.be/CCI/viewer can be browsed, and details of data processing and validation can be found at (Santoro et al. 2017).

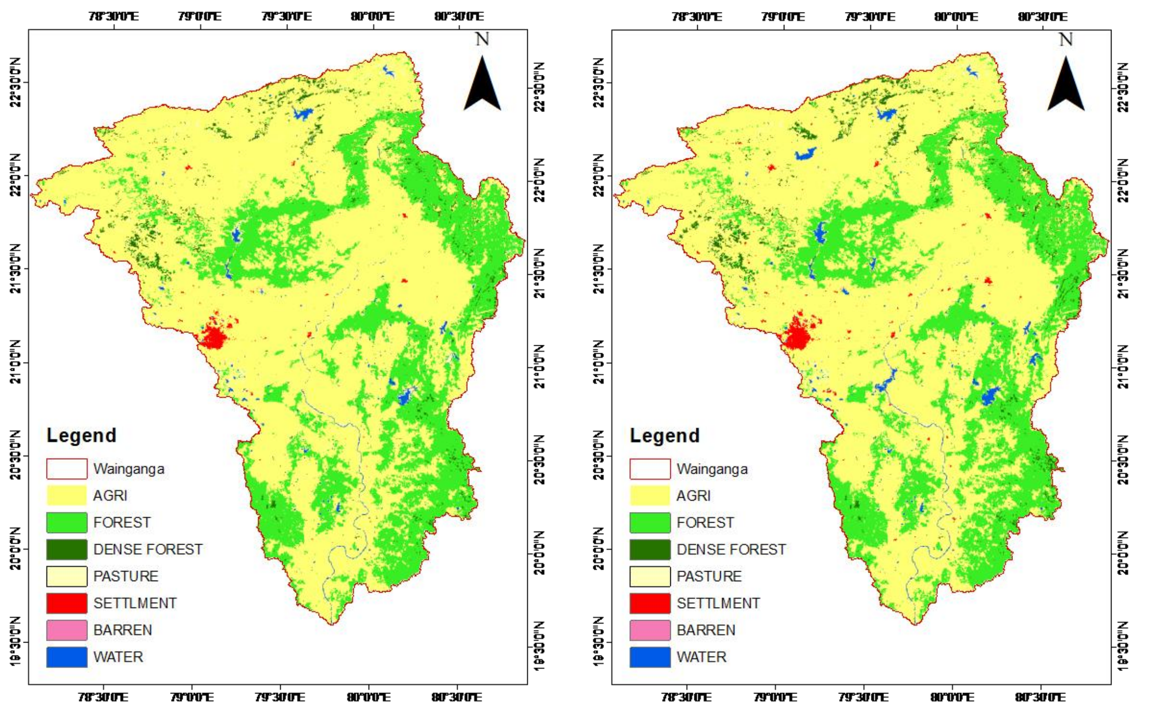

Fig. 2.1 Land-use maps of the WRB for the year 2000 and 2020

The region has seen changes in land use over the last couple of decades, the rate change in the different land-use classes has accelerated, particularly in the human settlement area. All kind of human settlements, including residential areas (including urban and rural), the industrial areas are considered as one category and named as urban area in the study. The urban area accounted for 337.64km^2 in the year 2020 after an exponential growth of 109% from the conditions of the year 2000. The water bodies and the barren areas have increased during the twenty years from the year 2000 to 2020. About 35.55% of the total basin is under forest cover which is more than the India's national average of 21.54%, and covers 40% of the Maharashtra state's total forested area (FSI 2017). This land-use change indicates that anthropogenic activities are increasing in the WRB. Further, it may be noted that the forest area in the south is converted into agricultural land. Also, most of the barren lands are in the central part.

Table 2. 3 Land-use classes and respective areas in the WRB over the years

Class Name	2000		2020		Change (2000 to 2020)
	Area (Km²)	Area (%)	Area (Km²)	Area (%)	(%)
Water Bodies	393.19	0.76	558.03	1.08	41.92
Forest	17289.97	33.55	17499.94	33.95	1.21
Agriculture	33668.07	65.31	33113.7	64.24	-1.65
Built-up	161.36	0.31	337.64	0.66	109.25
Barren land	34.75	0.07	38.04	0.07	9.47

CHAPTER 03: CLIMATE EXTREME ANALYSIS

3.1 GENERAL

Climate change is a complex and multi-dimensional phenomenon. It has a pervasive impact on the physical (i.e. water, air, land), chemical (agriculture, food security) and biological (terrestrial ecosystems, biodiversity) systems of the earth. Analysis of historical climatic variables in terms of trends and variability on the annual and seasonal basis can assist in understanding the behaviour of climatic changes occurred in a region. Thus, the detection of trends in climatic extreme considered as one of the main requirements for exploring climate science (Fankhauser et al. 1997). Study of major climatic changes, particularly variations in the incidence and distribution of precipitation and temperature, is essential for long-term sustenance of water resources. Arbitrary and/or systematic deviations of annual precipitation have solemn repulsion on the planning of command area development (Gadgil 1986).

Investigation of climate change over a region begins with the testing of long-term climatic data using different parametric and non-parametric statistical tests and detecting the trends and variabilities of climatic variables. Trend detection for a long time series of climatic data has more practical utility. A lot of research has been carried out across the globe as well as in India, for detecting the trends and forecasting the likely behaviour of the variable in the near future on a broader scale. An extensive collection of review of existing statistical methods and various tests used for investigation of trends and tendencies commonly used of water resources can be perceived in the research of Helsel and Hirsch (1992). With the rising apprehension about influences of climate change on the water sector, the investigators have applied the non-parametric Mann-Kendall (MK) test (Mann 1945, Kendall 1975) to ascertain whether a monotonous trend or tendency existing in hydro-climatic time-series data.

The identification and quantification of climatic change are essential for sustainable development of Indian agriculture. The fast retreat of the glaciers triggered by global warming and climate change may lead to significant soil erosion and flooding. In this general context, and especially in India, agriculture largely relies on monsoon (June–October) rainfall. The agricultural sector generates about twenty percent of the national gross domestic production (GDP), and more than sixty percent of the country's population depends on agriculture and associated activities for their livelihoods. In India, Rainfed agriculture has a vital role in total crop production, covering about

68 % of the total agriculture land and meeting the food demands of 40 % of inhabitants and 60 % of cattle population (Sharma and Soni 2006).

In the Indian context, using daily rainfall data from 1951 to 2000, Goswami et al. (2006) reported the rising trends in occurrence and magnitude of extreme rainfall events, and also informed noticeably drop in the frequency of moderate events in the central region of the Indian subcontinent during the monsoon seasons. The precipitation trend investigations of Ganges, Brahmaputra, Meghna and Subansiri river basins (Mirza et al. 1998, Mirza 2002, Deka and Sarma 2011, Goyal and Sarma 2017) it was reported that the precipitation in the Ganges basin is stable. Furthermore, it is also reported that one of three sub-divisions of the Brahmaputra basin suggests an increasing rainfall, while another indicates a decreasing trend. Based on the study of nine river basins of northwest and central India, Singh et al. (2008) concluded that there was a rising trend of 2–19% of average annual rainfall over 100 years. Sinha and De (2003) reported that annual rainfall and surface pressure over all-India, indicating a non-significant trend, except for some periodic behaviour. It has been reported that observations of an increasing trend of the occurrence of extreme and heavy storm events during the monsoon season, whereas decreasing trend during winter, pre-monsoon and post-monsoon seasons.

Besides rainfall, the fluctuations in atmospheric temperature were too studied by the researchers, the review of various methodologies and approaches for analysing trend for changing temperature regime in Indian context can be found in the investigation of Bhutiyani et al. (2007), Srivastava et al. (2009), Sonali and Kumar (2013) and Sonali and Nagesh Kumar (2016).

Spatial and temporal changes in a climatic data may occur either gradually (a tendency) or abruptly (with a change point) or in a more complex way (Kundzewicz and Robson 2004). Based on the study of monthly, seasonal and annual trends of rainfall of 135 years (1871–2005) for 30 sub-divisions (sub-regions) in India, Kumar et al. (2010) testified rising trends in rainfalls on an annual basis for half of the sub-divisions and decreasing only in one sub-division (Chhattisgarh). In the district wise rainfall analysis of 115 years (1901-2015) of Chhattisgarh, Nema et al. (2018) also reported a decrease in annual and monsoon rainfall and increased in rest of the seasonal rainfall.

The study of climatic extreme variability for past and future periods is reported in this chapter for the study basin, where agriculture is a primary economic activity. Nearly 80% of the community of the region belongs to the rural area, and agriculture and farming is the primary source of their livelihood. Rice is the principal crop, cultivated on almost 77% of the net sown area. On average, only about 20% of the total cultivated land of the basin is covered with irrigation facility; the rest depends on rains.

During Kharif crop season (July to October), growing rice is a tradition and is widely accepted. While, in Rabi crop season (October to March), there are limited choices of crops for the local farmers. With the accessibility to partially or assured irrigation, they commonly go for the combination of rice-wheat, rice-mustard and rice-winter vegetables. Under the rainfed situation, combination the rice-fallow, rice-utera (Lathyrus, chickpea and linseed) are the most common practices in the region. Thus, analysis of changing rainfall and temperature pattern in the region and their impacts on water availability plays a critical and vital role for managing the demand and supply for the water managers. Some studies (Bhutiyani et al. 2007, Jain and Kumar 2012, Chakraborty et al. 2013, Bhelawe et al. 2014, Dandodia and Sastri 2015, Meshram et al. 2016, Nema et al. 2018) have already been conducted on detecting rainfall and temperature trends at central regional and national scales.

In this context, this chapter aims at quantifying the a few indices for extreme rainfall and temperature series in sub-basins of the WRB and demonstrating the spatial pattern of their trends.

3.2 DATA USED

The current study utilizes the bias-corrected daily projections of PCP for the WRB from the dataset developed by (Mishra et al. 2020) using outputs from six CMIP6 GCMs as specified in Table 3.1, with their respective details. This dataset is available for two time periods; the Baseline Period (BLP) for 1951-2014 and the Future Period (FP) of 2015-2100 using Empirical Quantile Mapping (EQM) as the bias-correction method. This dataset is well validated against the observed data with a spatial resolution of 0.25^o (Jose et al. 2022). CMIP6 provides Shared Socioeconomic Pathways (SSPs), which include various future scenarios. The current study mainly considers two scenarios: SSP2 and SSP5. The study also leverages the ability of the Extreme Climate Indices (ECIs), which are recommended by the ETCCDI and ET-SCI. The indices were calculated using Python Programming, utilising the xclim library). Also, the computed ECIs were used to understand the WCEE variation at the sub-basin level using QGIS and ArcMap. In addition to this, the variation in the sub-basin for both BLP and FP is graphically presented. The four GCMs are averaged for the preparation of the MMEA dataset, and further, this data is used for the evaluation of WCEEs. Detail of the GCM data are given in Table 3.1. The data were analysed using the six indices provided by Expert Team on Climate Change Detection and Indices (ETCCDI) and Expert Team on Sector-Specific Climate Indices (ET-SCI).

The cell size of the dataset was kept at (0.25X0.25) degrees for analysis. The indices used are listed in Table 3.2.

Table 3. 1 Details of all the GCMS considered in the study

GCM Name	Country	Resolution (Degree Decimal) Latitude	Longitude	Description
BCC-CSM2-MR	China	1.1215°	1.125°	Beijing Climate Center Climate System Model-Medium-Resolution
EC-Earth3	Europe	0.70°	0.70°	EC-Earth Earth System Model Version 3
MPI-ESM1-2-HR	Germany	0.93°	0.93°	Max Planck Institute for Meteorology Earth System Model version 1.2 higher resolution
NorESM2-LM	Norway	1.9°	2.5°	Norwegian Earth System Model version 2 with low-resolution atmosphere/land and medium-resolution ocean/sea ice

Table 3. 2 Selected ECIs provided by ETCCDI and ET-SCI for rainfall and temperature

Index	Name	Definitions	Units
Rx1	Max 1-day PCP	Annual maximum 1-day PCP	mm
Rx5	Max 5-day PCP	Annual maximum 5-day PCP	mm
TXx	Max Tx	Annual maxima value of daily Tx	℃
TNx	Max TN	Annual maxima value of daily Tn	℃
TXn	Min Tx	Annual minima value of daily Tx	℃
TNn	Min TN	Annual minima value of daily Tn	℃

3.3 EXTREME RAINFALL ANALYSIS

The Fig. 3.1 shows that there is a net increase in the 1-day maximum rainfall event in SSP2-FP and SSP5-FP with PCP ranging from 38.4-53.9 mm and 39.4-53.6 mm, as compared to 32.8-45.2 mm for BLP. This increase in Rx1 can be subjected to threshold-exceeding events such as short-duration rainfall events, resulting in flash floods. Concerning the spatial changes, the Vidarbha region (western part) is subjected to drying conditions, while south (SB9) and south-eastern (SB7) part of basin fall for the heavy rainfall spell, showing more intense runoff and the possibility of flash floods. In addition to that, Northern part (SB2) is also prone to heavy rainfall.

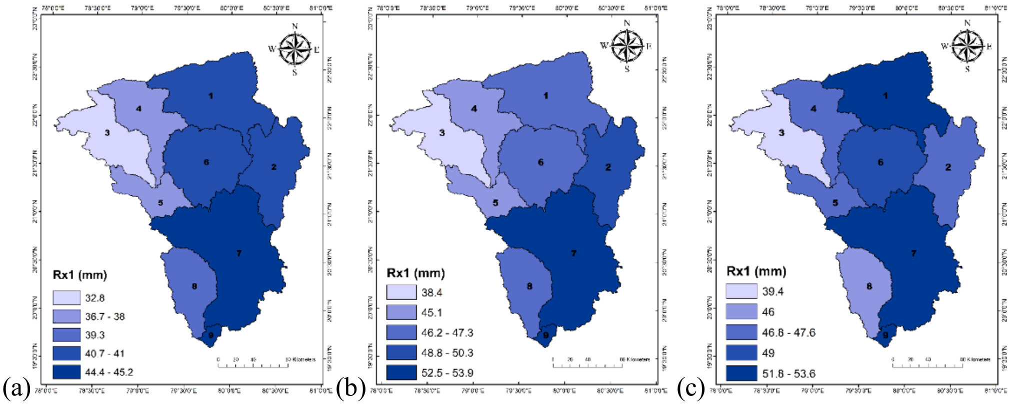

Fig. 3. 1 Trends of Rx1 for (a) BLP for 1951-2014, (b) SSP2-FP for 2015-2100, (c) SSP5-FP for 2015-2100

Similarly, according to Fig. 3.2, 5-day maximum rainfall also shows a sharp increase in PCP for SSP2-FP and SSP5-FP with values ranging from 120.9-156.7 mm and 122.3-159 mm, respectively, as compared to the range of 101-135.8 mm for BLP. An increase in Rx5 suggests the occurrence of river flooding and soil saturation, which can lead to flood events.

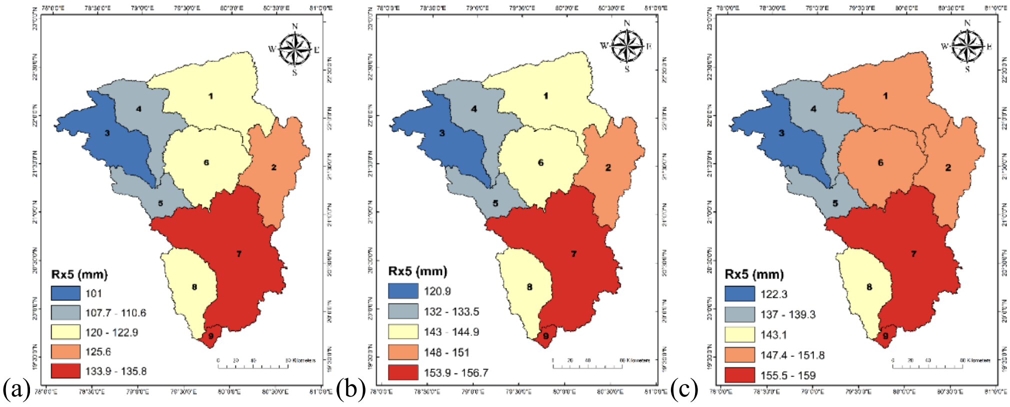

Fig. 3. 2 Trends of Rx5 for (a) BLP for 1951-2014, (b) SSP2-FP for 2015-2100, (c) SSP5-FP for 2015-2100

3.4 EXTREME TEMPERATURE ANALYSIS

The temperature intensity analisys compute and present the magnitude of extreme climate events, i.e., it showcases how the intensity of coldness/warmness of the days/nights in a year is presented. TX_x (Max Tx) and TX_n (Min Tx) denote the annual maxima and minima of the maximum TMP, while TN_x (Max Tn) and TN_n (Min Tn) denote the annual maxima and minima of the minimum TMP. Fig. 3.3 shows the TN_n, which is the annual minima of the minimum TMP for Fig. (3.3a) BLP and two future periods, i.e., Fig. (3.3b) SSP2-FP and Fig. (3.3c) SSP5-FP. The TN_n denotes the coldest nights, a direct indicator of cold intensity extremes. The range of TN_n varies from 7.5 - 13 °C for BLP, 6 - 11.5 °C for SSP2-FP and 10 - 15°C for SSP5-FP, respectively. It is clearly depicted that an extreme is observed in SSP5-FP, i.e., 15°C.

Also, it is clearly observed that LWG is experiencing the coldest nights in all three scenarios, with cold extremes rising from 11 - 13°C for BLP, 10 – 11.5°C for SSP2-FP, and 13.5 - 15°C for SSP5-FP. While Bagh is consistently in the lower extreme, comparatively warmer nights as compared to the whole basin, with 7.5 – 9°C for BLP (Fig. 3.3a), 6 – 7.5°C for SSP2-FP (Fig. 3.3b) and 10 - 11°C for SSP5-FP (Fig. 3.3c). In addition to that, Andhari and Chulbandh are also in extreme cold nights following LWG as shown in Figure 3.3. It is also to be noticed that Bawanthadi maintain almost similar TN_n throughout all the scenarios.

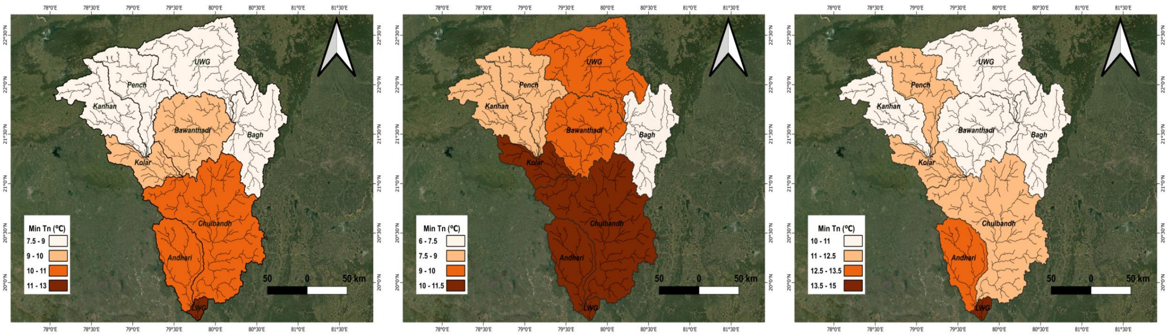

(a) (b) (c)

Fig. 3. 3 Trends of TN_n for (a) BLP for 1951-2014, (b) SSP2-FP for 2015-2100, (c) SSP5-FP for 2015-2100

Figure 3.4 illustrates Max Tn, i.e., annual maxima of the minimum TMP, depicting the warmness of the warm nights. The range of TN_x varies from 25 - 30°C for BLP, 27.5 – 31.5°C for SSP2-FP and 28.5 – 32.5 for SSP5-FP, respectively. Similar to TN_n, extremes are reported in SSP5-FP. Alike TN_n, LWG is showing the warmest nights amongst all the SBs with TN_x 28.5 – 30°C for BLP (Fig. 3.4a), 30.5 – 31.5°C for SSP2-FP (Fig. 3.4b) and 31.5 – 32.5°C for SSP5-FP (Fig. 3.4c), respectively, followed by Chulbandh and Andhari for all the scenarios. On the contrary, Kanhan and Pench show comparatively less intense warm nights in the whole WRB.

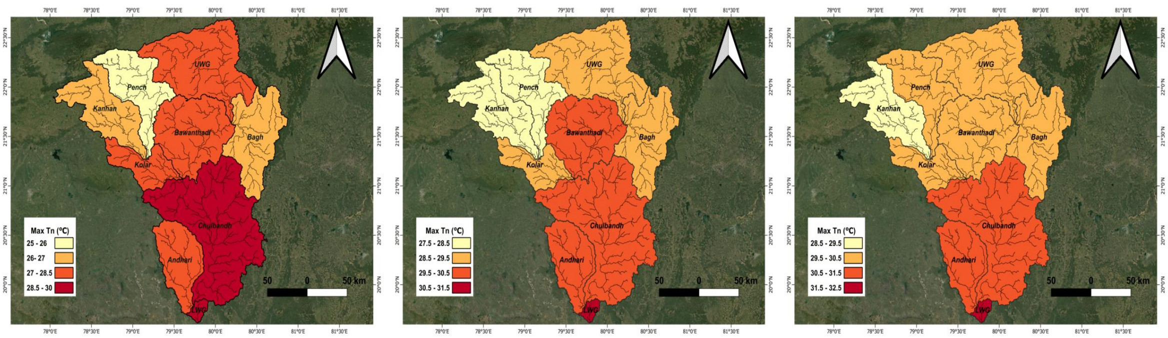

(a) (b) (c)

Fig. 3. 4 Trends of TN_x for (a) BLP for 1951-2014, (b) SSP2-FP for 2015-2100, (c) SSP5-FP for 2015-2100

Figure 3.5 shows the TX_x for the WRB, denoting the strongest heat intensity during daytime of each year. The TX_x for BLP varies from 40 – 44 °C, 41 – 45 °C for SSP2-FP, and 42 – 46°C for SSP5-FP, respectively. Referring to Fig. 6, it is observed that LWG is depicting heavy extremes, i.e., 43 – 44 °C for BLP (Fig. 3.5a), 44 – 45°C for SSP2-FP (Fig. 3.5b) and 45 - 46°C for SSP5-FP (Fig. 3.5c), respectively. Similarly, Pench is offering comparatively colder days as compared to other basins with TMP varying from 40 – 41°C for BLP, 41 – 42°C for SSP2-FP and 42 - 43°C for SSP5-FP, respectively. Maximum warmth is observed for SSP5-FP, which shows the presence of extreme heat waves, concluding that future scenarios of SSP5-FP will consist of more heat events.

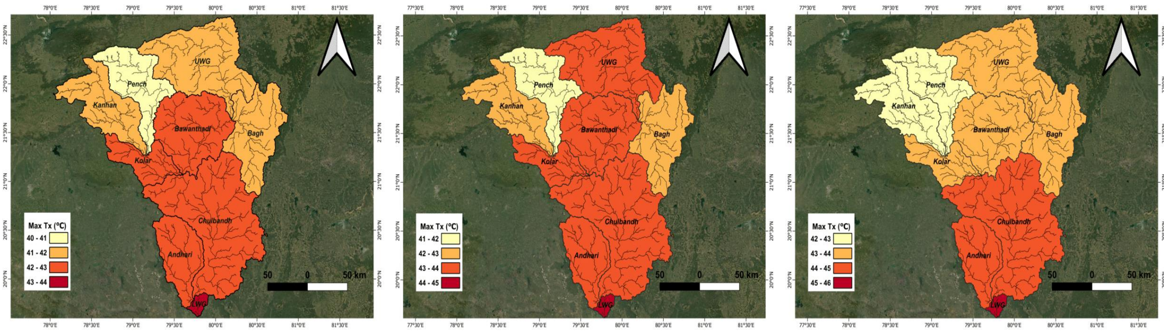

(a) (b) (c)

Fig. 3. 5 Trends of TX_x for (a) BLP for 1951-2014, (b) SSP2-FP for 2015-2100, (c) SSP5-FP for 2015-2100

Fig. 3.6 shows TX_n, the annual minima of the maximum TMP, showing the intensity of how cold the day extremes can be. It is clearly depicted that extreme coldness is more observed in the BLP as compared to SSP5-FP, with TMP ranging from 23 – 28°C for BLP (Fig. 3.6a), 21 - 27°C for SSP2-FP (Fig. 3.6b), and 22 - 29°C for SSP5-FP (Fig. 3.6c), respectively. As shown in TX_x, TN_x and TN_n, LWG is the warmest in the whole basin with 26 – 28°C for BLP, 26 - 27°C for SSP2-FP and 26 - 29°C for SSP5-FP, respectively for TX_n. On the other hand, Pench and Bagh show the presence of the cold extremes in the WRB, with TMP ranging from 23 – 25°C for BLP (Fig. 3.6a), 21 – 24°C for SSP2-FP (Fig. 3.6b), and 22 – 24°C for SSP5-FP (Fig. 3.6c), respectively. This analysis concludes that LWG is experiencing warmth, while Pench and Bagh endure coldness. The SBs which are located at higher elevations, with dominating forest reserves and vegetation forest cover, with some localized urbanization adding regional warming..

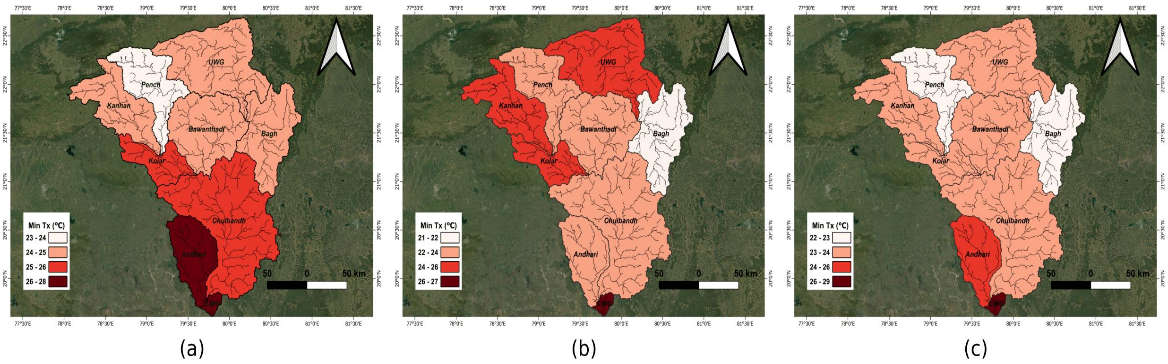

Fig. 3. 6 Trends of TX_n for (a) BLP for 1951-2014, (b) SSP2-FP for 2015-2100, (c) SSP5-FP for 2015-2100.

CHAPTER 04: SIMULATION OF FUTURE LAND-USE OF WRB

4.1 GENERAL

Land-use changes are considered as one of the most pertinent drivers of terrestrial ecosystems dynamics at local as well as global scales (Kanianska et al. 2014, Visconti et al. 2016, Cegielska et al. 2018). The changing pattern of land-use may cause impacts on a riverine system and its ecosystem services. Especially the urban sprawling and conversion of agricultural land into human settlements is the major challenge reported across the globe (Partoyo and Shrestha 2013, Pandey et al. 2018).

With the recent advancements in the geospatial technology and availability of global remotely sensed data, simulation of spatial changes in land-use is getting easier and more precise. These are helpful in monitoring the various phenomenon and variables relating to the earth and atmospheric system. Satellite-based remote sensing data provide a synoptic view of the earth system at low cost at a defined repetitive time interval (Lillesand and Kiefer, 2005). With the availability of satellite-based earth observations at a different period, the user or/and decision-maker can analyse the pattern of change in land-use and land cover at desired periods. These data can also be used as inputs for simulating the future land-use scenario, which is essential for environmental planning and management.

The quality of simulation of future land-use changes primarily depends on the level of an accurate analysis of the past and present land-use conditions, the data quality of input drivers, and the model used for the simulation. In recent past, many spatial models have been developed and attempted by integrating remote sensing and GIS for simulating the changes is land-use pattern and urban growth such as cellular automata (CA) models (White and Engelen 1993, Batty et al. 1999, Samat et al. 2011), logistic regression (LR) models (Congalton and Green 2009, Partoyo and Shrestha 2013, Wu et al. 2015, Arunyawat and Shrestha 2018), Markov chain (MC) models (Arsanjani et al. 2011, Tattoni et al. 2011, Paul et al. 2018), agent-based models (Crooks 2007, Matthews et al. 2007), artificial neural networks (ANNs) (Pijanowski et al. 2002, Maithani et al. 2010, Ahmadizadeh et al. 2014), optimisation models (Chu et al. 2010), modified CA-based SLEUTH model (Clarke et al. 1997, Jantz et al. 2004), and conversion of land-use and its effects (CLUE) model (Veldkamp and Fresco 1996, Verburg et al. 2002).

Each model has certain advantages and limitations (Araya and Cabral, 2010, Triantakonstantis and Mountrakis, 2012). Therefore, to overcome the limitations of these models, researchers attempted various hybrid or integrated models to complement the shortcomings of each other and most of them adapted to simulate urban growth (Arsanjani et al. 2013, Surabuddin Mondal et al. 2013, Basse et al. 2014, Maithani 2015, Ozturk 2015).

The early approaches of land-use simulations were confined to the urban area expansion and due to lack of a proper understanding of land surface dynamics with temporal changes they suffered from a substantial amount of errors. The incorporation of space-varied, time-varied, and others relevant drivers in land-use modeling was further improved with the development of Cellular automata (CA) models (White and Engelen 1993, Batty et al. 1999, USEPA 2000, Allen 2012). The CA models are simple to use and have greater compatibility with any raster-based GIS interface. These also have the flexibility to model different land-use scenario at one go. The CA model theory-based approach is most commonly and widely used in the land-use model simulations in a GIS environment (Kocabas and Dragicevic 2006, Guan et al. 2011, Samat et al. 2011). The development of Markov random process systems for the land-use simulation and optimum regulation is the main principle of the Markov model (Pandey and Khare 2017). The Markov model primarily quantifies the states and rates of conversion among the different land-use classes.

The CA and the Markov model have their own merits and demerits. The CA incorporates the spatial components and can address the dynamism with user-defined rules thus improve the computational efficiency but poor at modeling the anticipated spatial changes (Sang et al. 2011, Jokar et al. 2013, Garg et al. 2017, Siddiqui et al. 2017). On the other hand, Markov model is good at predicting the spatial trends of change. Thus, the CA-Markov model is a vigorous method within the spatial and temporal modeling of terrestrial changes which can be incorporated in a GIS framework and consider the remotely sensed data as inputs. The CA-Markov model considers the land-use changed occurred in the past along with the other drivers of changes such as the effect of natural, social and economic variables to model the land-use changes (Sang et al. 2011).

Artificial neural network (ANN) technique resembles the human biological nervous system. Like any other artificial neural network, it also comprises of basic processing elements, called neurons and connection links operating in parallel. A neural network architecture typically comprises three layers of nodes: an input layer, a hidden layer and an output layer. It is widely being used to define and model the complex non-linear relations among variables. Since, ANN model itself generates various parameter values automatically to involve less data for training and save the model calibration time (Civco 1993, Atkinson and Tatnall 1997). One of the imperative advantages of MLP is its aptitude for modeling all the land-use transitions at one time (Eastman 2012a). Many researchers reported (Alberti and Waddell 2000, Maithani 2015, Mishra and Rai 2016, Zhang et al. 2016a) the multilayer perceptron (MLP) based neural network-based land-use modeling. Ozturk (2015) used Cellular Automata-Markov Chain (CA-MC) and Multi-Layer Perceptron-Markov Chain (MLP-MC) hybrid models to simulate LULC changes and urban growth in Turkey and found that the MLP-MC model provided the best simulations rendering to the validation based on the kappa index. Many researchers have reported a high level of accuracy for LULC change simulation by the integration of MLP-NN with Markov chain (Dadhich and Hanaoka 2011, Ahmed and Ahmed 2012, Mozumder and Tripathi 2014, Ozturk 2015, Mishra and Rai 2016).

It has been witnessed in the past few decades, the urban areas are expending and green cover, including agriculture and forest, are shrinking. To determine the consequence of these changes on the various basin characteristic, the land-use modeling was carried out for the WRB, which has agriculture as dominant land-use. Agriculture is the primary livelihood for the basin community. About 65% of the basin area belongs to agriculture. The basin has two distinct cropping seasons, monsoon (*Kharif:* mid-June to October*)* and post-monsoon (*Rabi:* November to mid-April). Paddy is the major crop of monsoon, which covers about 95% of the cropped area during *Kharif*. Wheat, summer paddy, pulses and oilseeds are the other crops grown in the study are during *Rabi*.

The land-use modeling was conducted for the WRB located in the Chhattisgarh state, which is a relatively new state and known as the rice bowl of India. This state has an agrarian economy and homogeneous climatic conditions. Since its formation in the year 2000, the region has seen rapid changes in the land-use patterns.

These changes have significantly altered the landscape of the region. Increasing population and rapid urbanisation witnessed the unprecedented land-use changes. Probably, this is the first attempt in the study area, wherein the simulation for the future LULC is being made, with the validation of the land-use change model with past data. Moreover, the specific objective of this chapter was to carry out a regional analysis from 2000 to 2015 of land-use changes in the central part of state Chhattisgarh of India and to develop the scenarios of future land-use change for 2030, 2060, and 2090. Specifically, this chapter focuses on (i) determination of the spatial and temporal land-use changes, (ii) identification of the major drivers of changes and transitions among land classes, and (iii) simulation of the future land-use and validating the model output with actual land-use maps using MLP-NN-Markov model.

4.2 DATA USED

Various spatial and temporal datasets from different sources were used in this investigation for prediction of future land-use of WRB, India. This section describes the details of those datasets and their respective sources.

4.2.1 Land-use Maps

Being primary inputs, the land-use and land cover maps of study basin for the year 2000, 2005, 2010 and 2015 were used. Under the climate change initiative programme of European space agency (ESA), global land cover inventory from 1992-2020 has been developed to help the research community, particularly for climate-related modeling. This inventory contains the processed and uniformly classified global land-use maps from different available satellite sensor data (http://maps.elie.ucl.ac.be/CCI/viewer/). The land-use data for the year 2000, 2005, 2010, 2015 and 2020 was downloaded for the study area. As the input land-use images are available for the globe, the original raster images have 22 major land-use class and 15 sub-classes. These data are available with the geographic coordinate system based on the world geodetic system 84 (WGS84) reference ellipsoid. The land-use maps were processed in GeoTiff file format in ArcGIS initially then land-use modeling was performed in TerrSet software friendly RST file format. Then land-use maps were resampled at a cell size of 30m to match with the DEM and other input driver maps. The images of the study area cropped from the global map, and twelve land-use classes were merged into six distinct land-use classes given in Table 4.1. Land-use maps of the study area for the periods of 2000, 2005, 2010, 2015 and 2020 are shown in Fig. 4.1.

Table 4. 1 Descriptions of land-use and land cover classes used in the study

LULC Class	Description
Agriculture Land	Agricultural area, cultivated and fallow lands and Horticulture areas
Forest	Deciduous forest, mixed forest lands, Open-forest, scrub, tree cover and others
Barren Land	Open soils, exposed rocks, dumping sites and areas of active mining, banks of streams
Water Body	River, reservoirs, lakes etc.
Built-up	Human settlements, industrial, transportation, roads, mixed urban and rural

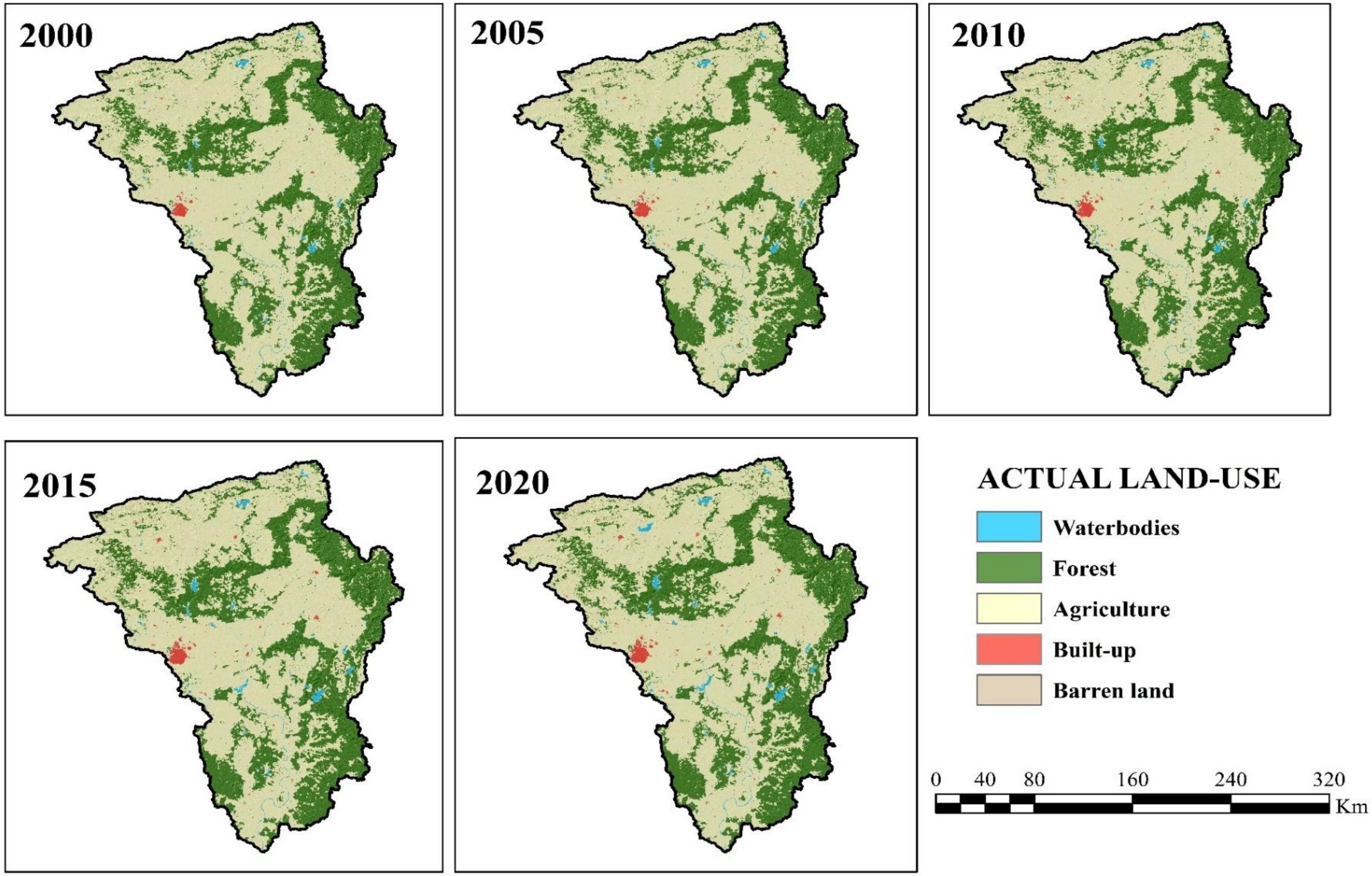

Fig. 4. 1 Land-use map of the WRB for the year 2000, 2005, 2010, 2015 and 2020.

4.2.2 Driving Variable

The other datasets are mainly comprised of the different variables and factors which directly or indirectly contributes to the land-use changes. These variables are called as drivers of land-use changes and had been used to develop the land-use prediction model for the WRB. These drivers of changes were categorised as biophysical, socio-economical and infrastructural drivers and acquired from different sources such as open street maps, population census data of India, SRTM data and spatial trend maps of transitions from existing land-use maps. A list of these drivers and their description is given in Table 4.2.

Table 4. 2 Description of the drivers of land-use Changes

Category	Driver	Description	Sources
Topographic	Elevation	Surface Elevation Map	SRTM, DEM
	Slope	Percentage Slope map prepared from DEM	SRTM, DEM
Hydrological	Canal_Distance	Distance to the canal network	Open Street Map
	River_Distance	Distance to the river network	River network from SRTM, DEM
	Reservoir_Distance	Distance to the reservoir	Open Street Map
Demographic	Population Density	Population density	Census Organization India (2011)
	Literacy Rate	Total Literacy Rate	Census Organization India (2011)
Infrastructural	Road_Distance	Distance to the road network	Open Street Map
	Rail_Distance	Distance to the rail	Open Street Map
	Urban_Distance	Urban disturbance	Land use map of 2010
Spatial Trend Maps of land-use class transition	Trend_AG_UR	Agriculture to Urban	Land use map of 2000 and 2005
	Trend_FOR_UR	Forest to Urban	Land use map of 2000 and 2005
	Trend_ALL_UR	All to Urban	Land use map of 2000 and 2005

The Euclidean distance method was adopted to produce all the distances maps such as distances to road, canal, river, railway lines, urban area, etc. within the ArcGIS framework and the produced maps were converted into RST format before being used for modeling the land-use change. All the inputs were resampled at a grid size of 30m to that of SRTM, DEM. The maps of these drivers of changes are shown in Fig. 4.2 to Fig. 4.6.

From DEM map it can be observed that the northern and eastern part of the basin under study is hilly and undulating, the central part is mostly plain and featureless, and the southern part also has hill but with less elevation. The slope map shows that there is not much slope variation in the basin, and it is bound only in the ridges of the basin. A minor canal network is present in the basin. The canal density is higher in the central-southern part of the basin, which has major reservoirs of the basins. The drainage map suggests that the basin is well-drained with the presence of many small tributaries of the WRB.

WRB is a sparsely populated basin with a few high populated urban clusters. The average population density of the basin is ~200 persons/km^2. The basin has a fair literacy rate of ~63% on average.

The basin has a good transportation infrastructure, including railway and road networks, which were also considered as one of the criteria contributing to changing land-use scenarios. A few main urban clusters in the basin, are the cities Nagpur, Gondia, Balaghat, Chhindwara, and Wardha.

4.3 METHODOLOGY

The assessment of LULC changes that took place from the year 2000 to 2005 was performed with the ANN-based land-use change model. The land-use class wise gain and loss and net change experienced by each class from the year 2000 to 2005 were estimated, and transition maps were analysed. The potential transition from agriculture, barren and open forest class to urban areas were considered, and all these three possible transitions were included into the model structure.

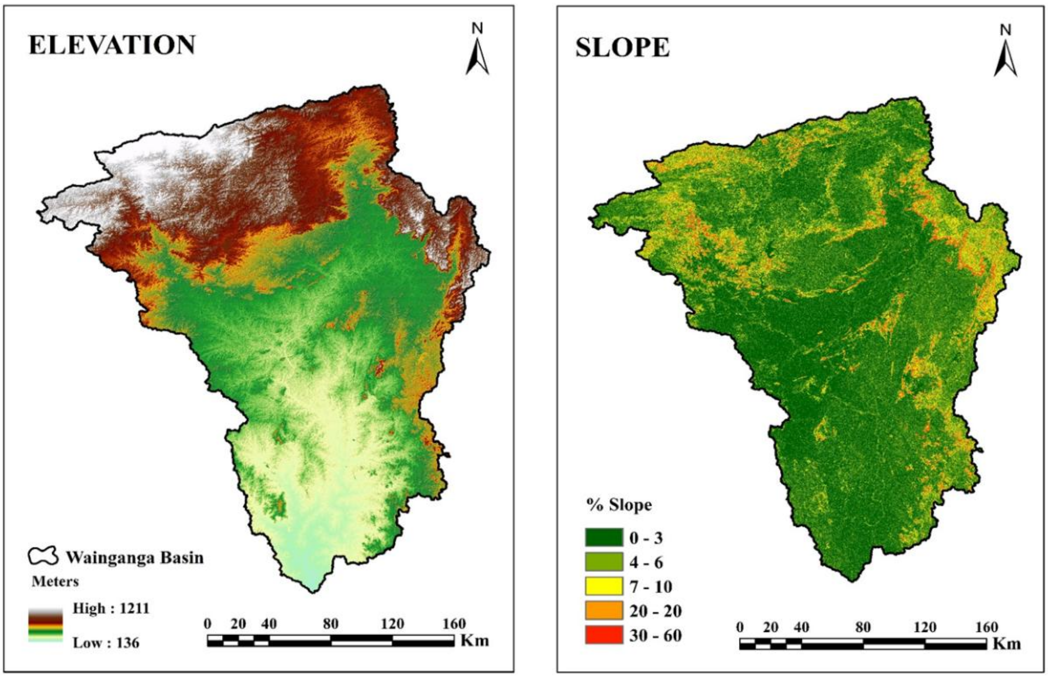

Fig. 4. 2 Topographic drivers of change including Elevation and Slope maps

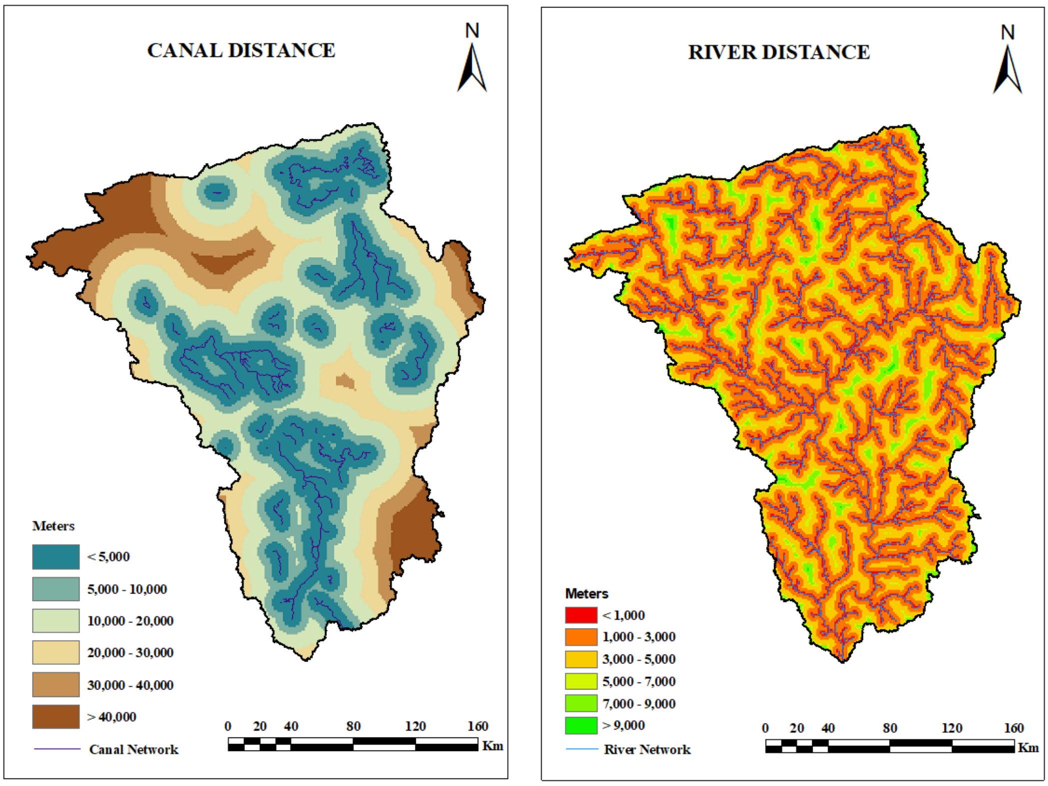

Fig. 4. 3 Hydrological drivers of change Canal Distance and River Distance maps

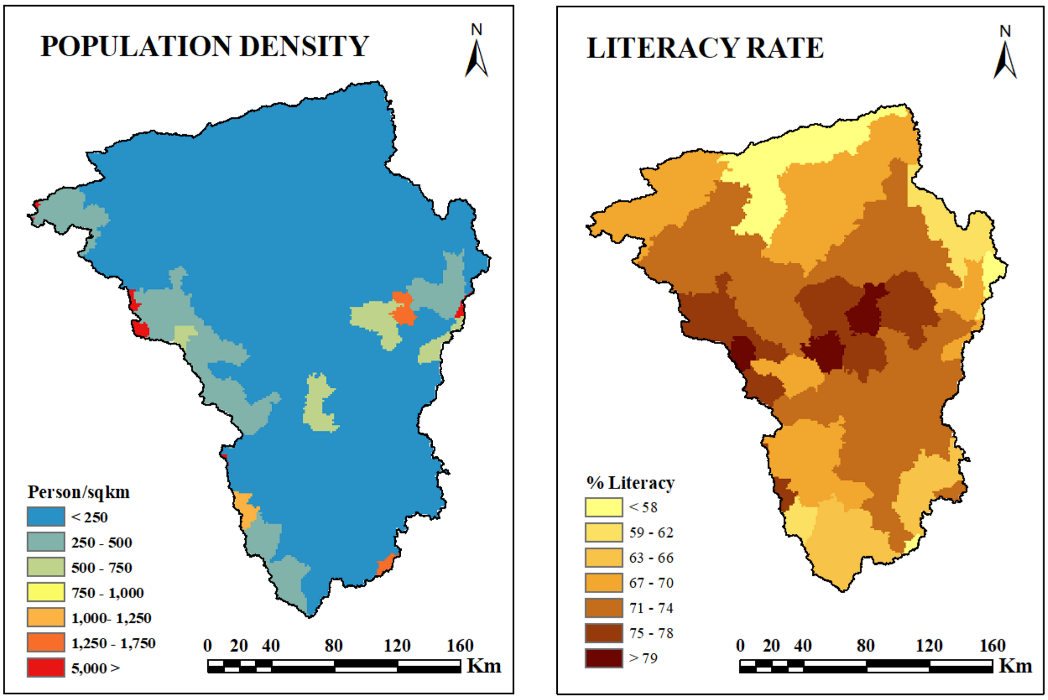

Fig. 4. 4 Demographic drivers of change including Population Density and Literacy Rate maps

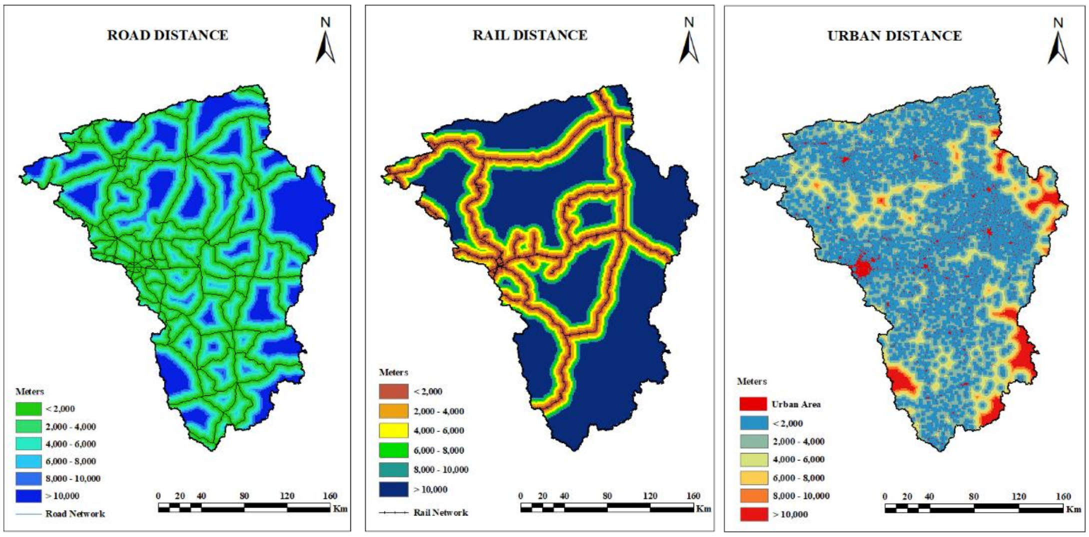

Fig. 4. 5 Infrastructural Drivers of change including distance maps of Road, Rail and Urban areas.

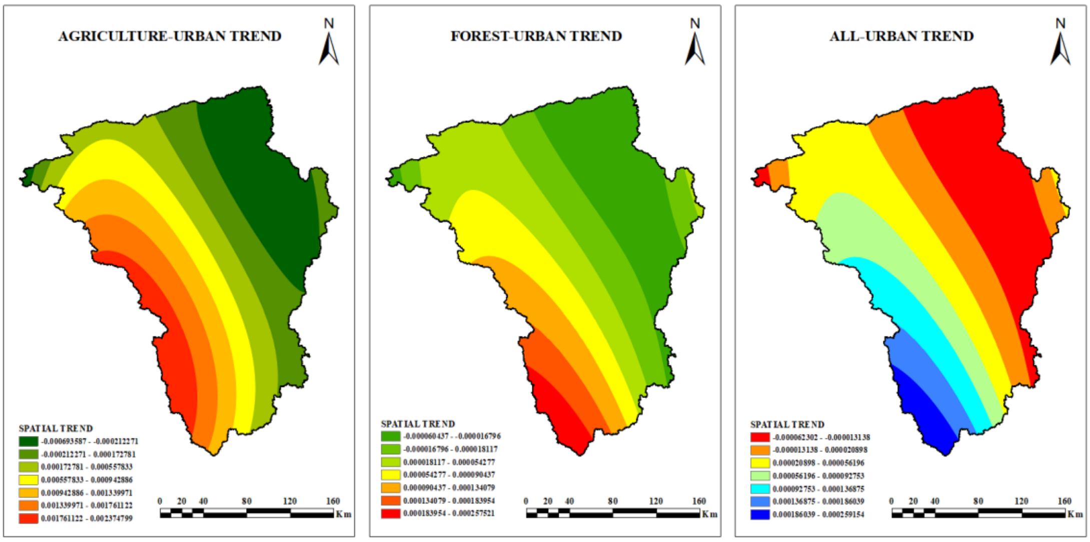

Fig. 4. 6 Spatial Trend Maps of Land use Transition.

4.3.1 Assessment of Predicting Potential of Drivers

The selection of drivers of changes or explanatory variable is a critical and peculiar task to be performed for land-use modeling. The land-use change model adopts a test procedure based on a contingency matrix analysis with a quantitative measure of the association named Cramer's *V* for this purpose, which is an asymmetrical measure of the relationship between two discrete variables, giving a value between 0 and +1 (inclusive). It is based on Pearson's chi-squared statistic and was published by Harald Cramér (1946).

Let a sample of size n of the simultaneously distributed variables A and B for i=1,2,3,…r and j=1,2,3,…k be given by the frequencies

n_{ij} = number of times the values were observed.

The chi-squared statistic then is:

$$X^2 = \sum_{i,j} \frac{\left(n_{ij} - \frac{n_i n_j}{n}\right)^2}{\frac{n_i n_j}{n}} \qquad \ldots (4.1)$$

Cramér's V is computed by taking the square root of the chi-squared statistic divided by the sample size and the minimum dimension minus 1:

$$V = \sqrt{\frac{X^2/n}{\min(k-1, r-1)}} \qquad \ldots (4.2)$$

Where, X^2 = Derived from Pearson's chi-squared test

n = total numbers of observations

k = No. of column

r = No. of rows

This analysis used to test whether a driver of change explained a particular land-use class transition or not. A high value of Cramer's *V* indicates that the potential explanatory value or predicting power of the driver is good in general but does not assurance a resilient performance since it cannot explain for the mathematics of the model used and the intricacy among the drivers and land-use. The value of Cramer's *V* rages from 0-1. Any value of Cramer's *V* greater than 0.15 were considered to be useful, and 0.4 and higher are good (Eastman 2012b). In this study, initially, 14 drivers were considered, and 12 drivers with Cramer's *V* value greater than 0.15 were selected for model development.

4.3.2 Multi-Layer Perceptron Neural Network Model

In this study, the classical model of feed-forward backpropagation neural network MLP-NN was used for transition potential map generation. It is the most robust method for the transition potential modeling of land-use changes. These prediction models provide the temporal and spatial changes in the land-uses over a region of interest. A multi-layer perceptron neural network (MLP-NN) transition sub-model was used, where the actual modeling of the transition of land-use classes accorded. The schematic diagram of the MLP-NN is shown in Fig. 4.7. It is a three-layer structure: including one input layer, one output layer and one hidden layer. Input layer contains thirteen nodes corresponding to thirteen drivers of changes of various categories and output layer contains six nodes corresponding to six land-use classes. For this modeling approach, 2725 numbers of pixels per land-use classes were used for training and the same number for testing. As a total of 5450 pixels had undergone the transitions from 2000 to 2005. A network of artificial neurons among the drivers of changes and the land-use classes. Initially, the MLP-NN model randomly assigns some weights to the drivers and these were adjusted during each iteration to achieve an accurate result in terms of stopping criteria of RMS, and machine learning accuracy rate set as model parameters.

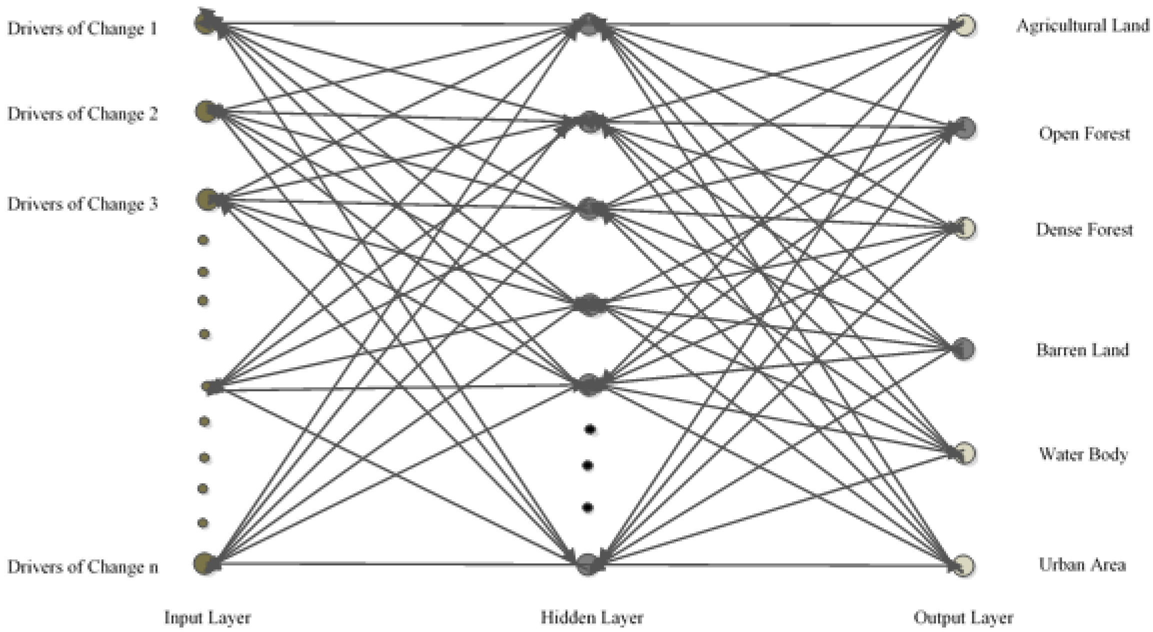

Fig. 4. 7 The structure of MLP neural network

The MLP-NN model was applied under self-learning mode, wherein the model makes its own decisions about the parameters utilisation and automatic updating them in order to achieve a greater model efficiency. During the simulation, the model also keeps on changing the start and end learning rate with the dynamic learning process. It starts with an initial learning rate and reduces it gradually over the iterations until the end learning rate is reached when the maximum number of iterations is reached. If major fluctuations in the RMS error are found after the first 100 iterations, the learning rates are reduced by half, and the procedure is started again. Since specific transitions were modeled, the model crops out of the transition potentials all cases that do not match the case of any other specific transition. For example, if the transition from agriculture to urban is being modeled, values will only change in pixels that were agriculture.

Separate transition potential maps were generated for each of the land-use class transition modeled through the MLP-NN after successful completion of the model. The automatic training and dynamic learning with the capability to model multiple transitions at one time make MLP-NN modeling technique most time-productive and dynamic (Eastman et al., 2012).

4.3.3 Markov Model

The theory of Markov chain analysis model is based on dynamic change prediction process. The model includes the formation of Markov random process for the prediction and optimum control theory method. In a Markovian process, the condition of a system can be predicted by knowing its previous condition and the probability of transition from each condition to each other condition. The Markov model provides details about the quantification of conversion conditions between the different land-use classes. It also conveys the rate of transitions among those classes. Using the earlier and later land-use conditions with identified time frames, Markov model finds out precisely how many pixels of a certain class would be likely to go under transition based on a prognosis of the transition potentials into the future. It does not perform a simple linear extrapolation since the transition potentials change over time are non-linear in nature. Based on the conditional probability formula (Bayes theorem), the forecast of changing land-use can be projected by the following equation (Sang et al. 2011, Waseem et al. 2015, Pandey and Khare 2017):

$$S(t+1) = P_{ij} \times S(t) \qquad \dots (4.3)$$

where S(t), S(t+1) are the status of the system at the time t and (t+1); P_{ij} is the transition probability matrix in a state, which is calculated by equation 4.4.

$$P_{ij} = \begin{bmatrix} P_{11} & P_{12} & \cdots & P_{1n} \\ P_{21} & P_{22} & \cdots & P_{2n} \\ \vdots & \vdots & \vdots & \vdots \\ P_{n1} & P_{n2} & \cdots & P_{nn} \end{bmatrix} \qquad \dots (4.4)$$

$$(0 \le P_{ij} < 1) \text{ and } \sum_{j=1}^{N} P_{ij} = 1, (i.j = 1,2,3,\dots,n)$$

The methodology adopted for modeling of land-use using MLP-NN-Markov model is shown in Fig. 4.8.

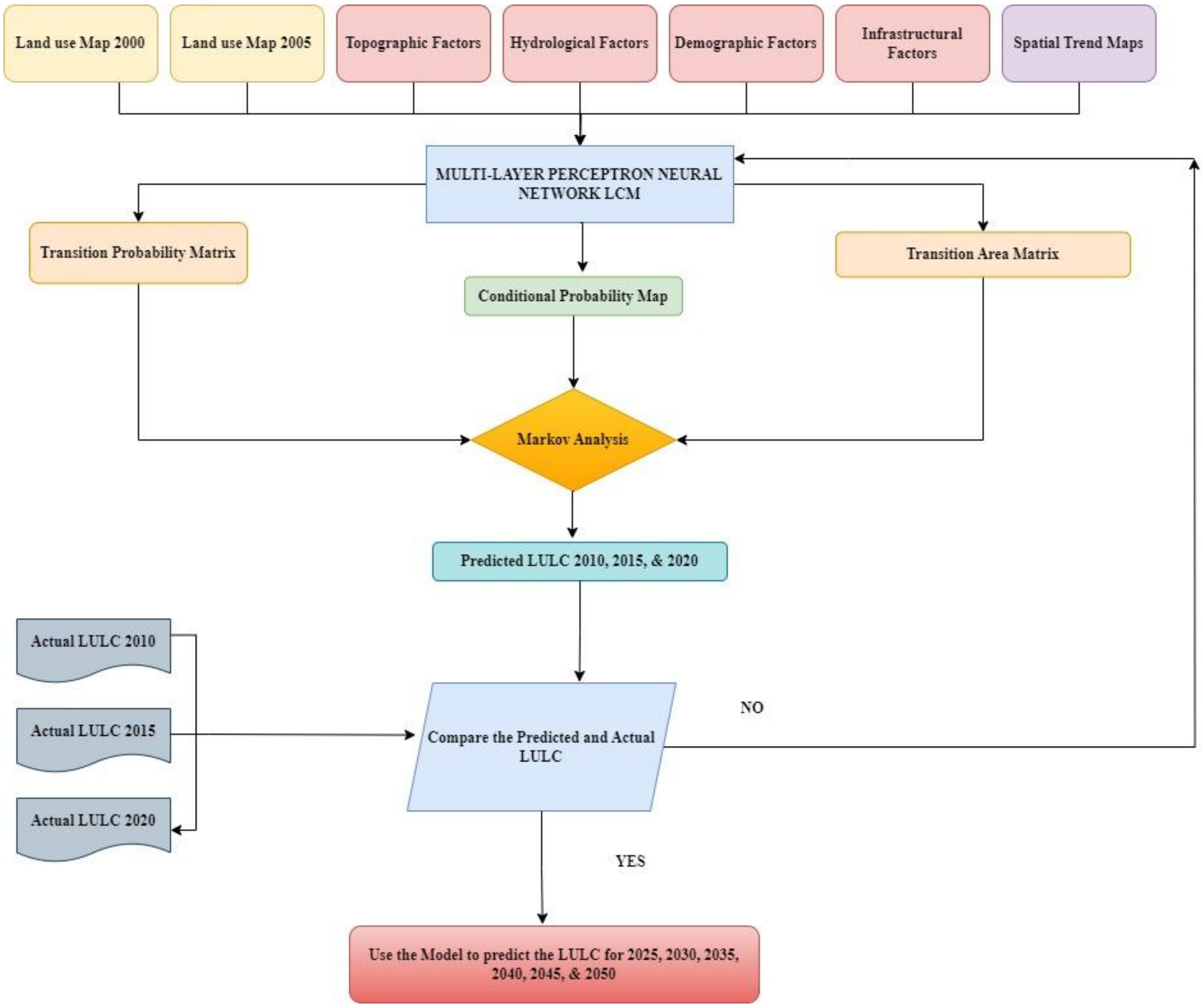

Fig. 4. 8 Flow chart of the methodology adopted for the prediction of LULC

4.3.4 Projection of Future Land-uses

In this study, transition probability matrices were developed using land-use maps for the year 2000 and 2005 and using the MLP-NN land-use change model. These matrices used in the Markov chain to simulate the land-use map of 2010 and 2015 and simulation results then compared with the actual land-use map of 2010 and 2015. After achieving the acceptable level of simulation accuracy, finally, land-use maps for 2030, 2060 and 2090 were produced based on the MLP-NN-Markov model. The overall methodology has already presented in Fig. 4.8.

4.4 RESULTS AND DISCUSSION

4.4.1 Land-use Change

The LULC maps for the years 2000, 2005, 2010, 2015, and 2020 are derived from the global land cover inventor, and they are classified into five classes (waterbodies, forest, agriculture, built-up and barren land). Description of these classes is already given in Table 4.1.

. In the Wainganga basin agriculture and forest area are dominating land use classes with 65% and 33% respectively to the total geographical area. The changes that occurred in LULC classes were analysed during the years 2000, 2005, 2010, 2015, and 2020. There has been a significant change in LULC classes especially for built-up agriculture, forests, and waterbodies over the years. In 2000 built-up was covered with an area of 161.36 km², which gradually increased to 228.51 km² in 2005, 264.30 km² in 2010, 319.28 km² in 2015, and 337.64 km² in 2020. The agriculture land covered an area of 33,668.07 km ² in 2000 with 65.31% which is gradually decreasing in 2020 with an area cover of 33,113.70 km² in 2020 with 64.24%. The forest land covered an area of 17,289.97 km² in 2000, which is gradually increasing to 17,499.90km² in 2020. During 2000 the forest land with 33.54% which grew with 33.56% in 2005, 33.60% in 2010, 33.5% in 2015, and 33.95% in 2020. Waterbodies which covered an area of 393.19 km² in 2000 and increased to 558.03km² in 2020. During 2000 the waterbodies were 0.76% which grew with 0.78% in 2005, 0.96 % in 2015, and 1.08% in 2020. Barren land is constant in the 20 years of changes. The changes in LULC are shown in Table 4.3. The increase in the built-up area indicates that some anthropogenic activities are increasing in the Wainganga basin. Furthermore, the LULC map of the years 2000, 2005, 2010, 2015, and 2020 shows that, there is a growth in settlement areas due to an increase in population growth and also it is one of the reasons for the decrease in the agriculture area.

Table 4. 3 Land-use classes and respective areas in the WRB over the years

Class Name	2000		2005		2010		2015		2020	
	Area (Km²)	Area (%)	Area (Km²)	Area (%)	Area (Km²)	Area (%)	Area (Km²)	Area (%)	Area (Km²)	Area (%)
Waterbodies	393.19	0.76	401.23	0.78	402.19	0.78	495.04	0.96	558.03	1.08
Forest	17289.97	33.54	17300.32	33.56	17317.40	33.60	17303.00	33.57	17499.90	33.95
Agriculture	33668.07	65.31	33582.31	65.15	33527.40	65.04	33394.20	64.78	33113.70	64.24
Built-up	161.36	0.31	228.51	0.44	264.30	0.51	319.28	0.62	337.64	0.66
Barrenland	34.75	0.07	34.98	0.07	36.12	0.07	35.87	0.07	38.04	0.07

Figure 4.1 and Table 4.3 reflect the areal extent and volume changes in land-use from 2000 to 2020. On comparison of changes in various LULC classes, the most apparent trend of expansion of urban area mainly at the cost of agriculture and barren lands can be noticed.

4.4.2 Accuracy Assessment

Numerous factors are acting on the earth system can lead to changes in the LULC. These can be either natural or anthropogenic. Among the anthropogenic factors, the human population and its growth rate are the most critical ones. In addition to these human factors, the natural factors also contribute toward the changes in LULC. Besides the topography, the climate is the most impactful and dynamic factor affecting LULC, over a period of time. It can be perceived that the growing population raises the demand potentials, and the climatic factors affect the supply potentials of the land resources. Various drivers of land-use changes have been considered and used as inputs to simulate the land-use maps for 2010, 2015 and 2020. The accuracy assessment of the study is simulated for the years 2010, 2015, and 2020 were performed with an error matrix. A total of 5006 random sample points were used for the accuracy assessment shown in Table 4.4, which are represented with user, producer, and overall kappa statistic accuracy. The overall accuracy for the year 2010 was evaluated at 99.42%, 2015 at 99.02%, and 2020 at 97.64% respectively. The kappa statistics for the classified images of 2010, 2015, and 2020 are 0.99%, 0.98%, and 0.95% respectively.

Table 4. 4 Error Matrix for the years 2020, 2015, and 2010

2020	Waterbodies	Forest	Agriculture	Built-up	Barren land	Total(User)
Waterbodies	52	0	2	0	0	54
Forest	0	1670	22	0	5	1697
Agriculture	3	36	3133	4	36	3212
Built-up	1	0	9	23	0	33
Barrenland	0	0	0	0	10	10
Total(Producer)	56	1706	3166	27	51	5006
User Accuracy	Waterbodies	Forest	Agriculture	Built-up	Barren land	
	96.30	98.41	97.54	69.70	100.00	
ProducerAccuracy	Waterbodies	Forest	Agriculture	Built-up	Barren land	
	92.86	97.89	98.96	85.19	19.61	
Overall Accuracy	97.64					
Kappa Coefficient	95.07	0.95				

2015	Waterbodies	Forest	Agriculture	Built-up	Barren land	Total(User)
Waterbodies	48	0	0	0	0	48
Forest	0	1668	10	0	0	1678
Agriculture	1	20	3205	2	11	3239
Built-up	0	0	5	26	0	31
Barrenland	0	0	0	0	10	10
Total(Producer)	49	1688	3220	28	21	5006
User Accuracy	Waterbodies	Forest	Agriculture	Built-up	Barren land	
	100.00	99.40	98.95	83.87	100.00	
ProducerAccuracy	Waterbodies	Forest	Agriculture	Built-up	Barren land	
	97.96	98.82	99.53	92.86	47.62	
Overall Accuracy	99.02					
Kappa Coefficient	97.92	0.98				

2010	Waterbodies	Forest	Agriculture	Built-up	Barren land	Total(User)
Waterbodies	32	3	3	0	0	38
Forest	1	1667	11	0	1	1680
Agriculture	0	3	3247	1	1	3252
Built-up	0	0	4	22	0	26
Barrenland	0	1	0	0	9	10
Total(Producer)	33	1674	3265	23	11	5006
User Accuracy	Waterbodies	Forest	Agriculture	Built-up	Barren land	
	84.21	99.23	99.85	84.62	90	
ProducerAccuracy	Waterbodies	Forest	Agriculture	Built-up	Barren land	
	96.97	99.58	99.45	95.65	81.82	
Overall Accuracy	99.42					
Kappa Coefficient	98.75	0.99				

4.4.3 Simulation of Land-use Maps and Their Validation

The MLP-NN-based land-use image change learning and processing were used to simulate the land-use of the year 2010, 2015 and 2020 for model calibration and validation. Firstly, the land-use transition potential maps were generated based on the transition probabilities for these changes, and then the land-use maps were simulated using Markov chain analysis. Transition probabilities matrix of land-use classes in the WRB during 2010, 2015 and 2020 are represented in Table 4.5. It can be seen that the barren land, open forest and the agricultural land have the highest probability to get converted into urban settlements for both the year cases. The probabilities become much higher in the case of the year 2015 then the case of the year 2010. Land-use pattern changes in the year 2010 and 2015 were predicted using an MLPNN–Markov model based on the year 2000 as an initial state and the year 2005 as final. (time interval of 10 years).

The model-simulated land-use maps for the year 2010 and 2015 were compared with the actual classified land-use of respective years. Fig. 4.9 shows the simulated land-use maps of the year 2010, 2015 and 2020 and Table 4.6 represents the area cover under different land-use classes for these two cases.

Table 4. 5 Transition probabilities matrix of land-use types in the WRB during 2000–2020

2010					
Class Name	Waterbodies	Forest	Agriculture	Built-up	Barren land
Waterbodies	0.9947	0.0010	0.0041	0.0002	0.0000
Forest	0.0001	0.9989	0.0007	0.0001	0.0001
Agriculture	0.0001	0.0006	0.9973	0.0020	0.0000
Built-up	0.0001	0.0001	0.0128	0.9871	0.0000
Barrenland	0.0000	0.0344	0.0002	0.0000	0.9654
2015					
Class Name	Waterbodies	Forest	Agriculture	Built-up	Barren land
Waterbodies	0.9985	0.0004	0.0004	0.0006	0.0000
Forest	0.0000	0.9992	0.0006	0.0001	0.0000
Agriculture	0.0003	0.0007	0.9977	0.0012	0.0000
Built-up	0.0001	0.0002	0.016	0.9837	0.0000
Barrenland	0.0000	0.0159	0.0004	0.0000	0.9837
2020					
Class Name	Waterbodies	Forest	Agriculture	Built-up	Barren land
Waterbodies	0.9976	0.0012	0.0009	0.0003	0.0000
Forest	0.0004	0.9982	0.0008	0.0001	0.0005
Agriculture	0.0017	0.0003	0.9964	0.0016	0.0000
Built-up	0.0001	0.0001	0.0131	0.9867	0.0000
Barrenland	0.0118	0.0072	0.0007	0.0000	0.9802

Table 4.6 Comparison of areal statistics of actual and simulated land-use of the year 2010, 2015 and 2020

Class Name	LULC 2010			LULC 2015			LULC 2020		
	Actual Area Km²	Predicted Area Km²	Prediction Accuracy (%)	Actual Area Km²	Predicted Area Km²	Prediction Accuracy (%)	Actual Area Km²	Predicted Area Km²	Prediction Accuracy (%)
Waterbodies	402.19	401.23	99.76	495.04	402.19	81.24	558.03	495.036	88.71
Forest	17317.40	17299.6	99.90	17303.00	17316.00	99.92	17499.90	17302.9	98.87
Agriculture	33527.40	33553.4	99.92	33394.20	33521.90	99.62	33113.70	33394.2	99.15
Built-up	264.30	258.11	97.66	319.28	271.16	84.93	337.64	319.363	94.59
Barrenland	36.12	34.9776	96.83	35.87	36.12	99.31	38.04	35.874	94.31

It can be concluded from the table that the MLP-NN model had simulated the land-use maps with the good agreement to actual land-use maps for the year 2010, 2015 and 2020. The prediction accuracy based on the absolute error difference of the respective land class was also estimated and found that for most of the classes, it is very high. It may be due to that fact that the changes are not very big in the dominative land-use classes. The maximum accuracy was recorded with water for the year 2010 simulation followed by agriculture and forest simulation. the least accuracy at the order of 81.24% was associated with the waterbodies simulation for the year 2015.

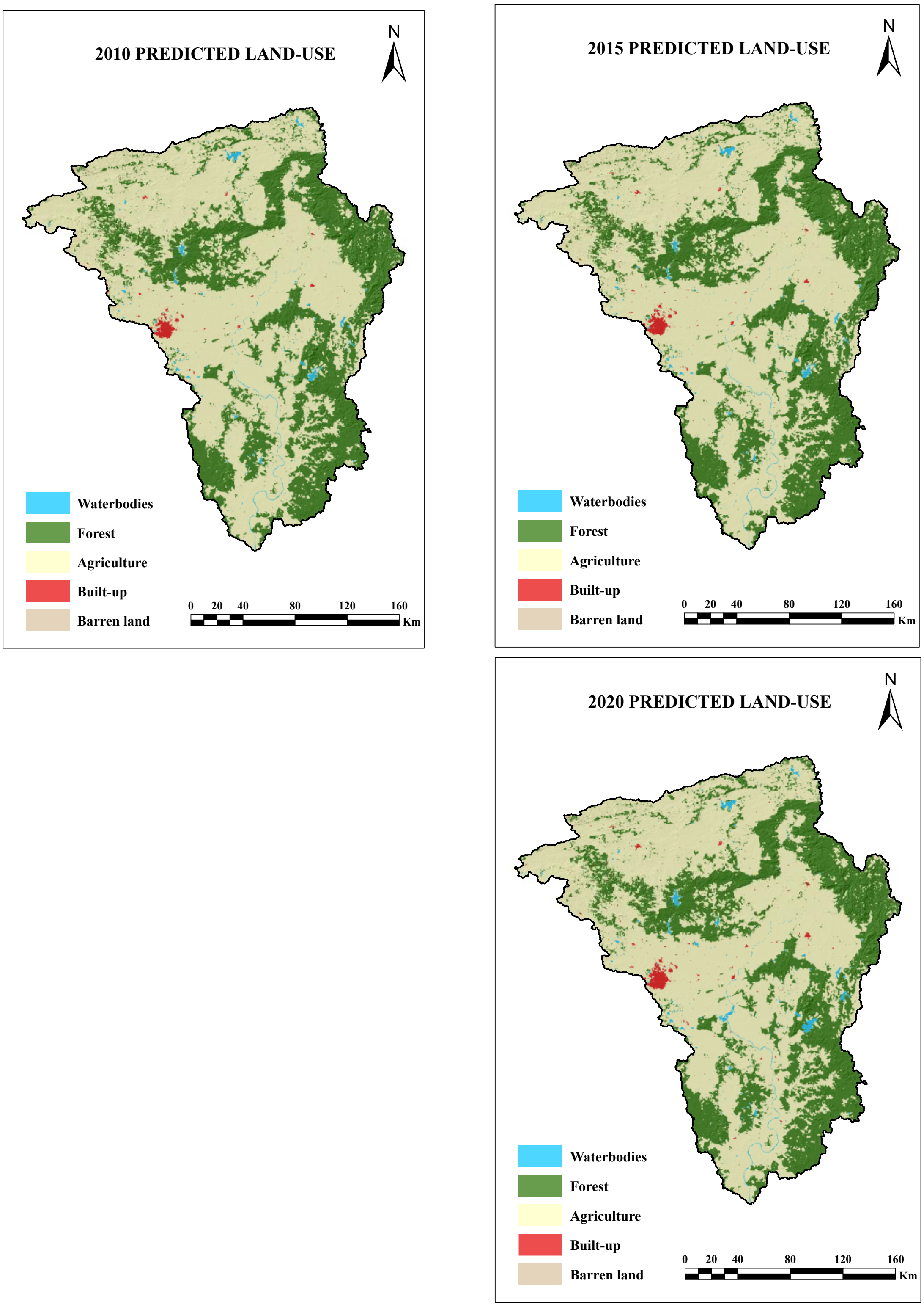

Fig. 4. 9 Simulated Land-use maps of WRB for the year 2010 and 2015.

4.4.4 Projection of Future Land-use

By using the MLPNN-Markov model, the future land-use map is created for the years 2025, 2030, 2035, 2040, 2045, and 2050. The built-up area is expanding in the Nagpur city of the study area, and some of the expansion is witnessed with urban clusters in parts of the basin. The future land use map is shown in Fig. 4.10 and Fig. 4.11, respectively. Table 4.6 indicates that the gradual increase in built-up and agricultural land will decrease by 64.19% in 2050. Similarly, the forest area will decrease by 33.88% in 2050. The model prediction indicates the future conversion of waterbodies, forests, agriculture, built-up, and barren land. Table 4.7 shows a growth in urban areas, still more than 65% of the area is covered by agriculture. This shows that the agriculture area is the future dominant activity in the Wainganga basin.

From Table 4.6, it can be seen that the basin is likely to witness exceptional changes in the urban land at the order of 18.52% by the mid (2050) of 21st century. The agricultural and forest land is reducing significantly. These lands nearby to settlements will be likely to be converted into the urban area. Model predicted a reduction in the agricultural land-use type by the early and mid of 21st century respectively. The model prediction indicates the conversion of barren, open forest and agricultural land into the urban land in future.

It can be concluded from Table 4.7 that even though there is exponential growth in urban areas, still more than 64% of the total basin area is likely to belong to the agricultural alone. This emphasis the presence and future dominance of agriculture activities in the basin.

The projected potential distribution of the land-use classes for the future indicates that the land-use changes experienced by the study basin in the recent past decades are likely to be continued with exceptional growth in the urban area. WRB is likely to witness exceptional urban growth of the order of 18.52%, towards the mid of 21st century. The agricultural land-use class will be expected to remain the dominating class in future periods. It is likely to have more than 64% of the total basin area. Area of the dense forest and water bodies are likely to almost static. The MLP-NN land-use model-simulated and predicted the land-uses for future periods with good accuracy. The ever-growing population is the reason for rapid urbanization in the future. The study provides the early and mid of the 21st century land-use projection which can be used for long-term planning and management of the land resources in the WRB.

Table 4. 6 Comparison of the areal statistics of predicted land-use maps for the future years to the actual land-use map of 2020

Class Name	Actual 2020	Predicted 2025	% Change	Predicted 2030	% Change	Predicted 2035	% Change	Predicted 2040	% Change	Predicted 2045	% Change	Predicted 2050	% Change
Waterbodies	558.03	558.029	0.0	558.029	0.0	558.029	0.0	558.029	0.0	558.029	0.0	558.029	0.0
Forest	17499.90	17496.3	0.0	17488.8	-0.1	17483.3	-0.1	17477.1	-0.1	17470.6	-0.2	17463.7	-0.2
Agriculture	33113.70	33104.2	0.0	33103	0.0	33102.8	0.0	33102.6	0.0	33100.5	0.0	33087.4	-0.1
Built-up	337.64	350.824	3.9	359.456	6.5	365.1	8.1	371.626	10.1	380.229	12.6	400.157	18.5
Barrenland	38.04	38.0385	0.0	38.0385	0.0	38.0385	0.0	38.0385	0.0	38.0385	0.0	38.0385	0.0

Table 4. 7 Land-use classes and respective areas in the WRB for the future years

Class Name	2025		2030		2035		2040		2045		2050	
	Area (Km²)	Area (%)	Area (Km²)	Area (%)	Area (Km²)	Area (%)	Area (Km²)	Area (%)	Area (Km²)	Area (%)	Area (Km²)	Area (%)
Waterbodies	558.03	1.08	558.03	1.08	558.03	1.08	558.03	1.08	558.03	1.08	558.03	1.08
Forest	17496.30	33.94	17488.80	33.93	17483.30	33.92	17477.10	33.90	17470.60	33.89	17463.70	33.88
Agriculture	33104.20	64.22	33103.00	64.22	33102.80	64.22	33102.60	64.22	33100.50	64.21	33087.40	64.19
Built-up	350.82	0.68	359.46	0.70	365.10	0.71	371.63	0.72	380.23	0.74	400.16	0.78
Barrenland	38.04	0.07	38.04	0.07	38.04	0.07	38.04	0.07	38.04	0.07	38.04	0.07

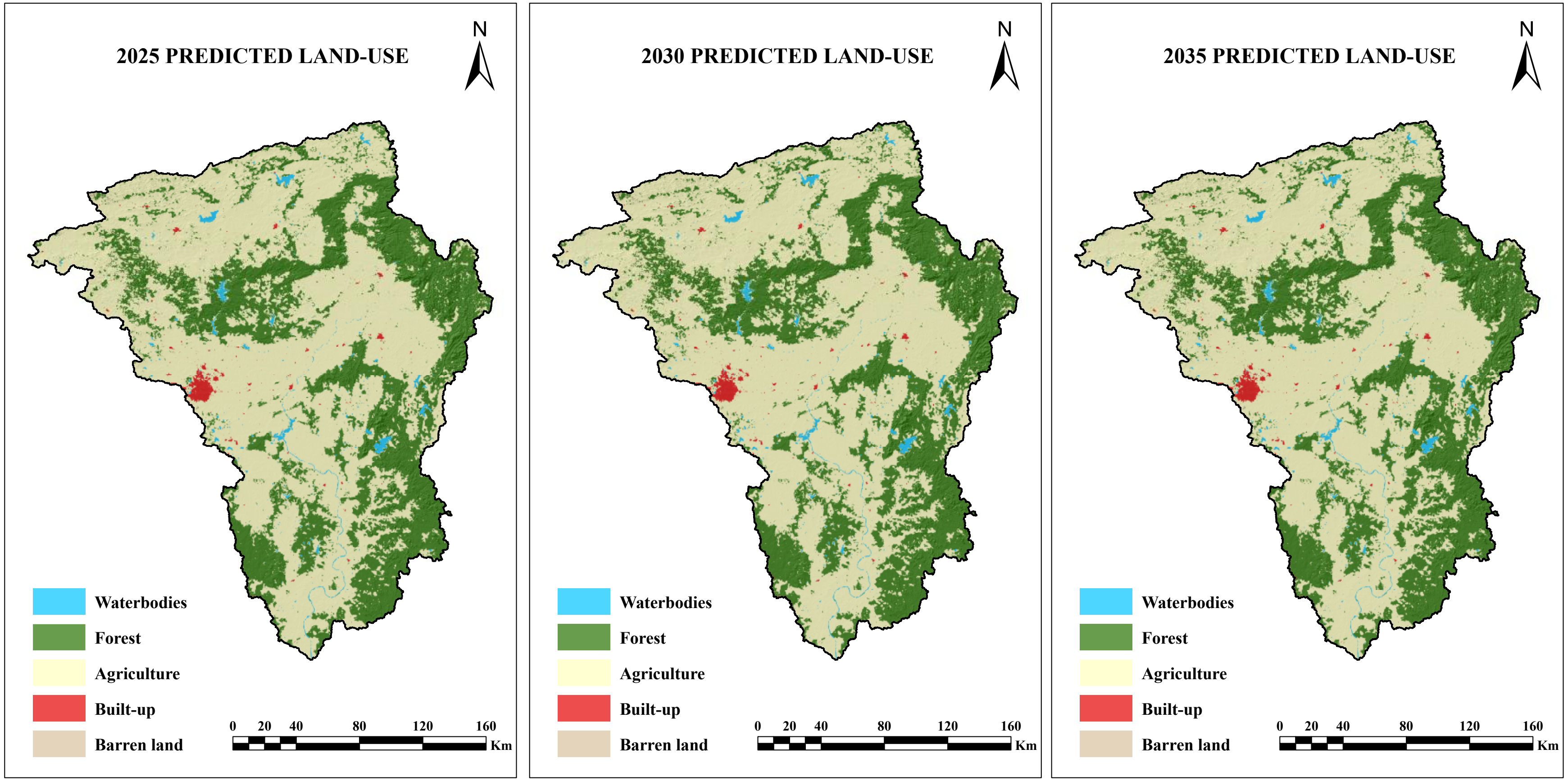

Fig. 4. 10 Projected Land-use map of the year 2025, 2030, and 2035 for WRB

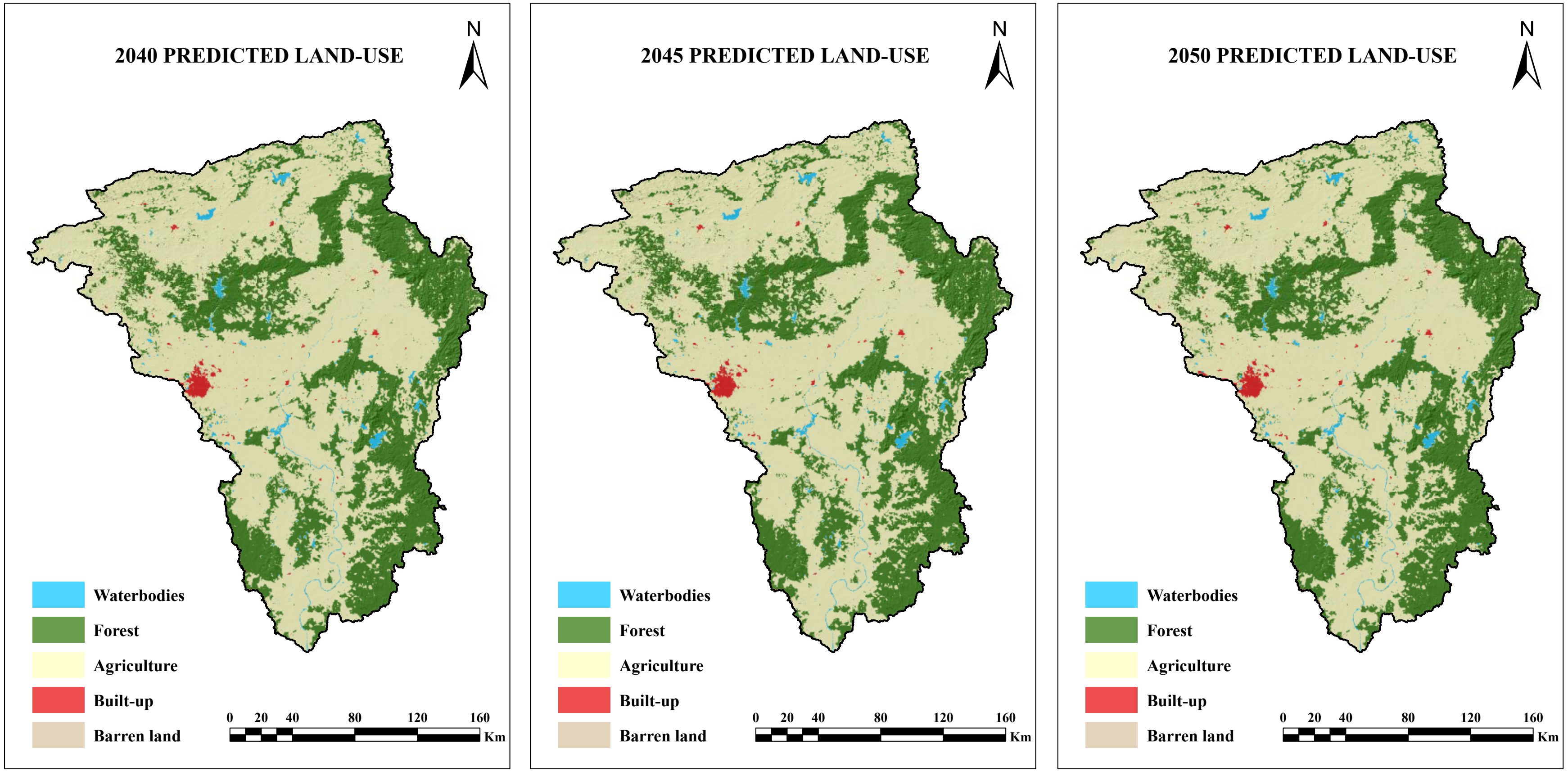

Fig. 4. 11 Projected Land-use map of the year 2040, 2045 and 2050 for WRB

CHAPTER 05: HYDROLOGICAL RESPONSE UNDER THE CHANGING CLIMATE AND LAND-USE

5.1 GENERAL

Water is the most vulnerable sector in view of the changing climate and physical landscape changes. The potential impacts of these changes must be considered while planning any developmental project pertaining to water resources. Variability in air temperature and precipitation caused by the enhanced accumulation of GHG gases in the atmosphere are the primary attributes of climate change. These variations will lead the intensification of the water cycle and result in water-related disasters such as short duration high magnitude flooding and long dry spell leading to drought conditions (Reshmidevi et al. 2018).

Many investigators have studied the impacts of climate change on hydrology (Sharma and Shakya 2006, Jean-Pierre et al. 2010, Basheer et al. 2016, Mall 2016, Jaiswal et al. 2017, Lu et al. 2017). These assessments are very important for the developing and high populated counties like India, which are exposed to severe threats of changing climate on water and agriculture sectors.

Changes in the patterns of land-use, i.e. urban growth, deforestation, land-use conversion etc. result in changes in the various pedological parameters such as infiltration capacity of soil strata, surface runoff, baseflow regime, evapotranspiration, etc., which can lead the alteration in hydrologic cycle (Sharma and Shakya 2006, Islam et al. 2012, Kim et al. 2013b)

Global circulation models (GCMs) are the most commonly used tools that provide the various climatic variables for the future. GCMs are the complicated models governed by mathematical equations based on the different atmospheric, oceanic and land surface physical processes. The spatial scale of output of CGMs are usually coarse and cannot be used directly by the hydrological models. Therefore, the GCM output projections need to be downscaled to capture and represent the catchment level heterogeneity (Tripathi et al. 2006, Chen et al. 2011, Meena et al. 2016). As the GCMs consider the global scale calculation, the downscaled variable is obsessed with some bias as compared to locally observed data. Therefore, the bias-corrections techniques are also applied to the downscaled variable before using them as input for the hydrological model (Teutschbein and Seibert 2012, Sharma and Babel 2013). The fifth version of assessment report

(AR5) of world apex climate body, the Inter-governmental Panel on Climate Change (IPCC), includes novel emission scenarios termed as representative concentration pathways (RCPs), which are the set of GHGs emission designed to support policy research on the impacts of climate change (Visconti et al. 2016). RCPs were then followed by the AR6 of IPCC in 2023.

A few of the studies carried out to examine the collective and specific effects of varying climatic and land-use patterns on the river hydrology (Tong et al. 2012, Kim et al. 2013b, Morán-Tejeda et al. 2015, Stigter et al. 2017). These studies indicated that the hydrological behaviour of rivers is more impacted by the variations in climate, then the land-use.

In impact assessment studies firstly the hydrological model calibration and validation is performed with the past data and then the same model is used for simulating the future hydrology with various future climate inputs to the model. Various sources of uncertainty are likely to be accumulated when the GCM data is being used. In order to take care of this large uncertainty introduced by the use of a single GCM model, multi-model ensemble approach has been used in recent studies. The output from the multi-model ensemble reported being more reliable compared to individual models (Nóbrega et al. 2011).

With the said background, hydrological responses of Wainganga River basin have been assessed under the changing climate and LULC scenarios using climate projections from five different CGMs. A semi-distributed and Soil Conservation Service Curve Number (SCS-CN) method based hydrological model (SWAT) was used for simulating the streamflow for different GCM inputs. Future LULC maps were predicted by a land-use change model and applied for flow simulations. In this study, ArcGIS graphical user interface (GUI) of SWAT, i.e. ArcSWAT, was used.

Four bias-corrected and statistically downscaled, Coupled Model Inter-comparison Project Phase Six (CMIP6) GCM dataset for two SSP scenarios, viz. SSP2 4.5 and SSP5 8.5 were used. The study covers the potential impacts of climate and land-use changes on the hydrology of the WRB. The significant work contributions of this study presented in this chapter are as follows:

a. Calibration, validation and application of the SWAT model for simulating the streamflow under various scenarios
b. Quantification of the impacts of varied climatic and land-use conditions on the streamflow
c. Assessment of the water availability in the near, mid and far future in the basin.

5.2 DATA USED

The largest and northernmost tributary of River Godawari, the Wainganga River is said to be the lifeline of central India. It mainly drains the fertile plains of Maharashtra and mountainous terrain of southern MP State. Majority of the terrain of the basin is featureless with few highlands in the northern and eastern ridge of the basin. The water availability in the basin chiefly depends on monsoon rainfall, which is about 80% of total annual rainfall. Hydrological modeling of WRB was done using a physically-based semi-distributed SWAT model. Various spatial and time-series data have been used in this study. The setting up the SWAT model mainly requires a DEM, thematic map for soil with its characteristics and LULC map for the basin and sub-basin delineation and creation of Hydrologic Responses Units (HRUs). The climate time series data needed by the model to simulate the streamflow at defined outlets.

5.2.1 Digital Elevation Map

The elevation or topographic information is the primary data used for studying the elevation profile, slope, aspect and flow-accumulation and flow-direction of a basin. These analyses were done with a Digital Elevation Model (DEM). The Shuttle Radar Topography Mission (SRTM) DEM of 1 Arc sec spatial resolution acquired from United State Geological Survey (USGS) (https://earthexplorer.usgs.gov.in) and used for hydro-geo-processing. DEM processing is an essential part of the hydrological modelling using SWAT. It has been used to delineate the watershed boundaries and drainage network (Fig. 5.1).

5.2.2 Soil Data

For the assessment of the streamflow, groundwater dynamics, soil erosion, sedimentation, the characteristics of the native soil is needed to be known. The hydrological properties of soil primarily are influenced by the percentage of sand, silt, clay, rocks and organic matter presents in it. For the investigation, soil-related information and data were acquired from the National Bureau of Soil Survey and Land-use Planning (NBSSLUP), Nagpur. Digitised soil map of MP and Maharashtra was obtained at 1:50,000 scale and thematic map for the study area (Fig. 5.2) has prepared. The soils of the WRB are largely classified as sandy-loam and clay-loam, which mainly falls under the class ‘B’ and ‘C’ hydrological soil groups.

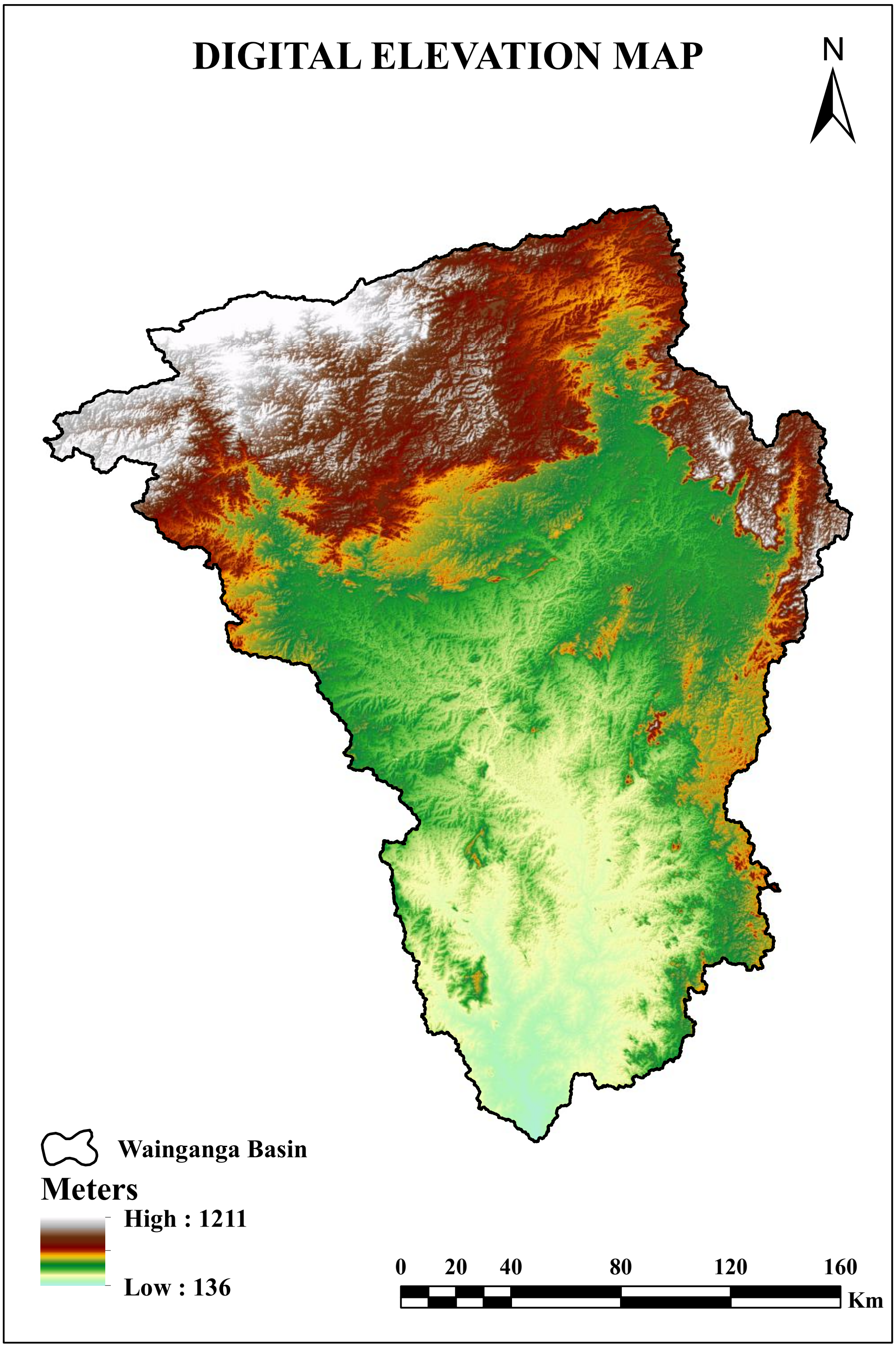

Fig. 5. 1 Digital Elevation Map of the WRB

5.2.3 LULC Map

The land-use and land-cover (LULC) information from the European Space Agency (ESA) has been used in this study. ESA provides LULC data for every year, starting from 1998 to 2018 under 21 distinct land-use classes at 300m of spatial resolution. LULC map for the year 2000 was considered for the calibration and validation of the hydrological model and LULC data of 2000, 2005, 2010 and 2015 were used to develop the land-use prediction model. Land-use map of the study basin for the year 2000, representing the baseline period can be seen in Fig. 5.3. Details about the prediction of LULC maps for the future periods are provided in chapter 4.

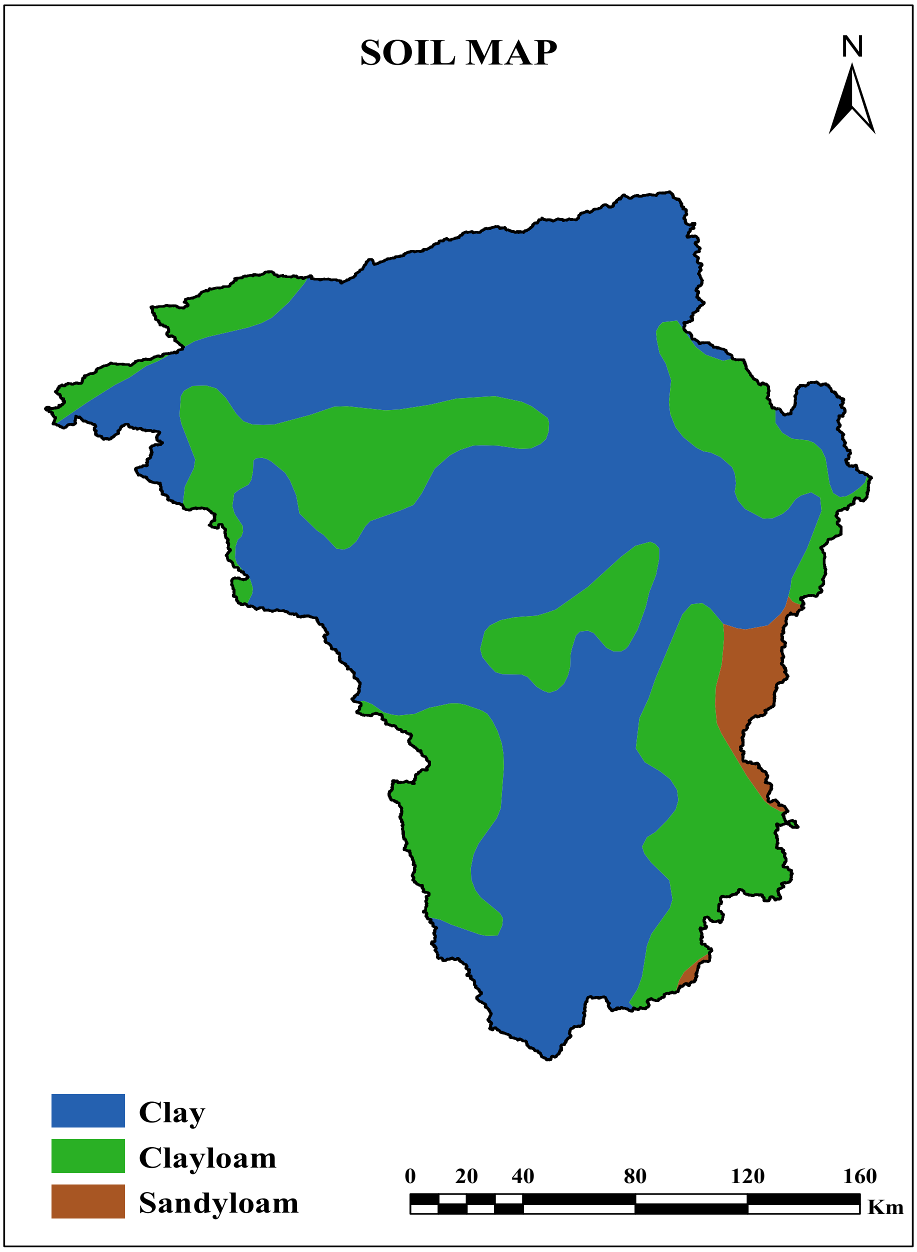

Fig. 5. 2 Soil Map of the Wainganga River basin

5.2.4 Hydro-meteorological Data

The average monthly streamflow time series at Ashti gauging site of Central Water Commission (CWC) was used for setting up the SWAT model. A total of 25 years (1980-2005) of discharge data has been acquired from India-WRIS project (http://indiawris.gov.in/wris/#/) used for the purpose. For hydrological simulation, SWAT model requires various meteorological variables, viz. rainfall, temperature (maximum and minimum), relative humidity, solar radiation, wind velocity at daily time steps. In order to cater for such a large basin, daily gridded rainfall data

(0.25^0 X 0.25^0) and temperature Data (re-gridded at 0.25^0 X 0.25^0) from the India Meteorological Department (IMD), Pune for 25 years (1980-2005) have been used. Remaining climatic parameters were estimated internally by SWAT weather generator.

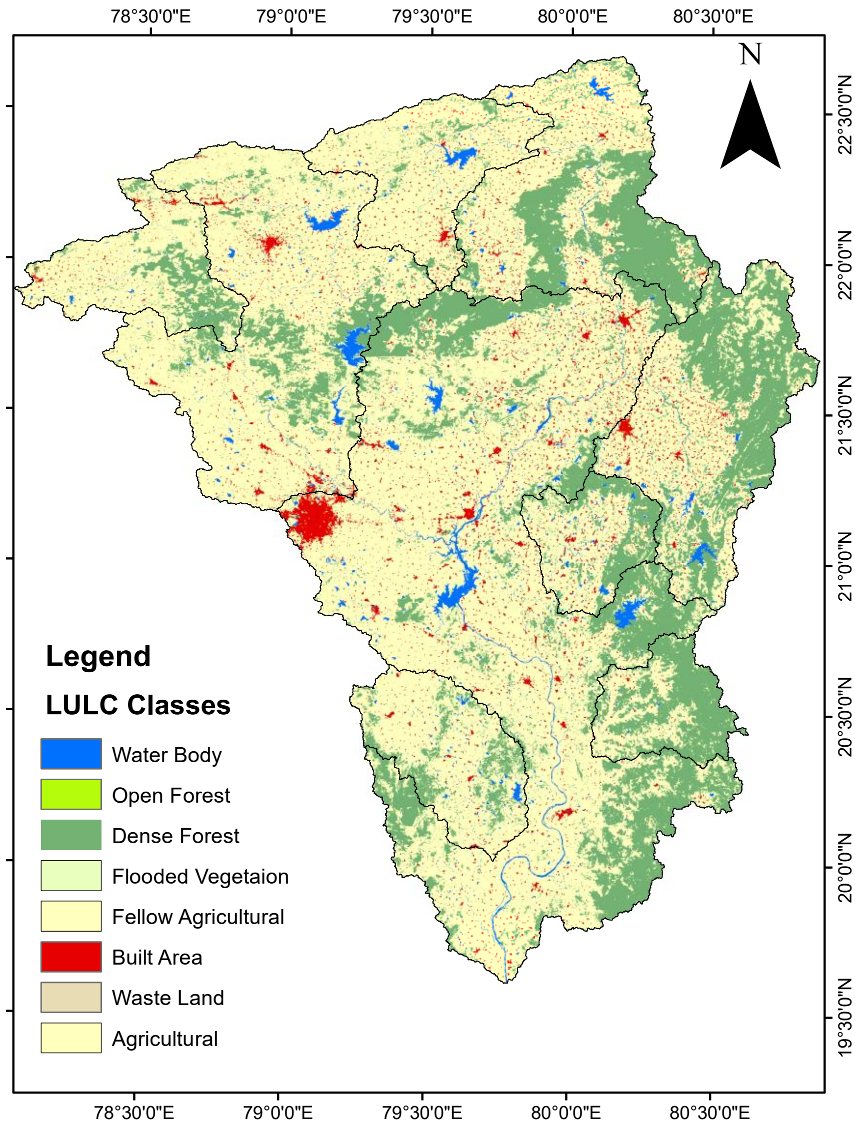

Fig. 5. 3 LULC map of the WRB of the Year 2000

CMIP6 climatic data were used for this study. CMIP6 is the sixth phase of the Coupled Model Intercomparison Project (CMIP) endorsed by the Working Group on Coupled Modelling (WGCM) of the World Climate Research Programme (WCRP). The details are provided in the Table 3.1 in chapter 3.

For this study, a period of 25 years (1980-2005) is designated as the baseline period. The impacts of climate change and land-use change were examined for three future periods, i.e. NFS: Near-Future Scenario (2025–2050), MFS: Mid-Future Scenario (2051–2075) and FFS: Far-Future Scenario (2076–2100). For each of the period impacts for both the SSP scenarios has been studied.

5.3 METHODOLOGY

5.3.1 LULC Simulation Model

A multi-layer perceptron neural network (MLP-NN) transition land-use model developed with actual land-use maps of the years from 2000-2015 of WRB and various drivers of change. The MLP-NN model performance in simulating the land-use distribution for the year 2010, 2015 and 2020 confirms the potential of this modeling approach for simulating the future land-use in the study area. After achieving the acceptable level of accuracy, the model has been used to predict the future land-use maps for the year 2030, 2040 and 2050 representing the projected potential distribution of the land-use classes in near, mid and far of 21st century respectively. The detailed methodology and various data used for simulating the future LULC maps have been discussed in Chapter 4.

5.3.2 Hydrological Simulation Model

The hydrological simulations were carried out using SWAT model for this research work SWAT was developed in collaboration of the United States Department of Agriculture, Agriculture Research Services (USDA-ARS) and Agriculture Experiment Station, Texas (Arnold et al. 1998).

Albeit, different rainfall-runoff models are available, choice of a reasonable model for a given watershed is most significant and challenging for proficient planning, management and the execution of watershed. Various models have been created by different analysts for precipitation based runoff simulation. However, the SWAT model outcomes are much superior to other hydrologic models (Devia et al. 2015).

The SWAT model has been applied in various local and regional scales of watersheds for assessment for present and projected management practices, for both water quantity and quality modeling, impact evaluation of changing global climate, modeling of flow under changing land-use practices, sediment yield and contamination assessment, analysis of extreme events, evaluation of point and non-point pollutant (Mango et al. 2011, Wilson and Weng 2011, Wang et al. 2014, Morán-Tejeda et al. 2015, Wu et al. 2015, Zhang et al. 2016b, Tan et al. 2017). The main purpose of SWAT development was to simulate the impacts of various land management practices on streamflows, sedimentation and chemical yields from agricultural areas with large complexity in terms of different soils, varying land covers and different agricultural management practices (Zahabiyoun et al. 2013, Sowmiya and Arul 2017, Khaniya et al. 2018). ArcSWAT, which is a graphical user interface (GUI) and sub-routine (module) of the SWAT model embedded in ArcGIS, is used in present research (Arnold et al. 2012).

The DEM, LULC map and soil map are the primary spatial inputs for SWAT model for the conceptualisation of Hydrological Responses Units (HRUs) within sub-catchments. First of all, the drainage network and catchment delineation are completed with the help of geo-processing of DEM data. Once the number of sub-catchments and other topographic processes completed HRU definition is the second task to be performed. Along with spatial input, temporal-climatic inputs such as precipitation, temperature, relative humidity, dew point temperature, wind velocity etc. are also needed for setting up the model. After a successful model run the monthly time series of simulated discharged was compared with observed discharge.

Irrespective of what kind of issue is being handled by the SWAT model, the water balance is the main impetus behind everything inside the watershed (Arnold et al. 1998). For precise evaluation of different phases of the hydrological cycle, water balance components are simulated by the model. The common equation for water balance utilised by the SWAT model is given beneath (Neitsch et al. 2011):

$$SW_t = SW_0 + \sum_{t-1}^{t}\left(R_{day} - Q_{surf} - ET_a - W_{seep} - Q_{gw}\right) \quad \dots (5.1)$$

Where, SW_t = Final water content of the soil (mm)

SW_0 = Initial water content (mm)

t = Time (day)

R_{day} = Precipitation (mm)

Q_{surf} = Surface runoff (mm)

ET_a = Evapotranspiration (mm)

W_{seep} = The water entering the vadose zone from the soil profile (mm)

Q_{gw} = Return flow (mm)

In SWAT, surface runoff sums can be evaluated either by utilising the SCS-CN or the Green and Ampt infiltration approach. In the present investigation, the SCS-CN based runoff generation technique has been utilised for the estimation of runoff. It is an exact model that estimates the rate of discharge under changing LULC and soil classes. The SCS-CN based runoff can be modeled as per the following formula (USDA 1972):

$$Q = \frac{(R-0.2s)}{R+0.8s}, \qquad R \geq 0.2s$$
$$Q = 0, \qquad R \leq 0.2s \qquad \ldots (5.2)$$

Where, Q is the daily runoff, mm; R is daily rainfall, mm, and s is a storage (retention) parameter, mm, which varies among sub-basin due to disparity in soil, land-use, management, and slope classes, and it varies with time also, due to of seasonal variation in volumetric water content of the soil. The retention parameter is associated with the SCS-CN by the following equation (USDA 1972).

$$s = 254\left(\frac{100}{CN} - 1\right) \qquad \ldots (5.3)$$

CN considered for the antecedent moisture content (AMC-II). In this study, the runoff curve number (AMC-II) values for the Indian condition were adopted by Narayana (1993).

The SWAT is a robust model, and apart from runoff, it provides all other water balance components by using various equations and algorithms. Like, the potential evapotranspiration (PET) can be calculated by any of the three available methods including Penman-Monteith (Monteith 1965); Hargreaves (Hargreaves and Samani 1985) and Priestley-Taylor (Priestley and Taylor 1972) depending on the data availability in the basin.

However, the Priestley-Taylor method requires solar radiation and air temperature data series as input, while the Hargreaves method requires air temperature data points only. In case of non-availability of the other meteorological data such as wind velocity, humidity, and radiation information, the Hargreaves method gives sensible outcomes by and large (Arnold et al. 1998, 2012). In the present research, the Hargreaves approach has been utilised for the estimation of evapotranspiration due to limited meteorological data on wind, relative humidity, sunshine hours etc.

$$\lambda E_0 = 0.0023\, H_0 \left(T_{max} - T_{min}\right)^{0.5} \left(T_{avg} + 17.8\right) \qquad \ldots (5.4)$$

Where λ is the latent heat of vaporisation (MJ/kg), E_0 is the potential evapotranspiration (mm/d), H_0 is the extraterrestrial radiation (MJ/m^2/d), T_{max} is the maximum temperature (^{0}C), T_{min} is the minimum air temperature (^{0}C), and T_{avg} is the mean temperature (^{0}C).

The percolation component of the SWAT model uses a storage routing technique along with a crack-flow model to forecast flow over each of the soil layers. Lateral sub-surface flow in the upper soil layer is accounted concurrently with percolation. A kinematic storage model (Sloan et al. 1983, Sloan and Moore 1984) is applied to predict lateral flow in the soil strata. The details about various theoretical considerations, inputs, process, file formats etc. are given in the manual of SWAT model available at Texas A&M University (TAMU) website (https://swat.tamu.edu/media/99192/swat2009-theory.pdf).

5.3.3 SWAT Calibration and Validation

Generally, the hydrologic modeling of a watershed involves (a) developing the model based on some theory, mathematical formulations and some assumptions such as SWAT; (ii) simulating the hydrological outputs for known observed data sets than conducting sensitivity analysis for the wide range of input parameters; (iii) carrying out model calibration and (iv) validation of the model (Abbaspour et al. 2017). The model calibration is one of the most significant tasks in all the simulation studies. Improving the model simulation capability and minimizing the uncertainty or error band is the central and fundamental point of a model calibration process (Engel et al. 2007). The minimisation of the difference between model-simulated and observed values is known as the process of model calibration. In the calibration process, the fine-tuning the hydrological model parameters is attempted so that the model reasonably simulates true processes in the real world or system (Abbaspour et al. 2017).

Commonly, sensitivity analysis performed before the model calibration. The input parameters sensitivity investigation is a method of detecting the order of changes in model outcome concerning those of model input parameters. The sensitivity examination decides the most sensitive model parameters for the calibration process, specific to the area under the study. By and large two kinds of parameter sensitivity investigation are used, viz. (a) "local sensitivity analysis or one at a time (OAT) sensitivity analysis in which just a single parameter is permitted to change while keeping every single other parameter at the fixed values" and (b) "global sensitivity analysis in which all parameter is permitted to change at the same time. Thus, global sensitivity analysis requires an exceptionally enormous number of simulations" (Abbaspour et al. 2017).

The SWAT model calibration can be done either in the ArcSWAT interface or by using a standalone SWAT Calibration and Uncertainty Program (SWAT-CUP) developed by (Abbaspour et al. 2007). The various component of water balance must be verified during the calibration procedure to ensure that the model results are meaningful and relevant. After finishing the calibration procedure, the model should be validated with the dataset which was not utilised during the calibration process. A comparison should be made between the model-simulated and field-observed values during both calibration and validation time frame, to test the performance and self-reliance of the developed model.

ArcSWAT (v.2012) was applied to simulate the monthly streamflow at the Ashti, gauging-discharge station located at the outlet of the WRB. Nine numbers of sub-basins, were considered for sub-basin level analysis. Each of the sub-basins was consist of HRUs of a unique combination of LULC, Soil and Slopes. The model sensitivity analysis was accomplished using Sequential Uncertainty Fitting (SUFI-2) algorithm of SWAT-CUP. SUFI-2 uses the Latin hypercube and one factor at a time (LH-OAT) method for performing the sensitivity analysis. The calibrated values of model parameters were then manually updated in the ArcSWAT. The model was validated for the period of 2001-2005. The model performance was tested with the coefficient of correlation (R^2), Nash and Sutcliffe model efficient (NSE), (RSR) and percentage bias (PBIAS) as suggested by Moriasi et al. (2007). The various steps of operations and processes are shown in the process flow diagram for the SWAT model was adopted from SWAT manual, as shown in Fig. 5.4.

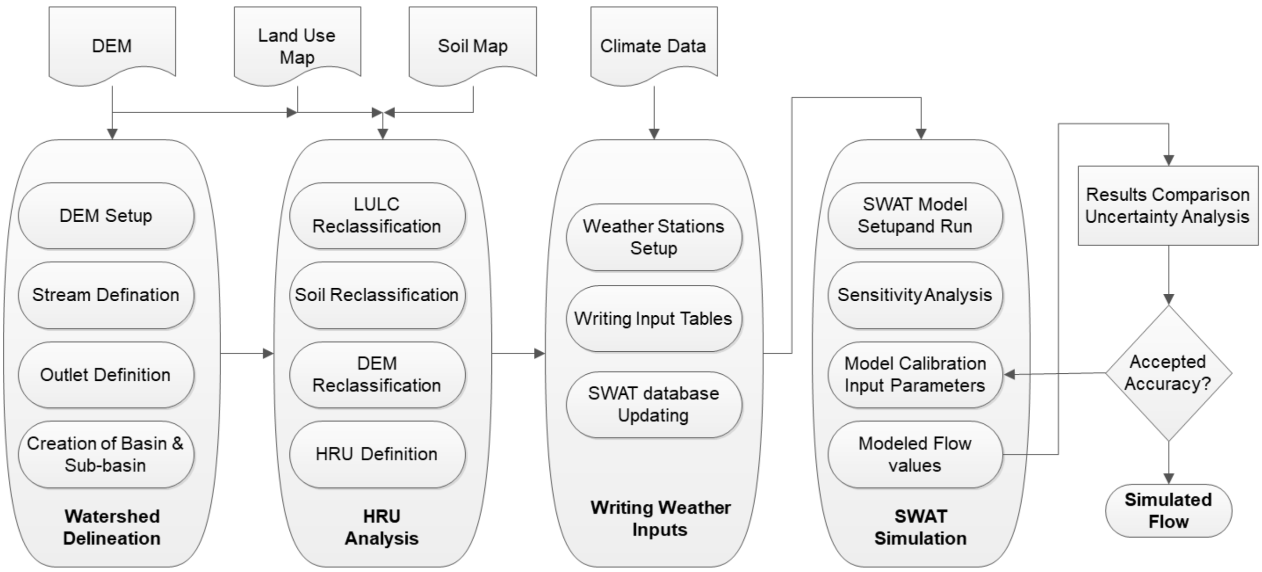

Fig. 5. 4 Flow chart showing the methodology of the SWAT model

Generally, the model assessments are compared with some observed variables to test the predicting power of that model based on certain established model evaluation criteria. When exhibiting model outcomes, the model designers ordinarily do not give steady or standard factual assessment criteria to help the users or clients in deciding how well their model provide the deliberate information and how well their model compares to other models (ASCE Task Committee 1993).

A time-series graph and scatter diagram for the actual field observed, and model-simulated streamflow was created and presented for visual interpretation. The scatter diagram technique and The Nash-Sutcliffe efficiency (NSE) used to test the model efficiency.

The NSE values vary from 0 to 1, 1, representing a perfect fit model. If the observed discharge approaches the mean value, the denominator tends to zero and the NSE approach negative infinity. This statistic works best when the coefficient of variation for the observed data set is large. The NSE characterizes amelioration over R^2 for evaluation of model performance as it is sensitive to the differences in the means and variances values of observation and simulation series. The NSE is one of the most commonly used indices for the performance evaluation of hydrologic models.

5.3.4 Multi-Model Ensemble under Future Scenario

In this study, future climatic inputs from four GCMs were used for simulating the impacts of changing climate. In order to overcome the uncertainty band of future climate, an ensemble of these simulations was used to evaluate the hydrological responses of the Wainganga River basin under three future periods, i.e. near, mid and far of 21^{st} century. These future simulations were compared with the baseline scenario for which the SWAT model was calibrated and validated, i.e. 1981-2005. Few of the studies (Yu and Yang 2000, Westerberg et al. 2011, Reshmidevi et al. 2018) indicated that when the two temporal periods do not overlap, then the flow regimes can be compared with the flow duration curves (FDCs) for any hydrological analysis. Therefore, the FDC of the baseline period and different future periods were compared for understanding the hydrological responses.

A weighted ensemble average approach adopted by (Reshmidevi et al. 2018) was used to get the multi-model ensemble mean simulation from all five GCMs. SWAT simulations for each GCM were performed, and FDCs were generated from these SWAT outputs for the annual and monsoon flows. Then, comparisons were made between the FDCs from GCMs-based SWAT outputs and the FDCs of the observed flows.

5.3.5 Setting Scenarios and Experiments

In the present investigation, three scenarios were considered to evaluate the hydrologic responses of the basin under independent and collective effects of the changing climate and/or land-use change under the SSP2 4.5 and SSP5 8.5:

a. Scenarios I: Changing climate with static LULC
b. Scenarios II: Changing LULC with static climatic conditions
c. Scenarios III: Changing climate with corresponding LULC scenario.

Streamflow at the Ashti gauging site was simulated according to each of the above scenarios from 2016 to 2099 under both SSP2 4.5 and SSP5 8.5 for the three future periods: Near-Future Scenario (2025–2050), MFS: Mid-Future Scenario (2051–2075) and FFS: Far-Future Scenario (2076–2100).

The projected flows for combinations of future period and scenario were compared with the baseline period (1981-2005) flows, considering the no-change scenario. The impacts of climate change on streamflow were examined by varied climate scenario in the future periods and streamflow was simulated with the assumption that the land-use will remain constant as per the prevailing condition of the year 2000.

5.4. RESULTS AND DISCUSSION

This section incorporates results identified with the LULC simulation model, calibration & validation of SWAT model and hydrological simulations at the outlet of Wainganga River basin under the various combination of future climatic and land-use scenarios. Results related to the analysis of different statistical indices used for appraising the SWAT model performances are also reported.

5.4.1 Future LULC

The future land-use maps for the year 2030, 2040 and 2050 were prepared, and results pertaining to these are described in chapter 4. These three maps used as inputs to the SWAT model for the hydrologic simulations under various combinations with climatic data of past and future.

5.4.2 SWAT Calibration and Validation

Being a physically based and semi-distributed parameter model, calibration of the SWAT model is only possible for watersheds with observational data (Arnold et al. 1998). Most of the model input is physically based and taken from the field observation and available literature. The SWAT model was calibrated using the monthly observed discharge data at the outlet of the WRB, viz. Ashti gauging site for the twenty years (1981-2000) and then, it was validated for the period of five years (2001-2005). There are three calibration methods commonly popular among the researchers, i.e. the manual method, automatic calibration method and a combination of these two. Manual calibration is the most commonly used method. However, it is cumbersome, time-taking, and highly dependable on the experience and knowledge of the modeller about the hydrological processes and the study area of interest. (Eckhardt and Arnold 2001).

The time-series of the observed monthly discharge values of Ashti gauging site were compared with the pre-calibrated simulated (SWAT model) values for the entire study period, and calibration was done in SWAT-CUP..

5.4.3 Model parameterization and sensitivity analysis

The sensitivity analysis parameter provides insights as to which parameters contribute most to the output variance due to input variability (Holvoet, Van Griensve, Seuntjes, & Vanrolleghem, 2005). The sensitivity analysis method implemented in the SWAT model is called the Latin hypercube One-At-a-Time (LH-OAT) design as proposed by Mories (1991). Sensitivity analysis was then performed to identify those parameters model outputs were sensitive. In general, a parameter should be included in calibration if sensitivity analysis identifies that there is a 95% probability that the sensitivity of a variable to a particular parameter is significant. Based on the sensitivity analysis, the SUFI-2 algorithm in SWAT-CUP and an artificial trial and error method were both used to calibrate the key parameters for different periods with different LULC conditions. Fig.5.5 and Table 5.1 shows the results of the sensitivity analysis.

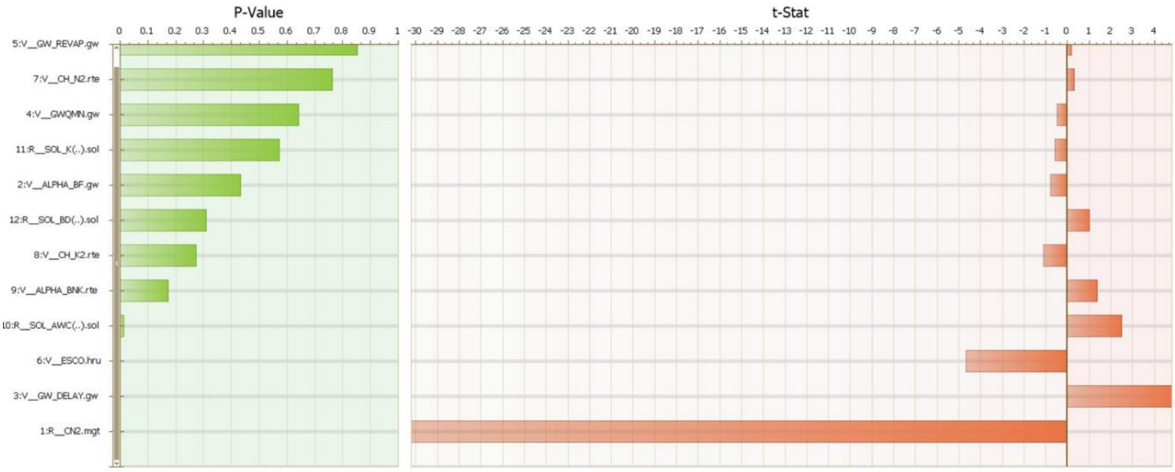

Fig. 5. 5 Results of the global sensitivity analysis of SWAT parameters for Wainganga River basin

In this study, an LH-OAT sensitivity analysis, which is incorporated in SWAT-CUP, is used to perform sensitivity analysis. The NSE was considered as the objective function of the 12 model parameters and ten intervals of LH sampling. After set-up of the SWAT model and including all the input parameters simulations were performed, and sensitivity analysis was executed. The parameter creating the maximum average percentage change in the objective function value is ranked as most sensitive representing by the minimum *p-value*. The result of the sensitivity analysis (Table 5.1) indicates that parameters namely; curve number (CN), groundwater delay time (GW_DELAY), soil available water capacity (SOL_AWC), saturated hydraulic conductivity (SOL_K) are the most crucial parameters for the study area and they were fine-tuned to achieve better model performance. The table contains the ranks, description, the related hydrological process of these model parameters. The calibrated values of top four sensitive parameters along with their upper, lower and default run values are also given in the same table.

Rest of the eight parameters viz. baseflow alpha factor for bank storage (ALPHA_BNK), Manning's "n" value for the main channel (CH_N2), soil evaporation compensation factor (ESCO), groundwater revap coefficient (GW_REVAP), soil bulk density (SOL_BD), groundwater recession factor (ALPHA_BF), Effective hydraulic conductivity in main channel (CH_K2) and Threshold depth of water in the shallow aquifer required for return flow (GWQMN), with their rank and default values are also shown in the table.

Table 5. 1 SWAT parameters with rank according to sensitivity with respective range and values for the case study

Rank	Name	Description	Lower Bound	Upper Bound	Process	Default Run-Value	Calibrated values
1	CN	SCS-CN for AMC-II	35	98	Runoff	83	74
2	GW_DELAY	Groundwater delay (days)	0	500	Groundwater	31	20
3	SOL_AWC	Available water capacity of the soil (mm/mm soil)	0	1	Soil	0.096	0.15
4	SOL_K	Soil conductivity (mm/hr)	0	100	Soil	18.66	18.66
5	ALPHA_BNK	Baseflow alpha factor for bank storage (days).	0	1	Channel	0	-
6	CH_N2	Manning coefficient for main channel	0	0.3	Channel	0.014	-
7	ESCO	Soil evaporation compensation factor	0	1	Evaporation	0.95	-
8	GW_REVAP	Groundwater -revap coefficient	0.02	020	Groundwater	0.20	-
9	SOL_BD	Moist bulk density (Mg/m3 or g/cm3).	0.9	2.5	Soil	1.5	-
10	ALPHA_BF	Baseflow alpha factor (1/days)	0	1	Groundwater	0.0482	-
11	CH_K2	Hydraulic conductivity in main channel (mm/hrs)	0	150	Channel	0	-
12	GWQMN	Threshold depth of water in the shallow aquifer required for return flow to occur (mm)	0	5000	Groundwater	1000	-

The sensitivity analysis specified the significance of all the model parameters in generating the flows in the basin. This result explains how the parameter sensitivities are so site-dependent and contingent by the local land-use practices, elevation profile and soil classes, as compared to other studies elsewhere.

5.4.4 Result of SWAT Model Simulation

The discharge monitored on the ground and monthly model-simulated discharge during the simulation period (1980-2018) along the 1:1 line is illustrated in Fig. 5.6. It can be seen from the figure that the model-simulated streamflow values are spread equally on both sides of the 1:1 line for low values of observed discharge. In case of the high-flow regime of observed data, the model-simulated values are marginally over the 1:1 line, signifying that the model slightly over-predicts in the high-flow regimes. During the validation, the value of the model evaluation criteria, viz., R^2 and NSE, were calculated for model simulations (Table 5.2) and found about 0.86, and 0.64 respectively. A comparison of various statistical parameters such as means, standard deviation etc. for the observed and simulated flows series is also given in Table 5.2. Fig. 5.7 shows the combined plot of observed versus SWAT model-simulated discharge values for the entire study period monthly, for both calibration and validation periods.

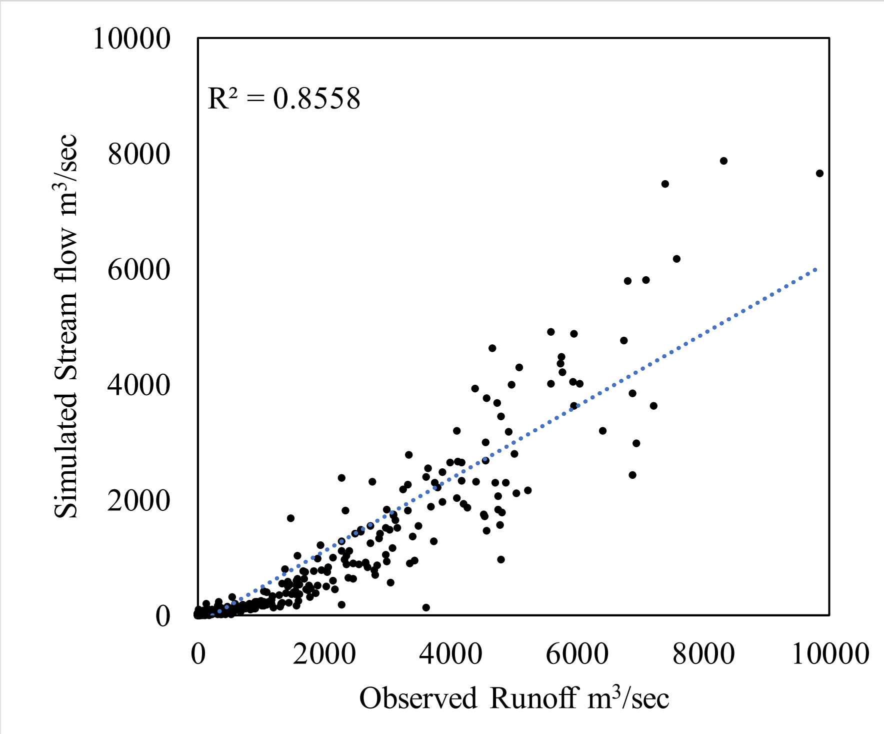

Fig. 5. 6 Scatter plot of observed and simulated discharge during the simulation period

Table 5. 2 Statistical analysis of monthly observed and simulated discharge during simulation

Statistical Parameters	**Discharge at Ashti during 1980-2018 (m^3/sec)**	
	Observed	**Simulated**
Mean	646.90	704.00
Standard Deviation	123.60	182.20
Maximum	7865.75	9850.40
Model Evaluation Criteria	**Value**	**Performance Rating**
Coefficient of determination	0.86	Very good
Nash-Sutcliffe Efficiency	0.64	Very Good

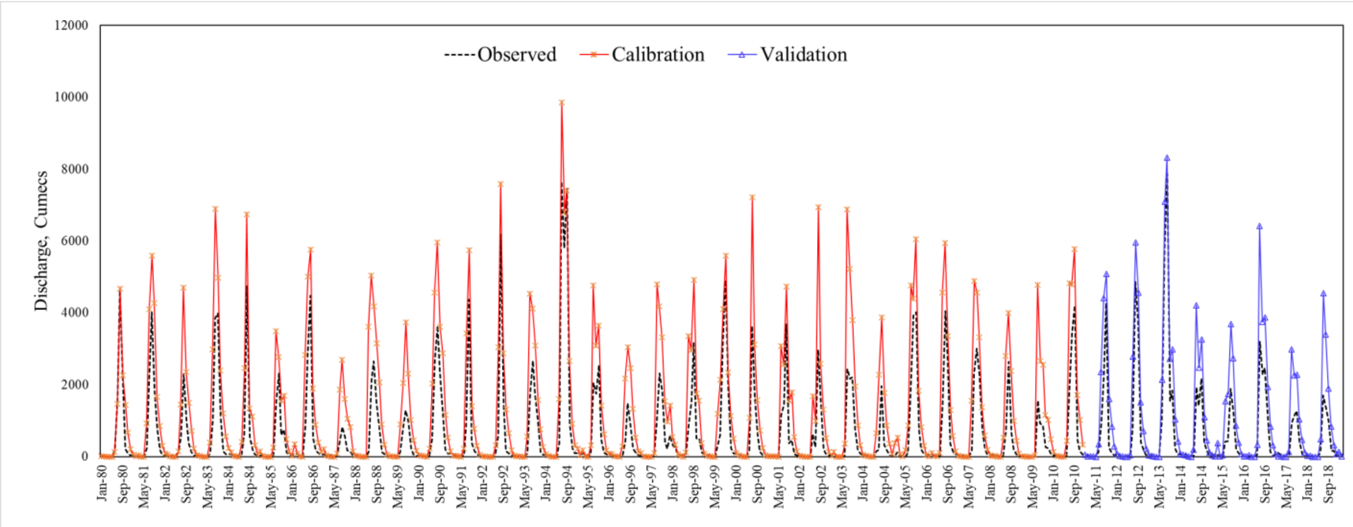

Fig. 5. 7 Comparision of observed and simulated discharge series at Ashti during calibration and validation period

5.4.5 Hydrologic Responses in the Future under Different Climatic and Land-use Change Scenario

In this study, the hydrological response of the WRB has been assessed with varying climatic and LULC scenarios. Four GCMs were considered to present the future climatic conditions with two SSPs, i.e. 24.5 and 58.5. Three different future periods were considered to see the changes in different time frames of the 21st century. Three LULC scenarios corresponding to the climatic period were also taken into account. The results of various permutation and combinations of theses change scenarios, and their impacts on the hydrologic responses of the WRB are described in the subsequent sections.

Hydrologic Responses due to Changing Climate

This section describes the hydrologic responses of WRB due to changing climate conditions with a static LULC condition of the baseline period, i.e. the year 2000. The calibrated and validated SWAT model was used to produce the flows times series while taking climatic inputs from each of the five CGMs for all three future periods, i.e. near, mid and far of the 21st century. To draw logical conclusion and minimize the uncertainty associated with the GCM models weighted average future time series for each of the future period has been reproduced, and the weighted ensemble average FDCs of the monthly flows for all three future periods with the FDC of the baseline are presented in Figure 5.8.

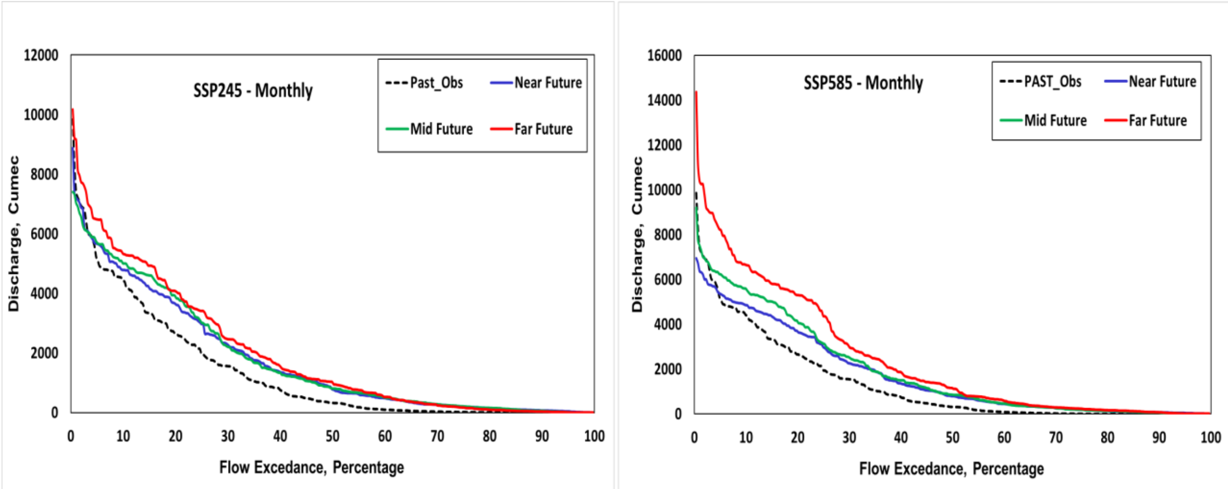

Fig. 5. 8 Weighted ensemble average FDCs of monthly flows for the baseline period, near, mid and far future period of the 21st century scenario under SSP245 & SSP585.

It is evident from Fig. 5.8 that the normal flows (representing 20–60% exceedance probability) and high flows (representing <20% exceedance probability) at monthly time-scales show slight decreases in the early of the 21st century, whereas in low-flows (representing >90% exceedance probability) there is accretion in the future periods for both the SSP scenarios. The increases in the streamflow projections for normal-flows and high-flows can be observed for the mid and end periods of the 21st century, whereas low-flows show some reduction in the future for both the SSP2 4.5 & SSP5 8.5.

These results may be ascribed to the alterations in the rainfall regime and its distribution pattern anticipated towards the end of the 21st century. Similar results have been reported by Reshmidevi et al. (2018) and Mehrotra et al. (2013) indicating a likely decrease in the number of short wet spells (less than four days) and moderate wet spells (four to seven days), whereas a rise in the quantum of rains from all the short, moderate and long (seven days and more) wet periods by the mid of the 21st century. On the contrarily, occurrences of short and moderate dry spells are likely to be increased under future scenarios. The expected rise in the dry spells is a prospective cause of the decline in the monthly and monsoon low-flows.

Figure 5.9 depicts the percentage deviation of flows on future periods with respect to the baseline period for both the SSP scenarios. It has interpreted that in the lean flow season, the variation is huge, but as the quantity of flow is very less in that period, it becomes significant particularly in February, March and April.

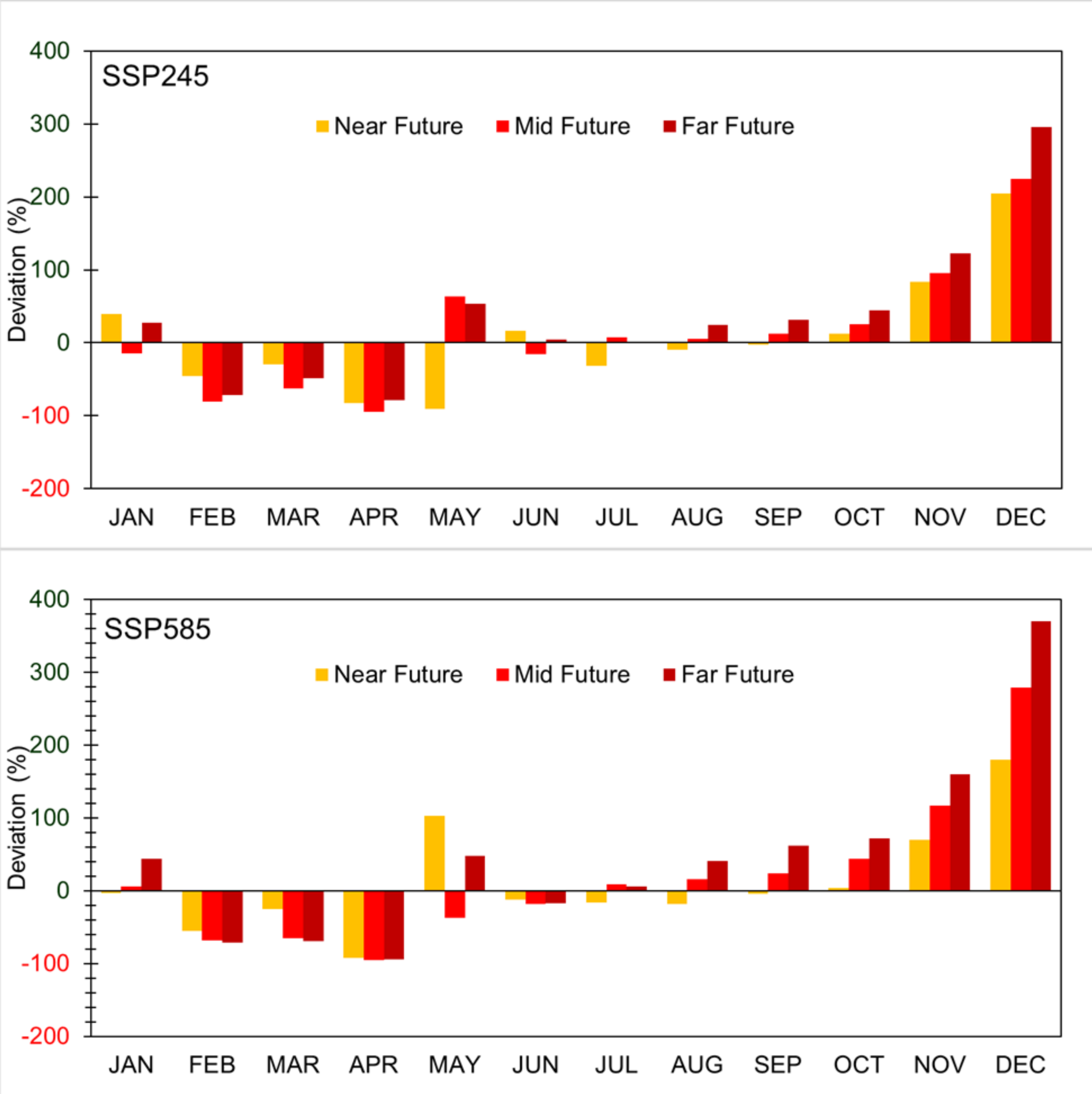

Fig. 5. 9 Percentage deviation of future flows with respect to the baseline period under both the SSP scenario

The Wainganga river hydrology seems to be intensified during the mid and far of the 21st century, particularly under the SSP5 8.5 scenario. Whereas both the SSPs are supporting the theory of decrease of river flows at the beginning of the century and when further moves ahead in future the streamflow and increasing. This can be attributed to future alterations in the precipitation pattern, which are analogous to that of discharge. The average monthly flows vary considerably throughout the year and reasonably high in monsoon months (i.e. June, July, August and September). It can also be noted that significant changes have occurred during the wet spells, whereas in the dry spells during the lean-flow season, there have been minor fluctuations for both the SSPs scenario. Even the lean-flow months of the study region, i.e. February, March April and

May are experiencing reduced flows in future, which may worsen the water availability situation and water quality may get impacted during these months.

The results are comparable with other similar kinds of studies (Mishra and Lilhare 2016, Nilawar and Waikar 2019). Results of the SWAT model flow projections suggest that availability of water does not seem to be a problem by this 21st century particularly during the wet seasons provided sufficient storages in the basin are created as the river may run with little flows during dry or lean seasons. The results indicate the influences of changing climate on the hydrologic response of the WRB in all three future periods.

Hydrologic Responses due to Changing LULC

This section describes the hydrologic responses of WRB due to changing land-use and land-cover (LULC) with static climate conditions of the baseline period. To assess these impacts, the climatic forcing of the past period kept uniform and the simulation performed for the three future LULC scenarios of years of 2030, 2040, and 2050.

Researchers have reported (Kim et al. 2013b, Júnior et al. 2015, Garg et al. 2017) that the changes in regional LULC, such as urban growth, affect the water resources in both the quantity and quality terms. Figure 5.10 shows the impacts of LULC of different periods (years 2000, 2030, 2040 and 2050) on the average monthly hydrographs of the river Wainganga assuming that the climatic factors were not changed over the time. It gives the idea that the changing LULC have a little impact on the streamflow as compared to the impacts of changing climate those presented in previous section. Figure 5.10 shows that changes in average monthly streamflow at the outlet of the WRB under the past and future LULC conditions.

The average value of monthly simulated streamflow was 1123m^3/s in the year 2020, and 1291m^3/s in 2050 under static climatic conditions of the baseline period. The streamflow is increasing in the case of future LULC scenarios, the major attribution of this could be increased in the settlement areas and reduction in the agricultural and open forest area, as reported in chapter 4.

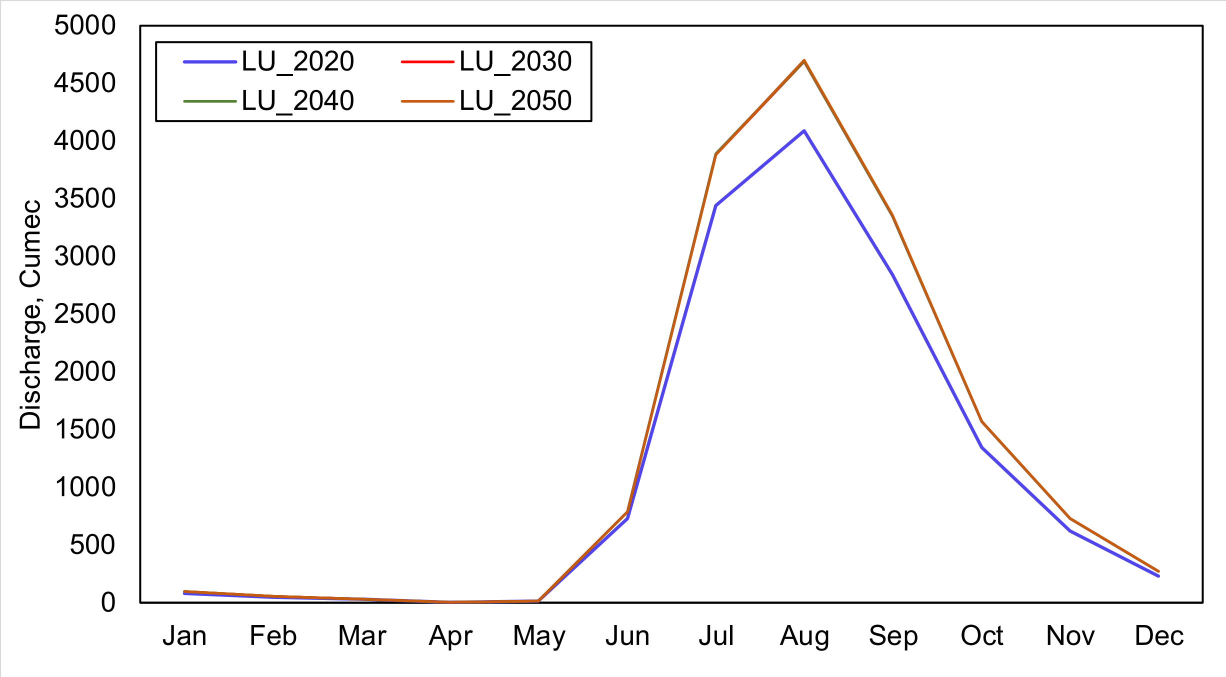

Fig. 5. 10 Average monthly streamflow variations under the changing LULC conditions

The average monthly values of simulated flows for the baseline period and future period LULC conditions are arranged in Table 5.3. It can be appreciated from the table that there is 14.9% escalation in the average annual streamflow by the year 2050 if the climate does not change. The year 2030 and 2040 LULC conditions are also contributing towards the incremental gain in the river discharge on average values. It can also be observed that the flow in the lean season or non-monsoon season is expected to be dropped, and during monsoon season there will be a surge in the river flows regimes.

Table 5. 3 Simulated average monthly streamflow under different land-use scenarios and static climate condition.

Month	LU_2020	LU_2030	LU_2040	LU_2050
Jan	80.4	94.9	94.9	94.9
Feb	50.0	55.1	55.1	55.0
Mar	27.4	28.3	28.3	28.3
Apr	3.4	3.7	3.7	3.9
May	11.4	14.8	14.9	14.9
Jun	729.6	789.1	789.7	790.0
Jul	3438.3	3884.0	3892.2	3885.8
Aug	4089.3	4690.3	4692.3	4701.3
Sep	2845.6	3352.6	3353.8	3355.5
Oct	1349.3	1567.0	1567.1	1568.7
Nov	625.5	726.6	726.6	726.4
Dec	230.9	272.1	272.1	272.0

The river flows of the WRB are found to be more responsive to changing climate rather the changes in land-use, and thus the variations in river flow under future scenarios of climate and land-use change are exceptionally coherent with those in which the only climate was changed (Tu 2009). Besides, the variations in the annual streamflow under climate change and land use change scenario III flow increases during February, March, and April and decreases in summer and autumn were similar to those in scenario I. The varied land-use in future periods brought out minor increment in river flows. However, in scenario III where both climate and land-use have to compound the alteration in the seasonal variability of flow (Praskievicz and Chang 2009).

5.5 CONCLUDING REMARKS

This chapter reports the impacts of isolated and combined effects of future climate and land-use on the hydrological behaviour of the WRB in central India. Three scenarios of changing climate and land-use were set up, and the SWAT model-simulated flows during three future periods under each scenario generated. Comparisons of the results of each scenario were performed with the baseline period observed flows data for concluding the impacts. Four numbers of statistically downscaled and bias-corrected GCM data, viz. BCC-CSM2-MR, EC-Earth3, MPI-ESM1-2-HR, and NorESM2-LM were used to get future climatic inputs. Two climatic projections, SSP2 4.5 and SSP5 8.5 for the climate change scenario were selected for the near future, mid future and far future. To take care of the uncertainty associated with GCMs, a weighted average ensemble of these five models was used to draw a rational conclusion.

The calibration and validation of the SWAT model were performed by simulating the historically observed discharge data for 25 years (1981–2005) at Ashti, gauging site. The good agreement between observed and model-simulated monthly values signalled that the calibrated model with the set of optimised parameters might be applied to examine the hydrological responses of the study basin under the varied future climatic and land-use conditions. Following conclusions can be made out of the study presented in this chapter:

i) The impacts of each scenario were apparent, especially in the monthly variations of streamflow. Results of the study confirmed the decreased streamflow initially in the near future periods of the 21st century and increased the streamflow towards the mid and far future of the 21st century under both SSP2 4.5 and SSP5 8.5.
ii) The monthly average streamflow fluctuates considerably throughout the year and is reasonably high in April, May, November and December months.
iii) Land-use change had a relatively minor impact on flows as compared to impacts caused by to changing climate. As urbanization advances, the flow in the river during the long

wet spells increase and declines during the dry periods. It is crucial to consider land-use change patterns and for the moderation of the ill effects of extreme events such as floods and droughts. Changing Land-use must be deliberated when formulating water resource planning and strategies.

iv) The collective impacts of changing climate and land-use in future periods on the flows of the Wainganga river were analogous to the impact of changing climate alone, but with the augmented monsoon and post-monsoon months' flow and reduced lean-flows in dry spells season in the combined scenario.

Development of predictive understanding of the flow alternation triggered by the distinct and combined influences of future climatic and land-use conditions is decisive for the sustenance of the water resource. The seasonal variation of streamflow in the WRB is likely to become more severe in the coming decades. Extreme hydro-climatic events are expected to increase in magnitude and frequency of occurrence in the study region.

CHAPTER 06: ADAPTATION MANAGEMENT STRATEGIES

6.1 GENERAL

Climate change is one of the greatest challenges ever faced by humankind today. As, the different spheres of the earth system are interconnected and affected by the changing climatic conditions, directly or indirectly. Precipitation and temperature are the primary indicators of climate and changes in their characteristics over a period of time define the phenomenon of climate change. The trend analysis of these essential meteorological variables, i.e. rainfall and temperature (maximum and minimum) of the WRB indicates that changes in the climatic conditions of the region have occurred over the years, and in future, it is likely to be continued. Results from Chapter 3 show that the basin is at high-risk condition due to its high exposure and sensitivity, and low adaptive capacity, making it vulnerable to climate change. Chapter 5 confirms that the hydrological responses of the study basin and water resources are expected to be impacted by changing climate and the changes in land-use.

Water resources in the WRB are randomly distributed in both, time and space and confronting a threat due to rapid industrial expansion and urbanisation (Kumari et al. 2016). Hence, sensible, scientific and coherent adaptive policies need to be formed to meet the challenge posed by climate change. In addition, evidence-based strategic planning and adaptations for short term and long term are required to reduce the vulnerability and develop resilience among various affected sectors of the state in the backdrop of climate change impacts.

Assimilated solutions that lead to the improvement in the quality of life and sustainability of the ecosystem, which are the primary goals of any adaptation strategies against climate change, are the need of the hour.

Proactive and preventive actions for adaptation to changing climate can significantly diminish many of the confrontational impacts. Climate change is likely to distress the economics of the contrary at large. The poorest of the poor are likely to hit harshly with its impact. As the poor have the least adaptive capacity.

In this light, the National Action Plan on Climate Change (NAPCC) clearly outlines “its first principle as protecting the poor and vulnerable sections of the society through inclusive and sustainable development strategy, sensitive to climate change”.

6.2 ADAPTATION AND MITIGATION STRATEGIES FOR COMBATING WATER RESOURCES VULNERABILITY

In order to develop a successful sub-basin, wise, sustainable adaptation strategy, it is imperative to understand the vulnerability profile of each sub-basin and the existing ground realities. The Wainganga river basin is an agriculture dominated basin and agriculture sector the largest consumer of water. There are two major crops in the basin which, sown in three cropping seasons:

Crop	Planting Date	Harvesting Date
Rice (Kharif crop)	15 Jun	21 Oct
Wheat (Rabi Crop)	06 Nov	15 Apr
Summer Rice (Rabi Crop)	12 Dec	14 Apr

The cropping season in the highlands of the basin has decreased from three seasons to two seasons (Rice, Wheat) due to reduction of water availability in these areas. For the second season, there was no adequate water supply for irrigation. Monsoon failure has resulted in changing the growing crops from two to one in recent decades. One of the common observations seen in these parts of the basin is a change in the planting and harvesting times.

During the field visits to study basin (2024-2025) and interactions with the local farmers, it was understood that most of the farmers of this basin are aware of the climate change phenomenon. They knew about the change in rainfall patterns, temperature rises and heatwaves and their possible impacts on agriculture. Many of the local farmers already started practising various adaptations measures during drought periods without proper adaptation strategies to climate change. Some of the common practices noted in this basin are shifting in the sowing dates depending on the onset of monsoons, increased use of chemicals and fertilisers, priority to the high yielding and short-duration crops variety over the traditional ones, involvement in non-farming activities along with the farming, adaptation of mixed cropping, inter-cropping and introduction of crop rotation. A few of the progressive farmers have started practising the drip and sprinkler irrigation with tube well irrigation for wheat and other horticulture crops. With the introduction of central government schemes such as Mahatma Gandhi Rural Employment Guarantee Act (MNREGA), farmers are now more interested in labour works than agricultural activities due to the higher payments.

Vulnerability mapping highlights the vulnerable areas for baseline as well as future periods for sustainable adaptation planning. Few of the coping strategies practised by farmers have been pointed out for the agricultural sector. But there is a need for an integrated modelling approach based on future climatic conditions. Hydrological modelling generated outputs, water resources vulnerability assessment, the local wisdom and peoples' perception and various physiographic characteristics of the sub-basins are the key considerations while framing the adaptation strategies and policies in views of the changing climate and land-use scenarios. Sub-basin wise formulation of integrated adaptation strategies must be framed such that it can spell out in action plans, which will moderate the risk of climate change and land-use related adverse effects.

The entire drainage area in the Wainganga river depends upon the monsoonal rainfall. The soil and water conservation practices such as water harnessing structures, mini percolation ponds, farm ponds, stagger trenches, check dams, contour bunds, boundary trenches etc. need to be adopted, which retard the flow velocity and increases the retention time, leading to enhancement in groundwater recharge and moderate the erosivity of runoff. The uplands present in the basin are suitable for groundwater storages by artificial recharge, whereas alluvium near the river course is suitable for surface water harvesting structures.

Water resources conservation is of major concern in semi-arid regions like the Wainganga river basin, where agriculture is the primary and most important economic activity playing a pivotal role in sustainable development. Moreover, the basin has high seasonality associated with the rainfall as 88% of the rain falls within a short span of three months and that is also non-uniformly distributed. Agriculture crop growth and production are highly linked to the atmospheric temperature at various stages such as the germination of seeds, flowering stage, the ripening of the crop etc. The projected climate towards the end of the 21st century indicates that the average annual minimum temperature is likely to be increased by 2.9^{0}C under the SSP2 4.5 and 3.6^{0}C under SSP5 8.5 scenarios. This significant temperature rising could lead to long hot spells. Hence, it is crucial to devise and implement suitable adaptation strategies to cope with such changes, for all the stakeholders of the basin, including farmers and decision-makers.

In the early periods of the 21st century, a reduction in summer and winter seasonal rainfall over the basin is expected. It may lead to reduced crop yields and quick-deplete of soil moisture. In contrast, by mid and end of 21st century, the future projected rainfall is likely to be high, particularly during the southwest monsoons, which may result in high soil moisture storage and small dry spells. Kharif is the main cropping period; therefore, the local farming community should go for short-duration high-yielding crop variety. Whereas, in case of Rabi season (non-monsoon) the flows are expected to get reduced (following a declining rainfall in winter season), the farmers must plan for less water consuming and water resistance crops. The climate variability can be more complicated if it gets integrated with the changes in the onset and withdrawal dates of monsoon, less number of rainy days, extreme events, higher temperatures, erratic rainfall events and increased potential evapotranspiration. This complexity will make agriculture and allied activities more vulnerable to climate change.

Many adaptive measures can be applied to moderate the adverse effects of climate change on water resources and agriculture to some extent. Focused planning is needed to overcome the negative effects of climate change on water resources. Some of the long term and short-term integrated adaptation strategies to climate change are suggested in subsequent sections.

6.2.1 Short-Term Strategies

The understanding of the impacts of climate change on water resources is not fully developed due to the interaction of various process among the different sectors. As such, a comprehensive climate-resilient plan for water resources and allied sectors can be taken up. It may start with a basic but very relevant activity, i.e. the development of a comprehensive database on water resources of the region may be at the sub-basin level. This database may be placed in the public domain for more transparency, awareness creation and inclusion of left-out issues. This database could be used for assessment of the potential impact of climate change projections on water sector by the various concerned agencies responsible for managing the different aspects of the sector. The progress can be updated from time to time for better monitoring and control over the objective. The short-term adaptation strategies may (Adger et al. 2007, Nyong et al. 2007, Epule et al. 2017, Pandey 2017):

- Review and strengthening of an existing network of hydro-meteorological monitoring sites including the automatic weather monitoring stations and self-recording rain gauge stations.
- Other vital information pertaining to the socio-economic, infrastructural, land-use pattern, geology, aspects etc. must be collected for reliable evaluation of the impacts of climate change on water resources of the basin. Such data can be used to analyse and identify the issues associated with projected climate change.
- Establishment and up-gradation of evaporation monitoring network with modern sensors and data loggers. It may incorporate different upgrades required in the existing hydro-meteorological observation stations.
- Strengthening of existing groundwater level and quality monitoring and expansion of the network in low-density areas.
- Compilation of the water quality information of various sources such as rivers, groundwater, lakes, wells, ponds, etc.

- Soil erosion, land degradation and sedimentation issues are fundamental, particularly in hilly regions; therefore, a regular monitoring mechanism of soil erosion and sedimentation must be evolved.
- Assessment of carrying capacity of the basin and sub-basins must be done considering ecological and social demands for various sectors.
- Development of a network of rainwater harvesting structures, check dams, farm ponds, percolation ponds, etc. for artificial recharge of groundwater storages so that the stored water can be used during the dry spells, in the events of early cessation of rain or in the form of groundwater extraction from the drilled or deepen bore wells.
- Development of the drought and heat-resistant varieties to sustain the prolonged dry spells. Promotion and plantation of vegetation species adapted to the new climate patterns must be endorsed.
- Promotion of the best management practices (BMPs) like the crop diversification, inter-cropping, adjusting the timing of field operations, soil fertility management and use of agroforestry, planting methods (e.g. on raised beds) etc.
- Increasing water use efficiency using micro-irrigation and precise agriculture. Adaption of the zero tillage to conserve soil moisture and save time and energy.
- Supplementary irrigation by drip and sprinkler, to extend the growing period for high-yield production.
- Increased use of organic manures and System of Rice Intensification (SRI) for increasing the productivity of irrigated rice.

6.2.2 Long-Term Strategies

Long-term strategies play a key role in changing the paradigm towards low GHG emissions and climate-resilient and sustainable development. The long-term goals set-out water resource development in view of the changing climate and earth landscapes. The long term strategies also direct short-term decision-making to facilitate the integration of climate change adaptation into implementation plans and processes (Epule et al. 2017, Pandey 2017).

- The sustainability of groundwater resources is most crucial for all the peninsular rivers. Intensified programs or missions for groundwater recharge in dark zones of the study basin must be taken up.
- Drinking water quality issues and their seriousness in light of climate change must be addressed by the authorities, particularly in rural areas. Whereas, in the urban setup, the improvement in water use efficiency (WUE) and reduction in per capita water uses must

be the priority. WUE can be achieved with promotional policies for water-efficient fixtures and devices, water-productive methods, and efficient public water supply system. The effective and timely implementation, operation and maintenance of water resources developmental projects can also be one of the major strategies that will result in the affirmative changes.

- Steps must also be taken to encourage integrated water resources management (IWRM) and planning along with their development.
- A climate change adaptation unit or climate resource centre must be set up for the necessary coordination and monitoring mechanisms. It may help the end-user such as farmer, etc. to access the appropriate technology for adaptation to climate change and serve as a link between the scientific and research institutions and end-user at the field.
- Provision of climate or weather linked insurance schemes for different sectors may a significant breakthrough in adaptation strategies.
- Strong documentation must be maintained for information flow, sharing of data and information, recording of responses, etc. for each of the stakeholder sector. This will help in learning what worked and what did not.
- Building the institutional and individual capacity within the water sector to integrate climate change concerns during the various stages of water resources project planning and execution.
- The gender dimensions of water sectors are well known, for example, that females generally assigned with the primary responsibility for collecting water for various domestic purposes such as drinking, cooking washing, etc., whereas men are responsible for using the water for outdoor activities such as agriculture, industries etc. The gender disparity must be considered while formulating adaptation strategies and projects.
- The private sector has substantial potential in terms of work experience, expertise over innovative technologies and competencies. Involvement of private and non-government organisations (NGOs) in the water sector by various means such as public-private partnership (PPP) ventures etc. could be a fruitful long-term adaptive strategy.

6.2.3 Basin Specific Strategies

The water sector needs to focus on collecting more data and information, developing appropriate infrastructure and improving water use efficiency, particularly in agriculture. There are a number of challenges are being faced by the WRB such as rapid growth of population, expending industrial activities, over-exploitation of water resources, unplanned urban growth, pollution, development of new infrastructure, maintenance and operation of existing infrastructure, etc. The overall key strategies for the WRB may be as follows:

1. Development of water storage infrastructure: To achieve climate resilience in the water sector, the storage capacity of the basin needs to be increased. The decentralized water storage infrastructure, e.g. dams, will make the basin to sustain the offset the alterations of precipitation and streamflow. Upgrading and restoring exiting water storage infrastructure should be given priority over creating new water storage infrastructure as many water storage infrastructures suffer from excessive sedimentation resulted in reduced storage capacity. The total storage capacity of the WRB is around 8.62% of its total annual flow needs to be improved. Apart from storage expansion perspective, these infrastructures must be considered for the safety perspective from extreme events i.g. floods.
2. Expansion of irrigated lands: Agriculture is still the largest user of water in the basin. Irrigated areas are one of the key adaptation measures that must be considered. Expanding irrigation in the command areas through creating of new canals and feeder channels networks shall provide the farming community liberty from the rainfed farming and they can go for more numbers of crops in a year.
3. Efficient use of water: As of now, the water-logged flood irrigation is being practised in most of the WRB. The farmers need to be educated about the proper & effective use of water. The water-conserving techniques such as the use of micro-irrigation, crop diversification, crop-rotation, zero tillage, mulching, etc. should necessarily be integrated into the overall plan of expanding command areas.
4. Water Pollution: Disposal of untreated sewage and industrial effluents from cities and towns located on the banks of the Wainganga and its tributaries results in chemical, biochemical and bacteriological contamination of the river water. The pollution of water effectively reduces freshwater availability for human and ecological needs. For example, the Kanhan and Kolar sub-basin has many industrial setups and largest urban centre, i.e. the city of Nagpur. The sub-basin needs special attention and checks on the water pollution and the groundwater extraction. Promotion and incentivisation of the recharging of groundwater, particularly in the regions with dark zones or water scarcity.
5. Analyses of baseline and future streamflow of the basin have clearly shown that there is high inter-annual variability in the runoff will result in a long dry spell of streamflow in the upper part of basins during lean-flows and could lead to hydrological droughts. This

can be dealt with the creation of additional water storages in large reservoirs and carry-over for use in years of drought.

6. The success of any project or adaptive strategy relies on the technical competence of the implementing agency. Institutional capacity building will play a crucial role to cope with climate change. A long-term program for capacity building on the significant aspects of climate change adaptation for different sectors will be a key strategy.

The integration of these adaptation strategies is essential for better managing the impacts of climate change and improving water and agricultural sector in the Wainganga River basin. It is also necessary for government agencies, water resources departments, meteorological departments and agriculture departments to raise awareness of the changes in climatic conditions by appropriate communication to the farmers through radio and television, extension services and non-governmental organizations.

6.3 CONCLUDING REMARKS

The adaption of human beings to climate change is a natural progression of the selection of surviving strategies. However, anthropogenic activities over the most recent couple of hundreds of years have accelerated the progression of climate, making it essential for the existent generation to take corrective measures. All-natural resources, including water, air, forest, soil, are a vital support system for life on earth.

CHAPTER 7: SUMMARY AND CONCLUSIONS

7.1 GENERAL

Changes in the climatic conditions are likely to impact several sectors, and the water resources are one of them to be impacted in many ways. Conversion of land-use to meet out multiple demands such as food, water, settlement, etc. for the ever-growing population have also created immense pressure on water resources, which is likely to intensify in future. These anticipated impacts of changing climate and land-use on the water resources will also impact other water-dependent sectors like agriculture, industry, forest, energy and urban. It is believed that these impacts of the changing climate and land-use will be felt more severely by the developing countries with agrarian-economy such as India. In India, about 85% of the water is used by the agricultural activities alone, and irrigation demands are likely to be increased substantially, water requirements for the human consumption are projected to be doubled, and water for the power sector is anticipated to increase many folds (ADB 2002). Therefore, considering the higher water demands in future and the anticipated adverse effects on the water resources in view of the changing climate and land-use, it is essential to investigate the impacts of changing climate and land-use on the future water availability and formulate appropriate adaptation strategies to cope up with the projected changes.

7.2 SUMMARY AND CONCLUSIONS

The research work reported in this report has been performed with the objectives of quantifying the impacts of changing climate and land-use on the hydrological response of the WRB in central India under various scenarios. The research focuses on historical as well as the expected future scenarios under varied climate and land-use conditions. In the present study, investigations the trends of the past and future data of temperature and precipitations was performed to ascertain that the climate change signs are apparent in the time-series.

For understanding the impacts of changing climate and land-use conditions on the streamflow in the study basin, it is imperative to simulate the future streamflow using the projected climate and land-use inputs for multiple scenarios. Therefore, the semi-distributed SWAT model was considered for the streamflow simulations. The model has been set up for the WRB up to Ashti, gauging site of Central Water Commission (CWC). The SWAT model performance was found very good during calibration and validation periods, and so, it has been used for simulating the flows under various combinations of climate and land-use.

Four numbers of bias-corrected and statistically downscaled GCMs, viz. BCC-CSM2-MR, EC-Earth3, MPI-ESM1-2-HR, and NorESM2-LM on half-degree grid size for four-time periods, viz., baseline (1951-2015) and three future periods, NFS: Near-Future Scenario (2025–2050), MFS: Mid-Future Scenario (2051–2075) and FFS: Far-Future Scenario (2076–2100). under two scenarios viz., SSP2 4.5 and SSP5 8.5 were used to examine the alterations in the coming climatic conditions as well for the modeling the hydrologic response of the study basin". An MLP-ANN-Markov based land-use model was used for simulating the land-use for the year 2030, 2040 and 2050 in future.

A weighted ensemble average approach was adopted to get the multi-model ensemble mean simulation from all four GCMs for three future periods. In this study, three different scenarios were considered to evaluate the individual and combined impacts of the changing climate and/or land-use change on streamflow.

Finally, the short-term and long-term adaptive strategies for the WRB are suggested to cope with the impacts on the flow regime caused due to the projected changes in the climate and land-use.

Based on the study, the following conclusions can be drawn:

1. The distinct impacts of changing climate and land-use on the hydrologic response of the WRB was observed, particularly in the monthly variations of streamflow. Results of the study confirmed the decreased streamflow initially in the early periods of the 21st century and increased streamflow towards the mid and end of the 21st century under both SSP2 4.5 and SSP5 8.5.

2. The Basin hydrology seems to be intensified during the mid and far future period, particularly under SSP-585 scenario.

3. Average monthly streamflow decreased for July, August and September months from 0.4% to 30.5% for SSP245 and 6.0% to 14.9% for SSP585 during the near future period of the 21st century.

4. The mid and far future periods are confirming the significant increase in these months, 4.1% to 34% for SSP245 and 8.1% to 65.2% for SSP585.

5. In the Monsoon season, flows are getting larger in the mid and far future periods of the 21st century.

6. In addition, monthly flows are increased in winter (Oct-Jan) and decrease in summer and autumn (Feb-April).
7. The mean monthly flows vary significantly throughout the year and are relatively high in monsoon Jun-Sep.
8. Land-use change had a relatively minor impact on flows as compared to impacts caused by to changing climate. As urbanisation advances, the flow in the river during the long wet spells increases and declines during the dry periods. It is crucial to consider land-use change patterns and for the moderation of the ill effects of extreme events such as floods and droughts.
9. The collective impacts of changing climate and land-use on hydrological behaviour were analogous to those of changing climate alone, however with augmented flows.
10. Effective adaption strategies need to be formulated to deal with the ill impacts of climate change by integrating future climatic conditions, hydrological modeling, physiography of basin, local wisdom and water resources vulnerability mapping.
11. Water harvesting structures such as check dam, farm pond, etc. and techniques, i.e. zero tillage, SRI, water-resistance crops etc. are recommended for the study basin.

7.3 SCOPE OF FUTURE WORKS

1. Impact assessment of climate change on the other hydrological processes such as sediment yield etc. may be investigated.
2. Responses of groundwater dynamics in the WRB can be explored under the changing conditions of climate and land-use patterns as the base flow is a significant regulator of the river flow.
3. The work can be extended for the whole of the Godavari basin, which might be a moderately challenging task and extensive data and information may be needed.

REFERENCES

Abbaspour, K. C., S. A. Vaghefi, and R. Srinivasan. 2017. A guideline for successful calibration and uncertainty analysis for soil and water assessment: A review of papers from the 2016 international SWAT conference. Water (Switzerland) 10(1).

Abbaspour, K. C., J. Yang, I. Maximov, R. Siber, K. Bogner, J. Mieleitner, J. Zobrist, and R. Srinivasan. 2007. Modelling hydrology and water quality in the pre-alpine/alpine Thur watershed using SWAT. Journal of Hydrology 333(2–4):413–430.

Adamowski, K., and J. Bougadis. 2003. Detection of trends in annual extreme rainfall. Hydrological Processes 17(18):3547–3560.

ADB. 2002. Water resources development in India: Critical issues and strategic options (2002):1–34.

Adger, W. N. 1999. Social vulnerability to climate change and extremes in coastal Vietnam. World development 27(2):249–269.

Adger, W. N., S. Agrawal, M. M. W. Mirza, C. Conde, K. L. O'brien, J. Pulhin, R. Pulwarty, B. Smit, and K. Takahashi. 2007. Assessment of adaptation practices, options, constraints and capacity (2007).

Ahmadizadeh, S., M. Yousefi, and M. Saghafi. 2014. Land use change detection using remote sensing and artificial neural network: Application to Birjand, Iran. Computational Ecology and Software 4(4):276–288.

Ahmed, B., and R. Ahmed. 2012. Modeling urban land cover growth dynamics using multi-temporal satellite images: A case study of Dhaka, Bangladesh. ISPRS International Journal of Geo-Information 1(1):3–31.

Ajami, N. K., Q. Duan, and S. Sorooshian. 2007. An integrated hydrologic Bayesian multimodel combination framework: Confronting input, parameter, and model structural uncertainty in hydrologic prediction. Water resources research 43(1).

Alberti, M., and P. Waddell. 2000. An integrated urban development and ecological simulation model. Integrated Assessment 1(3):215–227.

Alexandersson, H. 1986. A homogeneity test applied to precipitation data. Journal of climatology 6(6):661–675.

Alexandersson, H., and A. Moberg. 1997. Homogenization of Swedish temperature data. Part I: Homogeneity test for linear trends. International Journal of Climatology: A Journal of the

Royal Meteorological Society 17(1):25–34.

Allen, M. R., P. A. Stott, J. F. B. Mitchell, R. Schnur, and T. L. Delworth. 2000. Quantifying the uncertainty in forecasts of anthropogenic climate change . Nature 407(6804):617–620.

Allen, P. M. 2012. Cities and regions as self-organizing systems: models of complexity. Routledge.

Arnell, N. W. 1999. Climate change and global water resources. Global Environmental Change (1999):S31–S49.

Arnold, J. G., J. R. Kiniry, R. Srinivasan, J. R. Williams, E. B. Haney, and S. L. Neitsch. 2012. ArcSWAT Input Output Documentation 2012 (2012).

Arnold, J., R. Srinivasan, R. Muttiah, and J. Williams. 1998. Large Area Hydrologic Modeling and Assessment Part I: Model Development. JOURNAL OF THE AMERICANWATERRESOURCES ASSOCIATION 34(1):73–89.

Arsanjani, J. J., W. Kainz, and A. J. Mousivand. 2011. Tracking dynamic land-use change using spatially explicit Markov Chain based on cellular automata: the case of Tehran. International Journal of Image and Data Fusion 2(4):329–345.

Arunyawat, S., and R. P. Shrestha. 2018. Simulating future land use and ecosystem services in Northern Thailand. Journal of Land Use Science 13(1–2):146–165.

Atkinson, P. M., and A. R. L. Tatnall. 1997. Introduction neural networks in remote sensing. International Journal of remote sensing 18(4):699–709.

Basheer, A. K., H. Lu, A. Omer, A. B. Ali, and A. M. S. Abdelgader. 2016. Impacts of climate change under CMIP5 RCP scenarios on the streamflow in the Dinder River and ecosystem habitats in Dinder National Park, Sudan. Hydrology and Earth System Sciences 20(4):1331–1353.

Bhave, A. G., A. Mishra, and N. S. Raghuwanshi. 2014. A brief review of assessment approaches that support evaluation of climate change adaptation options in the water sector. Water policy 16(5):959–972.

Bhelawe, S., J. L. Chaudhary, A. S. Nain, R. Singh, R. Khavse, and S. K. Chandrawanshi. 2014. Rainfall Variability in Chhattisgarh State Using GIS 9(2):519–524.

Bhutiyani, M. R., V. S. Kale, and N. J. Pawar. 2007. Long-term trends in maximum, minimum and mean annual air temperatures across the Northwestern Himalaya during the twentieth century. Climatic Change 85(1–2):159–177.

Borah, D. K., and M. Bera. 2003. Watershed-scale hydrologic and nonpoint-source pollution models: Review of mathematical bases. Transactions of the ASAE 46(6):1553.

Bosshard, T., M. Carambia, K. Goergen, S. Kotlarski, P. Krahe, M. Zappa, C. Schär, and C. Schar. 2013. Quantifying uncertainty sources in an ensemble of hydrological climate-impact projections: UNCERTAINTY SOURCES IN CLIMATE-IMPACT PROJECTIONS. Water Resources Research 49(3):1523–1536.

Brakensiek, D. L., C. T. Haan, and H. P. Johnson. 1982. Hydrologic modeling of small watersheds. American Society of Agricultural Engineers.

Brooks, N., W. N. Adger, and P. M. Kelly. 2005. The determinants of vulnerability and adaptive capacity at the national level and the implications for adaptation. Global Environmental Change 15(2):151–163.

Cannarozzo, M., L. V. Noto, and F. Viola. 2006. Spatial distribution of rainfall trends in Sicily (1921-2000). Physics and Chemistry of the Earth 31(18):1201–1211.

Chen, H., S. Guo, C. yu Xu, and V. P. Singh. 2007. Historical temporal trends of hydro-climatic variables and runoff response to climate variability and their relevance in water resource management in the Hanjiang basin. Journal of Hydrology 344(3–4):171–184.

Chen, J., F. P. Brissette, and R. Leconte. 2011. Uncertainty of downscaling method in quantifying the impact of climate change on hydrology. Journal of Hydrology 401(3–4):190–202.

Chen, W., S. L. Cutter, C. T. Emrich, and P. Shi. 2013. Measuring social vulnerability to natural hazards in the Yangtze River Delta region, China. International Journal of Disaster Risk Science 4(4):169–181.

Dadhich, P. N., and S. Hanaoka. 2011. Spatio-temporal urban growth modeling of Jaipur, India. Journal of Urban Technology 18(3):45–65.

Dettinger, M. D., D. R. Cayan, M. K. Meyer, and A. E. Jeton. 2004. Simulated Hydrologic Responses To Climate Variations. Climatic Change 62 (2004):283–317.

Devia, G. K., B. P. Ganasri, and G. S. Dwarakish. 2015. A review on hydrological models. Aquatic Procedia 4 (2015):1001–1007.

Diem, J. E., T. C. Hill, and R. A. Milligan. 2018. Diverse multi-decadal changes in streamflow within a rapidly urbanizing region. Journal of Hydrology 556 (2018):61–71.

Dixon, B., and J. Earls. 2012. Effects of urbanization on streamflow using SWAT with real and simulated meteorological data. Applied Geography 35(1):174–190.

Eastman, J. R. 2012a. Idrisi selva tutorial. Idrisi Production, Clark Labs-Clark University 45 (2012):51–63.

Errasti, I., A. Ezcurra, J. Sáenz, and G. Ibarra-Berastegi. 2011. Validation of IPCC AR4 models over the Iberian Peninsula. Theoretical and Applied Climatology 103(1–2):61–79.

Epule, T. E., J. D. Ford, S. Lwasa, and L. Lepage. 2017. Climate change adaptation in the Sahel. Environmental Science & Policy 75 (2017):121–137.

Falkenmark, M. 1995. Land and water integration and river basin management. FAO Land and Water Bulletin 1 (1995):15–16.

Fankhauser, S., R. S. J. Tol, and D. W. Pearce. 1997. The aggregation of climate change damages: a welfare theoretic approach. Environmental and Resource Economics 10(3):249–266.

Früh, B., J. W. Schipper, A. Pfeiffer, and V. Wirth. 2006. A pragmatic approach for downscaling precipitation in alpine-scale complex terrain. Meteorologische Zeitschrift 15(6):631–646.

FSI. 2017. India State of Forest (ISF) Report 2017 of Forest Survey of India (FSI) an organization under the Ministry of Environment Forest & Climate Change Government of India. New Delhi.

Gadgil, M. V. 1986. Agricultural credit in India: A review of performance and policies. Indian Journal of Agricultural Economics 41(902-2018–2457):282–309.

Galkate, R., T. Thomas, R. Jaiswal, S. Singh, S. Awadhiya, D. Sonkusale, A. Verma, R. Sharma, T. Chandrakar, and J. Dass. 2014. Purpose Driven Study (PDS): Water Availability Study and Supply-Demand Analysis in Kharun Sub-Basin of WRB in Chhattisgarh State.

Garg, V., S. P. Aggarwal, P. K. Gupta, B. R. Nikam, P. K. Thakur, S. K. Srivastav, and A. Senthil Kumar. 2017. Assessment of land use land cover change impact on hydrological regime of a basin. Environmental Earth Sciences 76(18).

Giorgi, F., and L. O. Mearns. 2003. Probability of regional climate change based on the Reliability Ensemble Averaging (REA) method. Geophysical Research Letters 30(12):2–5.

Gosain, A. K., S. Rao, and D. Basuray. 2006. Climate change impact assessment on hydrology of Indian river basins. Current Science 90(3):346–353.

Goyal, M. K., and A. K. Sarma. 2017. Analysis of the change in temperature trends in Subansiri

River basin for RCP scenarios using CMIP5 datasets. Theoretical and Applied Climatology 129(3–4):1175–1187.

Van Griensven, A. 2005. Sensitivity, auto-calibration, uncertainty and model evaluation in SWAT2005. Unpublished report 25 (2005).

van Griensven, A., T. Meixner, S. Grunwald, T. Bishop, M. Diluzio, and R. Srinivasan. 2006. A global sensitivity analysis tool for the parameters of multi-variable catchment models. Journal of Hydrology 324(1–4):10–23.

Griggs, D. J., and M. Noguer. 2002. Climate change 2001: the scientific basis. Contribution of working group I to the third assessment report of the intergovernmental panel on climate change. Weather 57(8):267–269.

Guan, D., H. Li, T. Inohae, W. Su, T. Nagaie, and K. Hokao. 2011. Modeling urban land use change by the integration of cellular automaton and Markov model. Ecological Modelling (2011).

Guhathakurta, P., and M. Rajeevan. 2008. Trends in the rainfall pattern over India. International Journal of Climatology: A Journal of the Royal Meteorological Society 28(11):1453–1469.

Hargreaves, G. H., and Z. A. Samani. 1985. Reference crop evapotranspiration from temperature. Applied engineering in agriculture 1(2):96–99.

Haylock, M., and N. Nicholls. 2000. Trends in extreme rainfall indices for an updated high quality data set for Australia, 1910–1998. International Journal of Climatology: A Journal of the Royal Meteorological Society 20(13):1533–1541.

Helsel, D. R., and R. M. Hirsch. 1992. Statistical methods in water resources. Elsevier.

Helton, J. C., and F. J. Davis. 2003. Latin hypercube sampling and the propagation of uncertainty in analyses of complex systems. Reliability Engineering & System Safety 81(1):23–69.

Hendon, H. H., D. W. J. Thompson, and M. C. Wheeler. 2007. Australian rainfall and surface temperature variations associated with the Southern Hemisphere annular mode. Journal of Climate 20(11):2452–2467.

Her, Y., S. H. Yoo, J. Cho, S. Hwang, J. Jeong, and C. Seong. 2019. Uncertainty in hydrological analysis of climate change: multi-parameter vs. multi-GCM ensemble predictions. Scientific Reports 9(1):1–22.

Hiremath, D. B., and R. L. Shiyani. 2012. Evaluating regional vulnerability to climate change: A case of Saurashtra. Indian Journal of Agricultural Economics 67(3):334–344.

Hirsch, R. M., and J. R. Slack. 1984. A nonparametric trend test for seasonal data with serial dependence. Water Resources Research 20(6):727–732.

Hirsch, R. M., J. R. Slack, and R. A. Smith. 1982. Techniques of trend analysis for monthly water quality data. Water resources research 18(1):107–121.

Huang, D., W. Y. Licuanan, B. W. Hoeksema, C. A. Chen, P. O. Ang, H. Huang, D. J. W. Lane, S. T. Vo, Z. Waheed, and Y. A. Affendi. 2015. Extraordinary diversity of reef corals in the South China Sea. Marine Biodiversity 45(2):157–168.

Huang, J., J. Zhang, Z. Zhang, and C. Y. Xu. 2013. Spatial and temporal variations in rainfall erosivity during 1960-2005 in the Yangtze River basin. Stochastic Environmental Research and Risk Assessment 27(2):337–351.

Jain, M., and S. D. Sharma. 2014. Hydrological Modeling of Vamsadhara River Basin , India using SWAT (2014).

Jain, S. K., P. K. Agarwal, and V. P. Singh. 2007. Hydrology and water resources of India. Springer Science & Business Media.

Jain, S. K., and V. Kumar. 2012. Trend analysis of rainfall and temperature data for India. Current Science(Bangalore) 102(1):37–49.

Jain, S. K., and V. P. Singh. 2003. Water Resources Systems Planning and Management. First. Amsterdam: Elsevier Ltd.

Jain, S. K., J. Tyagi, and V. Singh. 2010. Simulation of runoff and sediment yield for a Himalayan watershed using SWAT model. Journal of Water Resource and Protection 2(03):267.

Jaiswal, R. K., H. L. Tiwari, and A. K. Lohani. 2017. Assessment of climate change impact on rainfall for studying water availability in upper mahanadi catchment, India. Journal of Water and Climate Change 8(4):755–770.

Jokar, J., M. Helbich, W. Kainz, and A. Darvishi. 2013. International Journal of Applied Earth Observation and Geoinformation Integration of logistic regression , Markov chain and cellular automata models to simulate urban expansion. International Journal of Applied Earth Observations and Geoinformation 21 (2013):265–275.

Jones, B., and B. C. O'Neill. 2016. Spatially explicit global population scenarios consistent with the Shared Socioeconomic Pathways. Environmental Research Letters 11(8).

Jones, B., and B. C. O'Neill. 2017. Global Population Projection Grids Based on Shared Socioeconomic Pathways (SSPs), 2010-2100. Socioecon. Data Appl. Cent.[online] Available from: https://doi. org/10.7927/H4RF5S0P (Accessed 3 July 2018) (2017).

Kampata, J. M., B. P. Parida, and D. B. Moalafhi. 2008. Trend analysis of rainfall in the headstreams of the Zambezi River Basin in Zambia. Physics and Chemistry of the Earth 33(8–13):621–625.

Kanianska, R., M. Kizeková, J. Nováček, and M. Zeman. 2014. Land-use and land-cover changes in rural areas during different political systems: A case study of Slovakia from 1782 to 2006. Land Use Policy 36 (2014):554–566.

Karl, T. R., and R. W. Knight. 1998. Secular trends of precipitation amount, frequency, and intensity in the United States. Bulletin of the American Meteorological society 79(2):231–242.

Kauffeldt, A., F. Wetterhall, F. Pappenberger, P. Salamon, and J. Thielen. 2016. Technical review of large-scale hydrological models for implementation in operational flood forecasting schemes on continental level. Environmental Modelling & Software 75 (2016):68–76.

Kavetski, D., G. Kuczera, and S. W. Franks. 2006. Bayesian analysis of input uncertainty in hydrological modeling: 1. Theory. Water resources research 42(3).

Kendall, M. 1975. Multivariate analysis. Charles Griffin & Company Ltd.

Khalkho, D. 2017. Distributed parameter modelling for development of effective watershed management plan of upper mahanadi basin. IGKV, Raipur.

Kim, J., J. Choi, C. Choi, and S. Park. 2013a. Impacts of changes in climate and land use/land cover under IPCC RCP scenarios on streamflow in the Hoeya River Basin, Korea. Science of the Total Environment 452–453 (2013):181–195.

Kim, J., J. Choi, C. Choi, and S. Park. 2013b. Impacts of changes in climate and land use/land cover under IPCC RCP scenarios on streamflow in the Hoeya River Basin, Korea. Science of the Total Environment 452–453 (2013):181–195.

King, A. D., L. V Alexander, and M. G. Donat. 2013. The efficacy of using gridded data to examine extreme rainfall characteristics: a case study for Australia. International Journal of Climatology 33(10):2376–2387.

Klein Tank, A. M. G., and G. P. Können. 2003. Trends in indices of daily temperature and precipitation extremes in Europe, 1946–99. Journal of climate 16(22):3665–3680.

Kocabas, V., and S. Dragicevic. 2006. Assessing cellular automata model behaviour using a sensitivity analysis approach. Computers, Environment and Urban Systems (2006).

Krause, P., D. P. Boyle, and F. Bäse. 2005. Comparison of different efficiency criteria for hydrological model assessment. Advances in geosciences 5 (2005):89–97.

Kumar, V., S. K. Jain, and Y. Singh. 2010. Analysis of long-term rainfall trends in India. Hydrological Sciences Journal–Journal des Sciences Hydrologiques 55(4):484–496.

Kumari, S., R. Jha, V. Singh, K. Baier, and M. K. Sinha. 2016. Groundwater vulnerability assessment using SINTACS model and GIS in Raipur and Naya Raipur, Chhattisgarh, India. Indian Journal of Science and Technology 9 (2016):1–6.

Kundzewicz, Z. W., M. Radziejewski, and I. Pinskwar. 2006. Precipitation extremes in the changing climate of Europe. Climate Research 31(1):51–58.

Kundzewicz, Z. W., and A. J. Robson. 2004. Change detection in hydrological records—a review of the methodology/revue méthodologique de la détection de changements dans les chroniques hydrologiques. Hydrological sciences journal 49(1):7–19.

Lal, R. 2015. World water resources and achieving water security. Agronomy Journal 107(4):1526–1532.

Landsea, C. W., and W. M. Gray. 1992. The strong association between western Sahelian monsoon rainfall and intense Atlantic hurricanes. Journal of Climate 5(5):435–453.

Lawin, A. E., N. R. Hounguè, C. A. Biaou, and D. F. Badou. 2019. Statistical analysis of recent and future rainfall and temperature variability in the Mono River watershed (Benin, Togo). Climate 7(1).

Lebel, T., and A. Ali. 2009. Recent trends in the Central and Western Sahel rainfall regime (1990-2007). Journal of Hydrology 375(1–2):52–64.

Lebel, T., G. Bastin, C. Obled, and J. D. Creutin. 1987. On the accuracy of areal rainfall estimation: a case study. Water Resources Research 23(11):2123–2134.

Legates, D. R., and G. J. McCabe Jr. 1999. Evaluating the use of "goodness-of-fit" measures in hydrologic and hydroclimatic model validation. Water resources research 35(1):233–241.

Letcher, R. A., B. F. W. Croke, and A. J. Jakeman. 2007. Integrated assessment modelling for water resource allocation and management: A generalised conceptual framework.

Environmental Modelling & Software 22(5):733–742.

Liu, Y., and H. V Gupta. 2007. Uncertainty in hydrologic modeling: Toward an integrated data assimilation framework. Water Resources Research 43(7).

Lu, J., X. Cui, X. Chen, S. Sauvage, and J.-M. Sanchez Perez. 2017. Evaluation of hydrological response to extreme climate variability using SWAT model: application to the Fuhe basin of Poyang Lake watershed, China. Hydrology Research 48(6):1730–1744.

de Luis, M., M. Brunetti, J. C. Gonzalez-Hidalgo, L. A. Longares, and J. Martin-Vide. 2010. Changes in seasonal precipitation in the Iberian Peninsula during 1946-2005. Global and Planetary Change 74(1):27–33.

Di Luzio, M., R. Srinivasan, and J. G. Arnold. 2004. A GIS-coupled hydrological model system for the watershed assessment of agricultural nonpoint and point sources of pollution. Transactions in GIS 8(1):113–136.

MacKellar, N., M. New, and C. Jack. 2014. Observed and modelled trends in rainfall and temperature for South Africa: 1960-2010. South African Journal of Science 110(7–8):1–13.

Madsen, H., D. Lawrence, M. Lang, M. Martinkova, and T. R. Kjeldsen. 2014. Review of trend analysis and climate change projections of extreme precipitation and floods in Europe. Journal of Hydrology 519 (2014):3634–3650.

Maithani, S. 2015. Neural networks-based simulation of land cover scenarios in Doon valley, India. Geocarto International 30(2):163–185.

Maithani, S., M. K. Arora, and R. K. Jain. 2010. An artificial neural network based approach for urban growth zonation in Dehradun city, India. Geocarto International 25(8):663–681.

Maity, R., A. Sharma, D. Nagesh Kumar, and K. Chanda. 2012. Characterizing drought using the reliability-resilience-vulnerability concept. Journal of Hydrologic Engineering 18(7):859–869.

Mall, R. K. 2016. Water resources in India and impact of climate change Water Resources in India and Impact of Climate Change 22(January 2007):157–176.

Mango, L. M., A. M. Melesse, M. E. McClain, D. Gann, and S. G. Setegn. 2011. Land use and climate change impacts on the hydrology of the upper Mara River Basin, Kenya: Results of a modeling study to support better resource management. Hydrology and Earth System Sciences 15(7):2245–2258.

Mann, H. B. 1945. Nonparametric tests against trend. Econometrica: Journal of the Econometric Society (1945):245–259.

Matthews, R. B., N. G. Gilbert, A. Roach, J. G. Polhill, and N. M. Gotts. 2007. Agent-based land-use models: a review of applications. Landscape Ecology 22(10):1447–1459.

McCabe, G. J., M. P. Clark, and L. E. Hay. 2007. Rain-on-snow events in the western United States. Bulletin of the American Meteorological Society 88(3):319–328.

McKay, M. D., R. J. Beckman, and W. J. Conover. 2000. A comparison of three methods for selecting values of input variables in the analysis of output from a computer code. Technometrics 42(1):55–61.

Meena, P. K., D. Khare, and M. K. Nema. 2016. Constructing the downscale precipitation using ANN model over the Kshipra river basin, Madhya Pradesh. Journal of Agrometeorology 18(1).

Mehrotra, R., A. Sharma, D. N. Kumar, and T. V Reshmidevi. 2013. Assessing future rainfall projections using multiple GCMs and a multi-site stochastic downscaling model. Journal of hydrology 488 (2013):84–100.

Meshram, S. G., V. P. Singh, and C. Meshram. 2016. Long-term trend and variability of precipitation in Chhattisgarh State, India. Theoretical and Applied Climatology(April).

Middelkoop, H., K. Daamen, D. Gellens, W. Grabs, J. C. J. Kwadijk, H. Lang, B. W. a H. Parmet, J. Schulla, and K. Wilke. 2001. Impact of Climate Change on Hydrological Regimes and Water Resource Management in the Rhine River Basin. Climatic Change 49 (2001):105–128.

Mirza, M. M. Q. 2002. Global warming and changes in the probability of occurrence of floods in Bangladesh and implications 12 (2002):127–138.

Mirza, M. Q., R. A. Warrick, N. J. Ericksen, and G. J. Kenny. 1998. Trends and persistence in precipitation in the Ganges, Brahmaputra and Meghna river basins. Hydrological Sciences Journal 43(6):845–858.

Mishra, V., and R. Lilhare. 2016. Hydrologic sensitivity of Indian sub-continental river basins to climate change. Global and Planetary Change 139 (2016):78–96.

Mishra, V. N., and P. K. Rai. 2016. A remote sensing aided multi-layer perceptron-Markov chain analysis for land use and land cover change prediction in Patna district (Bihar), India. Arabian Journal of Geosciences 9(4).

Monteith, J. L. 1965. Evaporation and environment. *In* Symposia of the society for experimental biology, 205–234. Cambridge University Press (CUP) Cambridge.

MoWR. 2008. Preliminary Consolidated Report on Effects of Climate Change on Water Resources. India.

Murthy, C. S., B. Laxman, and M. V. R. Sesha Sai. 2015. Geospatial analysis of agricultural drought vulnerability using a composite index based on exposure, sensitivity and adaptive capacity. International Journal of Disaster Risk Reduction 12 (2015):163–171.

Narayana, V. V. D. 1993. Soil and water conservation research in India. Publications and Information Division, Indian Council of Agricultural Research.

Narsimlu, B., A. K. Gosain, and B. R. Chahar. 2013. Assessment of Future Climate Change Impacts on Water Resources of Upper Sind River Basin, India Using SWAT Model. Water Resources Management 27(10):3647–3662.

Nash, J. E., and J. V Sutcliffe. 1970. River flow forecasting through conceptual models part I— A discussion of principles. Journal of hydrology 10(3):282–290.

Neitsch, S., J. G. Arnold, J. R. Kiniry, and J. R. Williams. 2011. Soil and Water Assessment Tool: Theoretical Documentation Version 2009. TEXAS.

Nema, M. K., S. K. Jain, and P. K. Mishra. 2014. Sptial and temporal distribution of rainfall trends in Bist-Doab region of Punjab (1901–2010) (2014).

Nema, M. K., D. Khare, J. Adamowski, and S. K. Chandniha. 2018. Spatio-temporal analysis of rainfall trends in Chhattisgarh State, Central India over the last 115 years. Journal of Water and Land Development 36(1).

New, M., and M. Hulme. 2000. Representing uncertainty in climate change scenarios: a Monte-Carlo approach. Integrated Assessment 1(3):203–213.

Nilawar, A. P., and M. L. Waikar. 2019. Impacts of climate change on streamflow and sediment concentration under RCP 4.5 and 8.5: A case study in Purna river basin, India. Science of the Total Environment 650 (2019):2685–2696.

Nóbrega, M. T., W. Collischonn, C. E. M. Tucci, and A. R. Paz. 2011. Uncertainty in climate change impacts on water resources in the Rio Grande Basin, Brazil. Hydrology and Earth System Sciences 15(2):585–595.

Pandey, B. K. 2017. Hydrological response simulation under land use and climate change scenarios. Unpublished PhD Thesis at Indian Institute of Technology, Roorkee

Pandey, B. K., and D. Khare. 2017. Analyzing and modeling of a large river basin dynamics applying integrated cellular automata and Markov model. Environmental Earth Sciences 76(22):1–12.

Pandey, B., Q. Zhang, and K. C. Seto. 2018. Time series analysis of satellite data to characterize multiple land use transitions: a case study of urban growth and agricultural land loss in India. Journal of Land Use Science 13(3):221–237.

Partal, T., and E. Kahya. 2006. Trend analysis in Turkish precipitation data. Hydrological Processes 20(9):2011–2026.

Partoyo, and R. P. Shrestha. 2013. Monitoring farmland loss and projecting the future land use of an urbanized watershed in Yogyakarta, Indonesia. Journal of Land Use Science 8(1):59–84.

Paul, S. S., J. Li, R. Wheate, and Y. Li. 2018. Application of Object Oriented Image Classification and Markov Chain Modeling for Land Use and Land Cover Change Analysis. Journal of Environmental Informatics 31(1).

Pettitt, A. N. 1979b. A non-parametric approach to the change-point problem. Applied Statistics 28(2):126–135.

Pijanowski, B. C., D. G. Brown, B. A. Shellito, and G. A. Manik. 2002. Using neural networks and GIS to forecast land use changes: A Land Transformation Model. Computers, Environment and Urban Systems (2002).

Praskievicz, S., and H. Chang. 2009. A review of hydrological modelling of basin-scale climate change and urban development impacts. Progress in Physical Geography 33(5):650–671.

Priestley, C. H. B., and R. J. Taylor. 1972. On the assessment of surface heat flux and evaporation using large-scale parameters. Monthly weather review 100(2):81–92.

Qin, N., X. Chen, G. Fu, J. Zhai, and X. Xue. 2010. Precipitation and temperature trends for the Southwest China: 1960–2007. Hydrological processes 24(25):3733–3744.

Räisänen, J., and T. N. Palmer. 2001. A probability and decision-model analysis of a multimodel ensemble of climate change simulations. Journal of Climate 14(15):3212–3226.

Raju, K. S., and D. N. Kumar. 2014. Ranking of global climate models for India using multicriterion analysis. Climate Research 60(2):103–117.

Rao, A. R., and K. H. Hamed. 1997. Regional frequency analysis of Wabash River flood data by

L-moments. Journal of Hydrologic Engineering 2(4):169–179.

Ravindranath, N. H., S. Rao, N. Sharma, M. Nair, and R. Gopalkrishnan. 2011. Climate change vulnerability profiles for North East India. Current Science 101(August):384–394.

Rebetez, M., and M. Dobbertin. 2004. Climate change may already threaten Scots pine stands in the Swiss Alps. Theoretical and applied climatology 79(1–2):1–9.

Rees, H. G., K. M. Croker, N. S. Reynard, and A. Gustard. 1997. 2 The Spatial and Temporal Variability of Hydrological Regimes: Mean Runoff-Estimation of renewable water resources in the European Union. IAHS Publications-Series of Proceedings and Reports-Intern Assoc Hydrological Sciences 246 (1997):23–30.

Reichler, T., and J. Kim. 2008. How well do coupled models simulate today's climate? Bulletin of the American Meteorological Society 89(3):303–312.

Renard, B., D. Kavetski, G. Kuczera, M. Thyer, and S. W. Franks. 2010. Understanding predictive uncertainty in hydrologic modeling: The challenge of identifying input and structural errors. Water Resources Research 46(5):1–22.

Reshmidevi, T. V., D. Nagesh Kumar, R. Mehrotra, and A. Sharma. 2018. Estimation of the climate change impact on a catchment water balance using an ensemble of GCMs. Journal of Hydrology 556 (2018):1192–1204.

Rosenthal, W. D., R. Srinivasan, and J. G. Arnold. 1995. Alternative river management using a linked GIS-hydrology model. Transactions of the ASAE 38(3):783–790.

Saltelli, A., K. Chan, and E. Scott. 2009. Sensitivity Analysis. New York: Wiley Online Library.

Samat, N., R. Hasni, and Y. A. E. Elhadary. 2011. Modelling Land Use Changes at the Peri-Urban Areas using Geographic Information Systems and Cellular Automata Model. Journal of Sustainable Development (2011).

Sang, L., C. Zhang, J. Yang, D. Zhu, and W. Yun. 2011. Simulation of land use spatial pattern of towns and villages based on CA-Markov model. Mathematical and Computer Modelling 54(3–4):938–943.

Santoro, M., G. Kirches, J. Wevers, M. Boettcher, C. Brockmann, C. Lamarche, S. Bontemps, I. Moreau, and P. Defourny. 2017. Land Cover CCI Product User Guide V2.0.

Sayemuzzaman, M., and M. K. Jha. 2014. Seasonal and annual precipitation time series trend analysis in North Carolina, United States. Atmospheric Research 137 (2014):183–194.

Sharma, K. D., and B. Soni. 2006. Land use diversification for sustainable rainfed agriculture. Atlantic Publishers & Dist.

Sharma, R. H., and N. M. Shakya. 2006. Hydrological changes and its impact on water resources of Bagmati watershed, Nepal. Journal of Hydrology 327(3–4):315–322.

Shekhar, M. S., H. Chand, S. Kumar, K. Srinivasan, and A. Ganju. 2010. Climate-change studies in the western Himalaya. Annals of Glaciology 51(54):105–112.

Shilpakar, R. L., W. G. M. M. Bastiaanssen, D. J. Molden, R. L. Shilpakar, W. G. M. M. Bastiaanssen, and D. J. Molden. 2011. A Remote Sensing-Based Approach for Water Accounting in the East Rapti River Basin, Nepal. Himalayan Journal of Sciences 17 (9)(9):15–30.

Shrestha, A. B., C. P. Wake, P. A. Mayewski, and J. E. Dibb. 1999. Maximum temperature trends in the Himalaya and its vicinity: an analysis based on temperature records from Nepal for the period 1971–94. Journal of climate 12(9):2775–2786.

Siddiqui, A. A., A. A. Siddiqui, S. Maithani, A. K. Jha, P. Kumar, and S. K. Srivastav. 2017. Urban growth dynamics of an Indian metropolitan using CA Markov and Logistic Regression. Egyptian Journal of Remote Sensing and Space Science 21(3):229–236.

Siebert, S., J. Burke, J. M. Faures, K. Frenken, J. Hoogeveen, P. Döll, and F. T. Portmann. 2010. Groundwater use for irrigation – a global inventory. Hydrol. Earth Syst. Sci. 14(10):1863–1880.

Sikorska, A. E., and B. Renard. 2017. Calibrating a hydrological model in stage space to account for rating curve uncertainties: general framework and key challenges. Advances in Water Resources 105 (2017):51–66.

Singh, J., H. V. Knapp, J. G. Arnold, and M. Demissie. 2005. Hydrological modeling of the Iroquois river watershed using HSPF and SWAT 1. JAWRA Journal of the American Water Resources Association 41(2):343–360.

Singh, P., V. Kumar, T. Thomas, and M. Arora. 2008. Changes in rainfall and relative humidity in river basins in northwest and central India. Hydrological Processes: An International Journal 22(16):2982–2992.

Singh, V. P., and V. P. Singh. 1992. Elementary hydrology. Prentice Hall Englewood Cliffs.

Sinha, R., and U. S. De. 2003. Climate change in India as evidenced from instrumental records. Bulletin of the World Meteorological Organization 52(1):53–58.

Sloan, P. G., and I. D. Moore. 1984. Modeling subsurface stormflow on steeply sloping forested watersheds. Water Resources Research 20(12):1815–1822.

Sloan, P. G., I. D. Moore, G. B. Coltharp, and J. D. Eigel. 1983. Modeling surface and subsurface stormflow on steeply-sloping forested watersheds (1983).

Smit, B., and J. Wandel. 2006. Adaptation, adaptive capacity and vulnerability. Global Environmental Change 16(3):282–292.

Sonali, P., and D. N. Kumar. 2013. Review of trend detection methods and their application to detect temperature changes in India. Journal of Hydrology 476 (2013):212–227.

Sonali, P., and D. Nagesh Kumar. 2016. Spatio-temporal variability of temperature and potential evapotranspiration over India. Journal of Water and Climate Change 7(4):810–822.

Sowmiya, S., and C. Arul. 2017. Simulation of Runoff for an Agricultural Watershed Using SWAT Model (2017):11505–11512.

Sreedevi, P. D., S. Owais, H. H. Khan, and S. Ahmed. 2009. Morphometric analysis of a watershed of South India using SRTM data and GIS. Journal of the Geological Society of India 73(4):543–552.

Srivastava, A., M. Rajeevan, and S. Kshirsagar. 2009. Development of a high resolution daily gridded temperature data set (1969 – 2005) for the Indian region. Atmospheric Science Letters 10(October):249–254.

Surabuddin Mondal, M., N. Sharma, M. Kappas, and P. K. Garg. 2013. Modeling of spatio-temporal dynamics of land use and land cover in a part of Brahmaputra River basin using Geoinformatic techniques. Geocarto International 28(7):632–656.

Tattoni, C., M. Ciolli, and F. Ferretti. 2011. The fate of priority areas for conservation in protected areas: a fine-scale Markov chain approach. Environmental Management 47(2):263–278.

Tebald, C., R. L. Smith, D. Nychka, and L. O. Meatns. 2005. J Climate 2005 Tebaldi (2005):1–17.

Tim, U. S., and R. Jolly. 1994. Evaluating agricultural nonpoint-source pollution using integrated geographic information systems and hydrologic/water quality model. Journal of environmental quality 23(1):25–35.

Tomer, M. D., and K. E. Schilling. 2009. A simple approach to distinguish land-use and climate-change effects on watershed hydrology. Journal of Hydrology 376(1–2):24–33.

Tong, S. T. Y., Y. Sun, T. Ranatunga, J. He, and Y. J. Yang. 2012. Predicting plausible impacts of sets of climate and land use change scenarios on water resources. Applied Geography (2012).

Tu, J. 2009. Combined impact of climate and land use changes on streamflow and water quality in eastern Massachusetts, USA. Journal of Hydrology 379(3–4):268–283.

USDA. 1972. Soil Conservation Service : National engineering handbook, Section 4, hydrology. Chapters 7, 8, 9, and 10.

USEPA. 2000. Projecting land-use change: A summary of models for assessing the effects of community growth and change on land-use patterns. US Environmental Protection Agency, Office of Research and Development.

Vallam, P., X. S. Qin, and J. J. Yu. 2014. Uncertainty Quantification of Hydrologic Model. APCBEE Procedia 10 (2014):219–223.

Vazquez-Amábile, G. G., and B. A. Engel. 2005. Use of SWAT to compute groundwater table depth and streamflow in the Muscatatuck River watershed. Transactions of the ASAE 48(3):991–1003.

Veldkamp, A., and L. O. Fresco. 1996. CLUE: a conceptual model to study the conversion of land use and its effects. Ecological modelling 85(2–3):253–270.

Verburg, P. H., W. Soepboer, A. Veldkamp, R. Limpiada, V. Espaldon, and S. S. A. Mastura. 2002. Modeling the spatial dynamics of regional land use: the CLUE-S model. Environmental management 30(3):391–405.

Vetter, T., S. Huang, V. Aich, T. Yang, X. Wang, V. Krysanova, and F. Hattermann. 2015. Multi-model climate impact assessment and intercomparison for three large-scale river basins on three continents. Earth System Dynamics 6(1):17–43.

Vilaysane, B., K. Takara, P. Luo, I. Akkharath, and W. Duan. 2015. Hydrological Stream Flow Modelling for Calibration and Uncertainty Analysis Using SWAT Model in the Xedone River Basin, Lao PDR. Procedia Environmental Sciences 28(SustaiN 2014):380–390.

Villarini, G., J. A. Smith, and G. A. Vecchi. 2013. Changing frequency of heavy rainfall over the central United States. Journal of Climate 26(1):351–357.

Walsh, R. D., and D. M. Lawler. 1981. Rainfall Seasonality: Description, Spatial Patterns and Change Through Time. Weather 36(7):201–208.

Wang, R., L. Kalin, W. Kuang, and H. Tian. 2014. Individual and combined effects of land use/cover and climate change on Wolf Bay watershed streamflow in southern Alabama. Hydrological Processes 28(22):5530–5546.

Waseem, M., A. Halmy, P. E. Gessler, J. A. Hicke, and B. B. Salem. 2015. Land use / land cover change detection and prediction in the north-western coastal desert of Egypt using Markov-CA. Applied Geography 63 (2015):101–112.

Westerberg, I., J. Guerrero, J. Seibert, K. J. Beven, and S. Halldin. 2011. Stage-discharge uncertainty derived with a non-stationary rating curve in the Choluteca River, Honduras. Hydrological Processes 25(4):603–613.

White, R., and G. Engelen. 1993. Cellular automata and fractal urban form: a cellular modelling approach to the evolution of urban land-use patterns. Environment and planning A 25(8):1175–1199.

Whitney, J. W., P. A. Glancy, S. E. Buckingham, and A. C. Ehrenberg. 2015. Effects of rapid urbanization on streamflow, erosion, and sedimentation in a desert stream in the American Southwest. Anthropocene 10 (2015):29–42.

Wibig, J., and B. Glowicki. 2002. Trends of minimum and maximum temperature in Poland. Climate research 20(2):123–133.

Wilhelmi, O. V, and D. A. Wilhite. 2002. Assessing vulnerability to agricultural drought: a Nebraska case study. Natural Hazards 25(1):37–58.

Willmott, C. J. 1981. On the validation of models, Physical Geography. Spatial statistic and models (1981):18.

Wilson, C. O., and Q. Weng. 2011. Simulating the impacts of future land use and climate changes on surface water quality in the Des Plaines River watershed, Chicago Metropolitan Statistical Area, Illinois. Science of the Total Environment 409(20):4387–4405.

Wu, F., J. Zhan, H. Su, H. Yan, and E. Ma. 2015. Scenario-Based Impact Assessment of Land Use/Cover and Climate Changes on Watershed Hydrology in Heihe River Basin of Northwest China. Advances in Meteorology 2015 (2015).

Xu, W., Q. Li, X. L. Wang, S. Yang, L. Cao, and Y. Feng. 2013. Homogenization of Chinese daily surface air temperatures and analysis of trends in the extreme temperature indices. Journal of Geophysical Research Atmospheres 118(17):9708–9720.

Yosef, Y., H. Saaroni, and P. Alpert. 2009. Trends in Daily Rainfall Intensity Over Israel 1950/1-

2003/4. The Open Atmospheric Science Journal 3(1):196–203.

Yu, P., and T. Yang. 2000. Using synthetic flow duration curves for rainfall–runoff model calibration at ungauged sites. Hydrological processes 14(1):117–133.

Zahabiyoun, B., M. R. Goodarzi, A. R. M. Bavani, and H. M. Azamathulla. 2013. Assessment of climate change impact on the Gharesou River Basin using SWAT hydrological model. CLEAN–Soil, Air, Water 41(6):601–609.

Zhai, P., and X. Pan. 2003. Trends in temperature extremes during 1951-1999 in China. Geophysical Research Letters 30(17):7–10.

Zhang, Q., C. Y. Xu, Z. Zhang, Y. D. Chen, C. ling Liu, and H. Lin. 2008. Spatial and temporal variability of precipitation maxima during 1960-2005 in the Yangtze River basin and possible association with large-scale circulation. Journal of Hydrology 353(3–4):215–227.

Zhang, Y., D. K. R. Robinson, A. L. Porter, D. Zhu, G. Zhang, and J. Lu. 2016a. Technological Forecasting & Social Change Technology roadmapping for competitive technical intelligence. Technological Forecasting & Social Change 110(May 2013):175–186.

Zhou, J., Y. Liu, H. Guo, and D. He. 2014. Combining the SWAT model with sequential uncertainty fitting algorithm for streamflow prediction and uncertainty analysis for the Lake Dianchi Basin, China. Hydrological Processes 28(3):521–533.